

## **ABSTRACT**

NAWALAKHE, RUPESH GAJANAN. Novel Atmospheric Plasma Enhanced Nanofiber/Gauze Composite Wound Dressings. (Under the direction of Dr. Marian G McCord and Dr. Xiangwu Zhang).

Traditional textile-based wound dressings are cost effective and highly absorbent but used alone, fail to provide optimal wound healing conditions (hemostasis, non-adherence, maintenance of a moist wound bed, etc.). Recently, many advanced wound dressings have been developed to provide enhanced functionalities and help to maintain an appropriate healing environment around wounds, but also led to higher cost and difficulty in handling. Another disadvantage of using modern wound dressing is that these dressings can either act as primary or secondary wound dressing (e.g. hydrocolloids, hydrogels, calcium alginate, transparent films, foam, hydrofibers, etc.). Electrospun nanofiber dressings have demonstrated the potential to revolutionize wound care by providing significantly enhanced moisture management, barrier properties, and bioactivity. However, nanofiber webs are inherently weak and difficult to handle. Deposition of electrospun nanofiber coatings on a traditional textile bandages addresses the need for structural support, but faces challenges of delamination due to compliance mismatch or poor adhesion. The goal of this research is to create biopolymer based nanofiber/gauze composite bandages that combine the desirable properties of each component, and to characterize the physical and mechanical properties of these materials in order to predict the performance of these novel materials for wound care applications.

In this research work, following tasks have been carried out:

- i) *Selection of appropriate substrate and nanofiber combinations*: Substrate material for the nanofiber coatings was chosen from existing commercially available 100% cotton gauze. Two bio-polymers, chitosan and silk fibroin (SF) were selected for electrospinning nanofiber web on to the cotton substrate in order to make composite wound dressing. Trifluoroacetic acid was selected as solvent to prepare electrospinning solution. In these composite bandages, chitosan/silk fibroin can act as primary wound dressing whereas cotton substrate can act as backing material and secondary wound dressing.
- ii) *Controlled deposition of nanofiber mat onto woven fabric substrate*: Electrospinning of chitosan and SF were carried out on to 100% cotton substrate in order to prepare composite bandages. Polymer solution concentration, electrospinning voltage, and deposition areal density were varied to establish the relationship of processing-structure-filtration efficiency for electrospun fiber mats. Optimum concentration of polymer in solvent was finalized based on SEM images, sturdiness of nanofibers, and its production rate.
- iii) *Improving interfacial adhesion between nanofiber mat and cotton substrate by plasma pretreatment of substrate fabric and plasma-post treatment of composite bandage*: Adhesion between nanofibers and substrate was studied using two test methods, quantitative and qualitative. The peel test which was quantitative test showed that plasma treatment of the substrate increased the adhesion between nanofiber layers and gauze substrate. . This force was further increased when composite bandages were given plasma pre-treatment to substrate as well as post-treatment to composite bandages. To

assess the improved adhesion between nanofiber layer and substrate, gelbo flex test was employed in which the composite bandages were subjected to 1000 cycles of twisting and flexing. Atmospheric plasma pretreatment of the gauze fabric prior to electrospinning and post treatment of composite bandages significantly reduced degradation of the nanofiber layer due to repetitive flexing. To understand the mechanism of improved adhesion between nanofiber layer and cotton substrate, surface elemental analysis of plasma treated/untreated cotton substrate and nanofiber layer were carried out.

iv) *Characterization of nanofiber/cotton substrate composite bandage*: Composite bandages were characterized for maintaining moist wound healing environment. These characterization techniques included moisture vapor transmission rate, air permeability, and absorbency. Antibacterial properties of chitosan based nanofiber/cotton substrate wound dressing were analyzed. To study the effect of atmospheric pressure plasma on storage modulus, crystallinity, glass transition temperature, and cell viability of chitosan and silk nanofiber, characterization techniques such as dynamic mechanical analysis, wide angle X-ray diffraction, and differential scanning calorimetry were carried out.

© Copyright 2012 by Rupesh Gajanan Nawalakhe

All Rights Reserved

Novel Atmospheric Plasma Enhanced Nanofiber/Gauze Composite Wound Dressings

by  
Rupesh Gajanan Nawalakhe

A dissertation submitted to the Graduate Faculty of  
North Carolina State University  
in partial fulfillment of the  
requirements for the degree of  
Doctor of Philosophy

Fiber and Polymer Science

Raleigh, North Carolina

2012

APPROVED BY:

---

Dr. Marian McCord  
Co- Chair

---

Dr. Xiangwu Zhang  
Co-chair

---

Dr. Mohamed Bourham

---

Dr. Saad Khan

## **DEDICATION**

I would like to dedicate this dissertation to my parents, Gajanan and Sandhya, and my sister Monali. I will always be thankful for their constant encouragement and support all along, without which I would not have reached these heights.

## **BIOGRAPHY**

Rupesh Gajanan Nawalakhe was born in Akola, Maharashtra State, India. He earned his bachelor degree in Textile Technology at Veermata Jeejabai Technological Institute, Mumbai, India in 2007. He joined NC State in 2007 to pursue his master in Textile Engineering and received his Master's degree in 2009. He started pursuing his PhD in Fiber and Polymer Science in 2009 under the guidance of Dr. Marian McCord. During PhD, his research work was focused on atmospheric plasma enhanced nanofiber/gauze composite wound dressings

## **ACKNOWLEDGMENTS**

I owe an immense gratitude to my advisors Dr. Marian McCord and Dr. Xiangwu Zhang for their constant support, guidance, and encouragement during this research work. This work would not have been possible without their knowledge, experience, and patience. I wish to express my high appreciation to my committee members Dr. Mohamed Bourham, and Dr. Saad Khan for their comments and suggestions to make this study successful. Also, I extend my thanks to our research group Dr. Narendiran Vitchuli, Dr. Quan Shi, Joshua Nowak and Michael Sieber for their moral support and guidance throughout my research. I would like to offer my high appreciation to Judy Elson, for her technical help with training on analytical laboratory equipment. I would also like to thank Traci Figura, Victoria Storman, for their time and hard work to make my graduate studies in NC State University convenient. I offer my special appreciation to my friends for their help, support and guidance throughout my graduate studies. I would like to thank the National Textile Center (NTC) of USA (Project No. F09-NS06), and North Carolina State University for the financial support without which this work would not have been possible. Last, but not the least, I am immensely grateful to my parents, Gajanan Nawalakhe and Sandhya Nawalakhe, my Sister, Monali Nawalakhe. I will always be indebted to these people for their support, encouragement and love without which the higher education would have remained a dream.

## TABLE OF CONTENTS

LIST OF TABLES .....	xii
LIST OF FIGURES .....	xiv
1. Introduction .....	1
1.1 Introduction.....	2
2. Literature Review.....	5
2.1 Wound Management .....	6
2.2 Wound Dressing .....	7
2.2.1Mechanisms of Injury .....	9
2.2.2 Wound Healing Process.....	11
2.2.3 Process of Blood Coagulation .....	13
2.2.4 Selecting a Proper Wound Dressing .....	15
2.3 Factors Affecting Wound Healing .....	15
2.4 Types of wound dressing .....	18
2.4.1 Calcium alginates .....	18
2.4.2 Hydrofibers .....	18
2.4.3 Hydrogel Impregnated Gauze .....	18
2.4.4 Hydrogels .....	19
2.4.5 Foams .....	19
2.4.6 Transparent Films .....	20
2.4.7 Hydrocolloids .....	20

2.5 Application of Textiles in wound dressings .....	21
2.6 Polymers used in Wound Dressings .....	22
2.7 Electrospinning .....	25
2.7.1 Applications of Nanofibers in Biomedical/ Biotechnology .....	27
2.7.1.1 Hemostasis .....	29
2.7.1.2 Absorption of Exudates from Wound .....	29
2.7.1.3 Maintaining Moist Environment and Permeability .....	29
2.7.1.4 Controlled Drug Release .....	30
2.7.1.5 Comfort and Flexibility .....	30
2.8 Selection of Polymer for Wound Dressings from Various Biocompatible and Biodegradable Polymeric Materials .....	31
2.9 Silk .....	34
2.9.1 Electrospinning of Silk Fibroin (SF) .....	33
2.10 Chitosan .....	39
2.10.1 Electrospinning of chitosan .....	40
2.10.1.1 Chitosan blends .....	41
2.10.1.2 Pure Chitosan Nanofibers .....	44
2.11 Plasma .....	46
2.11.1 Application of Atmospheric Plasma in Textiles .....	48
2.11.2 Plasma-Polymer Interactions .....	49
2.11.2.1 Adhesion .....	49
2.11.2.2 Etching .....	50

2.11.2.3 Cross-linking on Surface .....	52
2.11.2.4 Surface Activation .....	53
2.11.2.5 Enhancement in Mechanical Properties and Hydrophilicity .....	54
2.12 References .....	55
3. Motivation and Objective .....	66
3.1 Motivation .....	67
3.2 Objectives .....	70
4. Novel Atmospheric Plasma Enhanced Chitosan Nanofiber/Gauze Composite Wound Dressings .....	72
4.1 Abstract .....	74
4.2 Introduction.....	75
4.3 Materials and Methods.....	77
4.3.1 Materials .....	77
4.3.2 Electrospinning of nanofiber webs onto substrates .....	78
4.3.3 Plasma pre-treatment of substrate .....	78
4.3.4 Adhesion between Nanofiber Mats and Supporting Fabrics .....	80
4.3.5 Antibacterial Tests .....	81
4.3.6 Air Permeability.....	81
4.3.7 Moisture Vapor Transmission Rate (MVTR) .....	82
4.3.8 XPS Analysis .....	82
4.3.9 Absorbency .....	83
4.4 Results and Discussion .....	84

4.4.1 Electrospinning of chitosan nanofibers.....	84
4.4.2 Adhesion between nanofiber mats and supporting fabrics .....	85
4.4.3 Antibacterial Test.....	88
4.4.4 Air Permeability.....	90
4.4.5 Moisture Vapor Transmission Rate (MVTR) .....	92
4.4.6 XPS Analysis of Substrate after Plasma Treatment.....	92
4.4.7 Absorbency .....	95
4.5 Conclusions.....	96
4.6 Acknowledgements.....	97
4.7 References.....	98
 5. Novel Atmospheric Plasma Enhanced Silk Fibroin Nanofiber/Gauze Composite Wound	
Dressings.....	102
5.1 Abstract.....	103
5.2 Introduction.....	105
5.3 Materials and Methods.....	108
5.3.1 Materials .....	108
5.3.2 Electrospinning of nanofiber webs onto substrates .....	108
5.3.3 Plasma pre-treatment of substrate .....	109
5.3.4 Adhesion between Nanofiber Mats and Supporting Fabrics .....	111
5.3.5 Air Permeability .....	112
5.3.6 XPS Analysis of Substrate and SF Nanofibers after Plasma Treatment .....	112
5.3.7 Moisture Vapor Transmission Rate (MVTR) .....	113

5.4 Results and Discussion .....	114
5.4.1 Electrospinning of SF nanofibers.....	114
5.4.2 Peel test .....	115
5.4.3 Gelbo Flex Test.....	117
5.4.4 Air Permeability.....	119
5.4.5 Moisture Vapor Transmission Rate (MVTR) .....	120
5.4.6 XPS Analysis of Substrate after Plasma Treatment.....	121
5.4.7 XPS analyses of silk fibroin nanofibers .....	124
5.5 Conclusions.....	128
5.6 Acknowledgements.....	129
5.7 References .....	130
6. Electrospinning of Chitosan Nanofibers: Improving its Mechanical Properties and Adhesion with the Cotton Gauze with the help of Atmospheric Pressure Plasma .....	137
6.1 Abstract.....	139
6.2 Introduction .....	140
6.3 Materials and Methods .....	143
6.3.1 Material .....	143
6.3.2 Electrospinning of nanofiber webs onto substrates .....	143
6.3.3 Plasma pre-treatment of Substrate .....	144
6.3.4 Adhesion between nanofiber mats and supporting fabrics .....	146
6.3.5 Dynamic mechanical analysis (DMA) .....	147
6.3.6 Differential Scanning Calorimetry (DSC) .....	147

6.3.7 Wide angle X-ray Diffraction (WAXD) .....	148
6.3.8 X-Ray Photoelectron Spectroscopy (XPS) .....	148
6.4 Results and Discussion .....	149
6.4.1 Electrospinning of nanofiber webs onto substrates .....	149
6.4.2 Adhesion between nanofiber mats and supporting fabrics .....	151
6.4.3 Dynamic Mechanical Analysis .....	155
6.4.4 Differential Scanning Calorimetry .....	158
6.4.5 Wide angle X-ray Diffraction .....	160
6.4.6 XPS Analysis of Substrate after Plasma Treatment.....	162
6.4.7 XPS Analysis of Plasma treated Chitosan Nanofiber Webs.....	165
6.5 Conclusion .....	167
6.6 References .....	169
7. Electrospinning of Silk Fibroin Nanofibers: Improving its Mechanical Properties and Adhesion with the Cotton Gauze with the help of Atmospheric Pressure Plasma.....	173
7.1 Abstract .....	175
7.2 Introduction .....	176
7.3 Materials and Methods .....	178
7.3.1 Material .....	178
7.3.2 Electrospinning of nanofiber webs onto substrates .....	178
7.3.3 Plasma pre-treatment of Substrate .....	179
7.3.4 Dynamic mechanical analysis (DMA) .....	180
7.3.5 Differential Scanning Calorimetry (DSC) .....	180

7.3.6 Wide angle X-ray Diffraction (WAXD) .....	181
7.3.7 MTT assay: Viability Assessment of SF nanofibers.....	181
7.3.8 X-Ray Photoelectron Spectroscopy (XPS) .....	182
7.4 Results and Discussion .....	183
7.4.1 Electrospinning of nanofiber webs onto substrates .....	183
7.4.2 Dynamic Mechanical Analysis .....	184
7.4.3 Differential Scanning Calorimetry .....	185
7.4.4 Wide angle X-ray Diffraction .....	187
7.4.5 MTT assay: Viability Assessment of SF nanofibers .....	188
7.4.6 XPS Analysis of Plasma treated SF Nanofiber Webs.....	190
7.5 Conclusion .....	194
7.6 References .....	195
8. Conclusion and recommendations .....	199
8.1 Conclusion .....	200
8.2 Recommendations.....	204
APPENDICES: .....	206
Appendix A: Moisture Vapor Transmission rate .....	207
Appendix B: Absorbency .....	209
Appendix C: Air permeability .....	211
Appendix D: Peel test .....	213

## LIST OF TABLES

Table 2.1 Normal Wound-healing Process .....	11
Table 2.1 Normal Wound-healing Process (Continued).....	12
Table 2.2 Alginate-based wound dressings commercially available in the market.....	23
Table 4.1 Measurement of adhesion between nanofiber mats and supporting fabrics .....	85
Table 4.2 Antibacterial activities of Chitosan nanofiber coated gauze fabric against only gauze. ....	89
Table 4.3 Average Air Permeability and moisture vapor transmission rate (MVTR) of the composite wound dressing i.e. Chitosan nanofiber electrospun on untreated, He plasma treated and He-O <sub>2</sub> plasma treated cotton substrate .....	91
Table 4.4 Results of surface elemental analysis for plasma treated and untreated Cotton substrate with Atmospheric Pressure Plasmas.....	93
Table 4.5 Absorbency of Gauze and Composite wound dressing. ....	96
Table 5.1 Load (gf) required to peel the SF nanofiber layer off the substrate. ....	116
Table 5.2 Average Air Permeability and Moisture Vapor Transmission Rate (MVTR) of the composite wound dressing: SF nanofibers electrospun on untreated, He-plasma treated and He-O <sub>2</sub> plasma treated cotton substrate. ....	120
Table 5.3 Elemental and chemical composition of substrate with and without plasma treatment .....	123
Table 5.4 Results of chemical composition of C1s, N1 peaks and overall elemental analysis for treated and untreated SF nanofibers with atmospheric pressure plasmas. ....	125

Table 6.1 Measurement of adhesion between nanofiber mats and supporting fabrics .....	151
Table 6.2 Crystallinity of untreated, He-plasma treated and He/O <sub>2</sub> plasma treated chitosan nanofiber webs using WAXD.....	161
Table 6.3 Results of surface elemental analysis for atmospheric pressure plasma treated and untreated Cotton substrate .....	163
Table 6.4 Results of surface elemental analysis for atmospheric pressure plasma treated and untreated chitosan nanofibers .....	166
Table 7.1 Crystallinity of untreated, He-plasma treated and He/O <sub>2</sub> plasma treated SF nanofiber webs using WAXD.....	188
Table 7.2 Results of chemical composition of C1s, N1 peaks and overall elemental analysis for treated and untreated SF nanofibers with atmospheric pressure plasmas. ....	191

## LIST OF FIGURES

Figure 2.1 Conventional and Modern Wound dressing.....	7
Figure 2.2 Mechanisms of Injury.....	9
Figure 2.3 Blood coagulation. Clotting factors (proenzymes), identified by Roman numerals, interact in a sequential series of enzymatic activation reactions (coagulation cascade) leading to the amplified production of the enzyme thrombin, which in turn activates fibrinogen to form a fibrin polymer that stabilizes the clot or thrombus. ....	14
Figure 2.4 Schematic view of a typical electrospinning set-up .....	25
Figure 2.5 Formation of Taylor Cone and subsequent splaying of fibers .....	26
Figure 2.6 Use of polymer nanofibers for biomedical and biotechnological applications .....	28
Figure 2.7 Cell attachment and spreading of normal human fibroblasts plated onto SF nanofibers. (a) SEM images of the interaction between the NHEF and SF nanofibers. (b) Level of cell spreading of the NHEF plated onto the SF nanofibers .....	35
Figure 2.8. The proliferation of cells grown on the SF nanofibers membranes after different culture periods. MTT absorbency at 540 nm of cells on SF nanofibrous membranes were measured and viable cell numbers determined from standard curve .....	36
Figure 2.9 (A) Photographs and (B) the numbers of NHEK and NHEF adhered to chitin/SF blend nanofibrous matrices. (C) Percentage of cell spreading for NHEK and NHEF plated onto chitin/SF blend nanofibrous matrices. Data are expressed as mean $\pm$ S.E. ( $n = 4$ ). PS, polystyrene surface .....	38
Figure 2.10 SEM images of electrospun chitosan-PEO core-sheath nanofibers. (A-C) Samples before H <sub>2</sub> O rinse and (D-F) samples after H <sub>2</sub> O Rinse .....	42

Figure 2.11 Plasma etching: Hydrogen abstraction and Chain Scission .....	51
Figure 2.12 Possible Cross-linking Mechanism of Poly(p-phenylene terephthalamide) Film.....	52
Figure 2.13 Surface activation by oxygen plasma and nitrogen plasma.....	53
Figure 4.1 Schematic diagram of atmospheric pressure plasma system.....	79
Figure 4.2 SEM images of Chitosan nanofibers Concentration: A)2%, B)3%, C)4%, D)5%, E)6%, and F)7% in TFA. ....	84
Figure 4.3 Evaluation of nanofiber-fabric adhesion using the 90 degree peel test. ....	86
Figure 4.4 SEM images of composite bandages, before Gelbo testing and after 1000 cycles of Gelbo flex testing with no pre-treatment, 100% He, 99%He/1%O <sub>2</sub> plasma pre-treatment on substrate. ....	87
Figure 4.5 Antibacterial testing on control (untreated) gauze, He and He/O <sub>2</sub> treated substrate with and without chitosan nanofibers. ....	88
Figure 4.6 Possible sites for scission of cotton substrate after plasma treatment (A) Dehydroxylation, B) Dehydrogenation, C) scission between C1 and ring oxygen, D) dehydrogenation/dehydroxylation, E) scission between C1 and glycosidic oxygen .....	94
Figure 5.1 Depositing nanofibers onto the fabric by rotating collector. ....	109
Figure 5.2 SEM images of SF nanofibers electrospun at concentrations of A) 5%, B) 6%, C) 7%, D) 8%, E) 9%, F) 10% in TFA. Magnification: 2500 ×. ....	114
Figure 5.3 Distortion of SF nanofibers after 1000 cycles of Gelbo flex test, electrospun on 100% cotton gauze. First row: no plasma pre-treatment, second row: He plasma pre-	

treatment, third row: He/O <sub>2</sub> plasma pre-treatment. First column: no plasma post-treatment, second column: He plasma post-treatment, third column: He/O <sub>2</sub> plasma post-treatment. ..118	
Figure 5.4 Possible sites for scission of cotton substrate after plasma treatment A) Dehydroxylation, B) Dehydrogenation, C) scission between C1 and ring oxygen, D) dehydrogenation/dehydroxylation, E) scission between C1 and glycosidic oxygen. ....122	
Figure 5.5 Chemical composition of plasma-treated and untreated silk fibroin nanofibers with Atmospheric A) Untreated, B) He-plasma treated and C) He/ O <sub>2</sub> plasma treated SF nanofibers .1: Envelope, 2: C=O, 3: C=O/N-C=O, 4: C-O/C-N, 5: C-C/C-H. ....126	
Figure 5.6 Possible sites for scission after plasma treatment of SF nanofibers. ....127	
Figure 6.1 Schematic diagram of atmospheric pressure plasma system.....145	
Figure 6.2 SEM images of Chitosan nanofibers Concentration: a) 2%, b) 3%, c) 4%, d) 5%, e) 6%, and f) 7% in TFA. (Scale: 20 μm) .....149	
Figure 6.3 Distortion of chitosan nanofibers after 1000 cycles of Gelbo flex test, electrospun on 100% cotton gauze First row: no plasma pre-treatment, second row: He plasma pre-treatment, third row: He/O <sub>2</sub> plasma pre-treatment, First column: no plasma post-treat, second column: He plasma post-treat, third column: He/O <sub>2</sub> plasma post-treat .....154	
Figure 6.4 Storage modulus for the A) plasma untreated, B) He/O <sub>2</sub> plasma treated, and C) He-plasma treated chitosan nanofiber web. ....156	
Figure 6.5 DSC heating curves of A) plasma untreated, B) He/O <sub>2</sub> plasma treated, and C) He-plasma treated chitosan nanofibers .....159	

Figure 6.6 XRD patterns of A) plasma untreated, B) He/O<sub>2</sub> plasma treated, and C) He-plasma treated chitosan nanofibers. Plasma treatment showed increased crystallinity with the plasma treatment. ....160

Figure 6.7 Possible sites for scission of cotton substrate after plasma treatment (A) Dehydroxylation, B) Dehydrogenation, C) scission between C1 and ring oxygen, D) dehydrogenation/dehydroxylation, E) scission between C1 and glycosidic oxygen .....162

Figure 6.8 Possible sites for scission of chitosan after plasma treatment A) Dehydroxylation, B) Dehydrogenation, C) scission between C1 and ring oxygen, D) dehydrogenation/dehydroxylation, E) scission between C1 and glycosidic oxygen .....165

Figure 7.1 Depositing nanofibers onto the fabric by rotating collector. ....179

Figure 7.2 SEM images of SF nanofibers electrospun at concentrations of A) 5%, B) 6%, C) 7%, D) 8%, E) 9%, F) 10% in TFA. Magnification: 2500 ×. ....184

Figure 7.3 Storage modulus for the A) plasma untreated, B) He/O<sub>2</sub> plasma treated, and C) He-plasma treated SF nanofiber web. ....184

Figure 7.4 DSC heating curves of A) plasma untreated, B) He/O<sub>2</sub> plasma treated, and C) He-plasma treated SF nanofibers. ....186

Figure 7.5 XRD patterns of A) plasma untreated, B) He/O<sub>2</sub> plasma treated, and C) He-plasma treated SF nanofibers. Plasma treatment showed increased crystallinity with the plasma treatment. ....187

Figure 7.6 MTT viability of HEK grown on untreated, He plasma treated and He/O<sub>2</sub> plasma treated SF composite bandages. ....190

Figure 7.7 Chemical composition of plasma-treated and untreated silk fibroin nanofibers with Atmospheric A) Untreated, B) He-plasma treated and C) He/ O<sub>2</sub> plasma treated SF nanofibers .1: Envelope, 2: C=O, 3: C=O/N-C=O, 4: C-O/C-N, 5: C-C/C-H. ....192

Figure 7.8 Possible sites for scission after plasma treatment of SF nanofibers .....193

CHAPTER 1  
Introduction

## **Introduction**

Modern wound care products have advanced capabilities that can significantly enhance patient outcomes following serious injuries. An ideal dressing is the one that can provide an environment at the surface of the wound in which healing and regeneration of tissues can take place rapidly and with an acceptable cosmetic appearance. Conventional textile-based wound dressings are cost-effective and highly absorbent, but used alone, fail to provide optimal wound healing conditions (hemostasis, non-adherence, maintenance of a moist wound bed, etc.). Advanced wound dressings often incorporate multiple non-textile components (films, gels, antimicrobials, and biologicals) that provide multiple functionalities at a significantly higher cost. The goal of this research is to electrospin biopolymers onto conventional wound dressing substrates, to investigate the effect of atmospheric plasma treatment on the composite dressings, and to compare physical and mechanical properties of the composite dressings to those of advanced wound dressings. This work will mainly focus on chitosan and silk-fibroin, which are naturally occurring polymers having inherent applications in wound healing.

Chitosan is an N-deacetylated product of chitin, the second-most abundant natural polysaccharide next to cellulose. Chitin is embedded in a protein matrix of shells of crabs, crustaceans, shrimp and lobster, exo-skeleton of mollusks and insects, cell walls of some algae and fungi. Chitosan is preferred over chitin because of its solubility in acidic, neutral and alkaline solutions, which enables further processing. It has many useful properties such as biocompatibility, biodegradability, antimicrobial activity, wound healing properties, antitumor effects, etc. Chitosan has applications in a variety of areas, such as pharmaceutical

and medical applications, paper production, textile dyeing and finishing, fiber formation, wastewater treatment, biotechnology, cosmetics, food processing, and agriculture.

Other than chitosan, protein material from silkworms and spider silk are of specific interest because of combined strength and toughness. Silk fibroin is a natural fibrous protein, mainly consisting of amino acids with small side groups, such as glycine, alanine and serine. There have been increasing uses of silk fibroin from silkworm silk (*Bombyx Mori*) in various applications due to its biocompatibility, biodegradability, high oxygen and water permeability, drug permeability and resistance to enzymatic degradation. These properties make silk fibroin useful in biomedical applications, such as surgical sutures, skin treatments, and wound dressing materials, substrates for cell culture, controlled drug-delivery, cosmetics and food additives.

In the context of wound dressings, nanofibers are shown to demonstrate functional versatility, including desirable wound adherence, absorption, oxygen permeability, resorbability, and occlusivity. Their high specific surface area makes them effective matrices for controlled drug release. Nanofiber webs form highly effective filters for contaminants, particulates, and microorganisms. The combination of small interstices and high surface area make nanofibers is useful in accelerating hemostasis. Due to their high surface area to volume ratios, nanofibers of the same polymer give higher absorption than conventional fibers. The highly porous structures of nanofiber based dressings are ideal for providing oxygen and moisture vapor permeability while at the same time preventing wound desiccation. However, widespread use of nanofiber webs in wound dressings has been limited by challenges such as poor mechanical properties and difficulty in handling.

These shortcomings of nanofibers can be overcome by the treatment of substrate by atmospheric plasma. Atmospheric pressure plasma technology helps to modify the structures and properties of various materials, especially textile materials. Our hypothesis is that plasma treatment is capable of enhancing the bonds between nanofiber mats and textile substrates through pre-deposition surface activation of textile substrates, and improves the nanofiber strength and bonding through post-deposition crosslinking.

CHAPTER 2  
Literature Review

## 2.1 Wound Management

An ideal dressing is one that can provide an environment at the surface of the wound in which healing can take place at the maximum rate and with an acceptable cosmetic appearance [1]. A wound dressing is characterized by both form and function. The traditional category includes conventional and textile based wound dressing such as Gauze, Lint, Wadding, while the advanced category encompasses films, hydrocolloids, hydrogels, alginates, antimicrobials, etc. The basic function of wound dressing is to provide some level of absorbency and wound protection, which is usually provided by the conventional or traditional wound dressings.

Advanced functions include moisture occlusivity, antibacterial protection, hemostatic properties, etc. Figure 2.1 shows two types of wound dressing. Figure 2.1 A shows gauze, a traditional wound dressing material; whose main function is absorbency and protection, whereas Figure 2.1 B shows Sorbalgon<sup>®</sup> [2] which is an example of an advanced wound dressing which provides additional properties along with the absorbency and protection of wound. This particular product is made of calcium alginate fibers which form a hydrophilic non-adherent gel when in contact with the sodium salts contained in blood and wound exudates. This kind of wound dressing material is used in treatments of external bleeding and exudating wounds such as Ulcus cruris venosum, decubitus, abscesses, furuncles, burns and for difficult-to-treat wounds in accident or tumor surgery, etc. The gel-forming properties of the dressing promote the wound healing process. The cost of this particular dressing is \$54.31 (10/pack, 2" x 2") [2] whereas traditional cotton gauze wound dressing costs only for \$4.81 (80/pack, 3"x 3")[3].



a) Cotton Gauze, Conventional



b) Sorbalgon<sup>®</sup>, Modern

Figure 2.1. Conventional and Modern Wound dressing [4] [2]

## 2.2 Wound Dressing

This section will focus on the important characteristics of ideal wound dressings, selection of proper wound dressing depending on patients' priorities, importance of moist environment in wound dressing, wound healing mechanism, and blood coagulation.

It is now widely accepted that a moist wound environment enhances wound healing. Absorbptivity and oxygen permeability are key performance factors. Additionally, it has been recognized that ideal dressings should have the characteristics [5] of

- (1) Hemostasis,
- (2) Efficiency as a bacterial barrier,
- (3) Absorption of excess exudates,
- (4) Provision and maintenance of a moist environment,
- (5) Ability to conform to the contour of the wound area,
- (6) Adherence to healthy tissue but non-adherent to wound tissue,

(7) Ease of removal, and

(8) Low cost.

All dressings ideally should protect wounds from any damage and contamination by bacteria and foreign material. Dressings also should absorb exudates generated by the wound. If a wound produces a large amount of fluid (exudates) [6][7,8], it can hinder the wound healing process. Higher amounts of exudates can be a symptom of infection and increased edema. This would increase the risk of maceration of the surrounding skin [9] [10]. Another function which should be considered in construction of a wound dressing is compression to minimize edema i.e. swelling. Maintenance of a warm, moist environment is desirable to maximize the rate of wound healing [11] [12]. Based on the surface area of the wounds, for example, a wound with large surface area (e.g. burns), prevention of heat and fluid loss is important. While changing the dressing material and to avoid the disruption of healing tissue, non-adherence is advantageous [13].

However, a wound can heal without application of a wound dressing if a scab forms. As soon as skin suffers any cut or wound, blood platelets become activated. Platelets aggregate at the cut and are incorporated into the clot. This clot can be considered as a natural protective bandage over the wound or cut keeping the blood and other fluids from flowing out. The clot is full of other blood cells and fibrin obtained from fibrinogen that helps to hold the clot together. Scabs can be described as crust of dried serum with trapped erythrocytes, platelets, and other blood-borne cells [14]. Scabs provide almost same functions provided by wound dressing such as protections against foreign material, reduction in pain, holding the wound edges in approximation, facilitating of wound contraction and loss of fluid

and proteins. However, scabs undergo slow epithelialization [15] [16] and can provide a site for bacterial growth and infection.

### 2.2.1 Mechanisms of Injury:

Understanding mechanism of Injury is important because it would estimate the extent of wound infection and determine the choice of wound management. The mechanism of injury can be described as the forces applied to skin under injury conditions; shearing, tension and compression forces. These forces would result in five types of wounds; Incision, Laceration, Abrasion, Contusion, and Puncture (Figure 2.2).

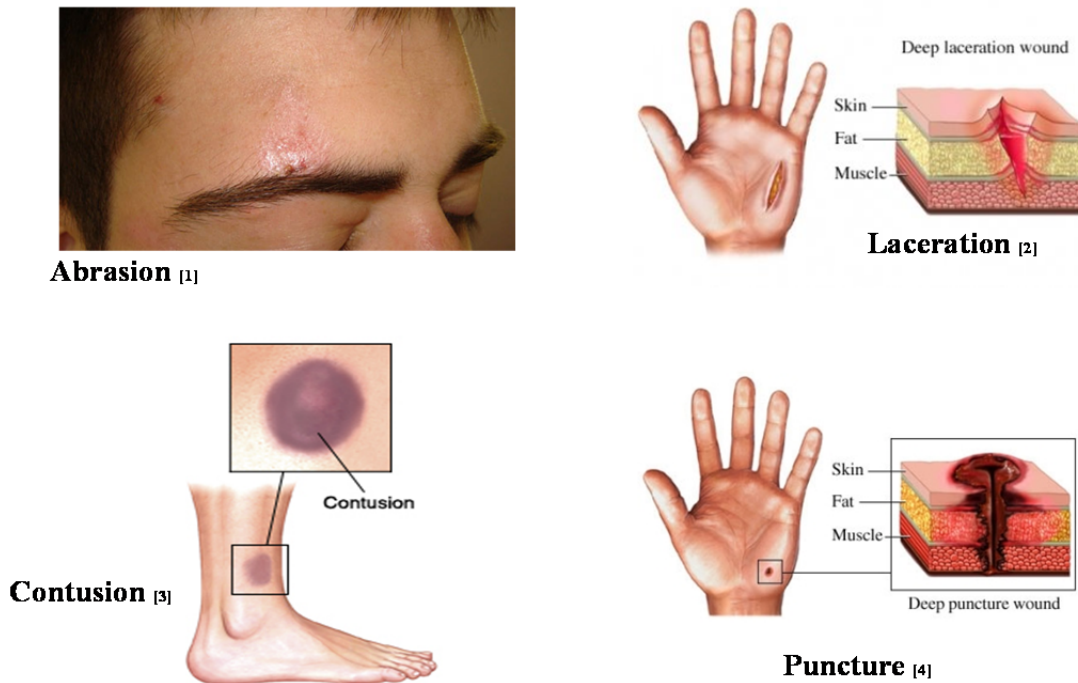


Figure 2.2 Mechanisms of Injury

**Incision**

An incision wound is a cut into a body tissue or organ, especially one made during surgery or caused by a sharp object such as a knife, broken glass or scissors. Incision wounds are 'neat' and the edges of the skin are usually smooth [17] [18].

**Laceration**

A laceration is an injury involving a cut, tearing or breaks in the skin. They can either be shallow injuring the surface skin or deep causing injury to the muscles, tendons, ligaments, blood vessels or nerves. Only difference between laceration and incision is that a laceration is generally jagged and skin is torn whereas in incision, skin is cut. Lacerations are most commonly observed in case of being hit with a fist or baseball bat [19]

**Abrasion**

An abrasion is a type of wound caused by damage to the skin due to scraping or rubbing. Abrasions are usually superficial wounds, meaning that only the outer layers of skin are affected. It is less severe than a laceration, and bleeding, if present, is minimal. Mild abrasions do not scar or bleed, but deep abrasions, one that penetrates to inner layers of the skin may lead to the formation of scar tissue. Knees and elbows having very thin layers of skin are more prone to the abrasions [20].

**Burn**

It is a type of injury to skin caused by heat, electricity, chemicals, light, radiation or friction. Burns are classified into first, second, third and fourth degrees according to the depth of injury to the dermis. It is usually treated by cleaning, removing blisters, applying grease gauze and soft gauze dressing, changed daily[21].

## **Contusion**

A contusion is a kind of closed wound and a type of relatively minor hematoma of tissue. In contusion capillaries and sometimes venules are damaged by trauma which allows blood to seep into the surrounding interstitial tissues meaning without breaking the skin [22]

## **Puncture**

A puncture wound is created when a sharp object enters the skin. These wounds are usually small and do not bleed a lot. Although these wounds tend to close over quickly, they still need treatment as infection is a possibility. Examples of puncture wounds include stepping on a nail or bites from animals [23].

### **2.2.2 Wound Healing Process**

The wound healing process is a complex series of events that begins at the moment of injury and can continue for months to years. It includes three phases [24] which can be stated as (table 2.1)

Table 2.1. Normal Wound-healing Process

Phases	Cellular and Bio-physiologic Events
Hemostasis	1. vascular constriction 2. platelet aggregation, degranulation, and fibrin formation (thrombus)
Inflammation	1. neutrophil infiltration 2. monocyte infiltration and differentiation to macrophage 3. lymphocyte infiltration

Table 2.1. Normal Wound-healing Process (Continued)

Phases	Cellular and Bio-physiologic Events
Proliferation	<ol style="list-style-type: none"> <li>1. re-epithelialization</li> <li>2. angiogenesis</li> <li>3. collagen synthesis</li> <li>4. ECM formation</li> </ol>
Remodeling	<ol style="list-style-type: none"> <li>1. collagen remodeling</li> <li>2. vascular maturation and regression</li> </ol>

I. Inflammatory Phase: This phase is immediate after the wound formation and lasts for 2-5 days. It includes a) hemostasis and b) inflammation. The first phase of hemostasis begins immediately after wounding, with vascular constriction and fibrin clot formation. The clot and surrounding wound tissue release pro-inflammatory cytokines and growth factors such as transforming growth factor (TGF)- $\beta$ , platelet-derived growth factor (PDGF), fibroblast growth factor (FGF), and epidermal growth factor (EGF). Once hemostasis controls the bleeding, the inflammatory phase starts, which is characterized by the sequential infiltration of neutrophils, macrophages, and lymphocytes[25] [26][27]. Neutrophils clear the invading microbes and cellular debris in the wound area. These cells also produce substances such as proteases and reactive oxygen species (ROS), which cause some additional bystander damage.

Macrophages have multiple roles in wound healing. In the early stage of wound healing, macrophages release cytokines which promote the inflammatory response by activating additional leukocytes. After clearing apoptotic cells, macrophages undergo a phenotypic transition to a reparative state that stimulates keratinocytes, fibroblasts, and

angiogenesis to promote tissue regeneration [28] [29]. Thus, macrophages stimulate the transition to the proliferative phase of healing.

T-lymphocytes migrate into wounds following the inflammatory cells and macrophages, and peak during the late-proliferative/ early-remodeling phase. The role of T-lymphocytes is not completely understood and is a current area of intensive investigation. T-cells regulate many phases of wound healing, including maintaining tissue integrity, defending against pathogens, and regulating inflammation.

The proliferative phase follows and overlaps with the inflammatory phase. It is characterized by epithelial proliferation and migration over the temporary matrix within the wound (re-epithelialization). In the reparative dermis, fibroblasts and endothelial cells are the most prominent cell types present and support capillary growth, collagen formation, and the formation of granulation tissue at the site of injury. Within the wound bed, fibroblasts produce collagen as well as glycosaminoglycans and proteoglycans, which are major components of the extracellular matrix (ECM). Following robust proliferation and ECM synthesis, wound healing enters the final remodeling phase, which can last for years. This is the longest phase in wound healing and can last for 3 weeks to 2 years [30]. It comprises new collagen formation which increases the tensile strength of the tissue. The scar tissue is only 80% as strong as original tissue.

### **2.2.3 Process of Blood Coagulation**

The mechanism of blood coagulation is as shown in Figure 2.3. At least 12 plasma proteins interact in a series of enzymatic and cofactor reactions leading to formation of a fibrin clot [31]. Thrombin is the enzyme that plays an important role in formation of clots.

Fibrinogen is a soluble glycoprotein that is converted to fibrin by thrombin. The fibrin, a fibrous protein, initially forms a loose mesh and then is cross-linked by Factor XIII to form a dense mesh that act as a hemostatic plug or clot over the wound site in the presence of calcium ions. Platelets and red blood cells get caught in the covalently cross-linked mesh

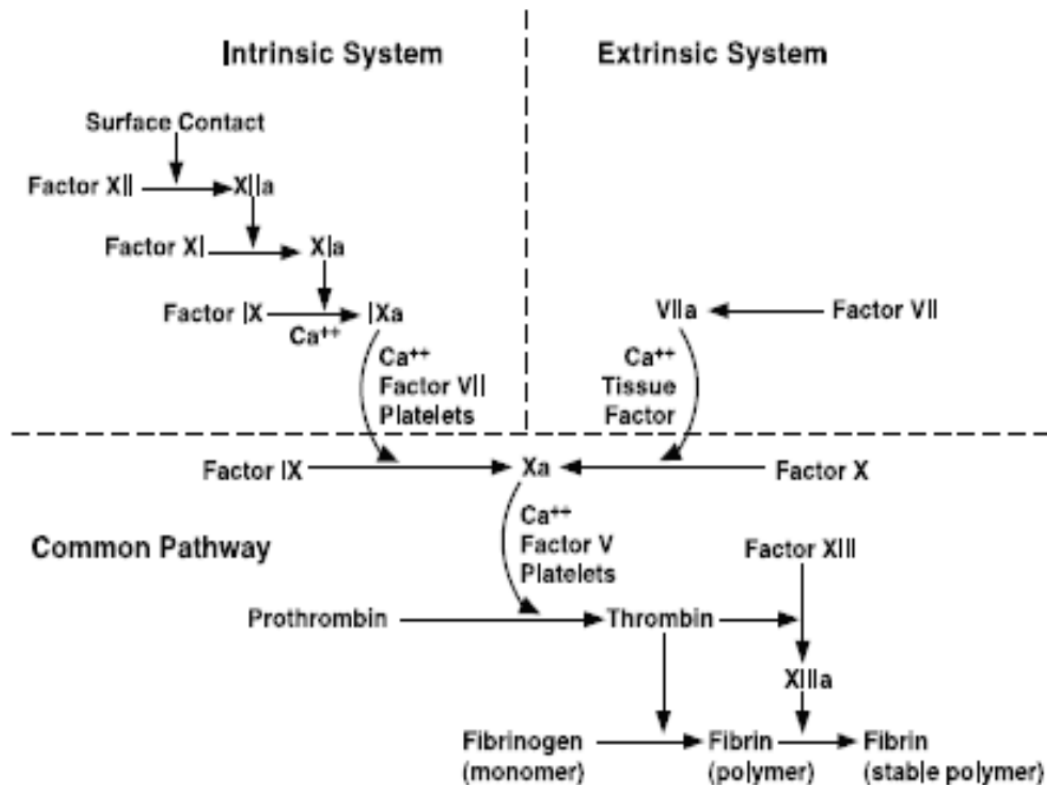


Figure 2.3. Blood coagulation. Clotting factors (proenzymes), identified by Roman numerals, interact in a sequential series of enzymatic activation reactions (coagulation cascade) leading to the amplified production of the enzyme thrombin, which in turn activates fibrinogen to form a fibrin polymer that stabilizes the clot or thrombus [32].

of fibrin, and the arrest of bleeding is accomplished. Hemostasis is eventually completed by fibrinolysis that removes the hemostatic plug and improves blood flow through the damaged vessel [31].

#### **2.2.4 Selecting a Proper Wound Dressing**

Though textile materials provide high absorbency, they may contribute to loss of wound moisture, or may become incorporated within the healing tissue. This incorporation of wound dressing in healing tissue can disturb a newly formed epithelializing layer during a wound dressing change. Current wound dressings are designed to have specific functions that address a narrow set of clinical demands for wound care in professional and self-care settings. Choice of wound dressings is dependent upon the severity and type of injury, as well as the stage of healing and the presence or absence of infection [33][34] [35].

Use of proper wound dressings maintains moisture levels by keeping ulcers moist and peri-ulcers dry. It provides protective barrier from environmental contaminants. Appropriate wound dressing selection increases healing rate, reduces pain and helps in decreasing infection rates. Along with these function, wound dressing material should be affordable to common people i.e. should be cost effective.

### **2.3 Factors Affecting Wound Healing:**

#### **Effect of pH:**

The literature has reported some studies of the effects of pH on cellular events in wound healing. The pH environment of chronic wounds has been recorded within the range of 7.15–8.9. This variability represents both healing and non-healing wounds. Wounds with an elevated alkaline pH have demonstrated lower rates of healing than wounds in which the pH is closer to neutral [36][37], [38]. As the wound progresses towards healing, the pH moves to neutral and then becomes acidic [39][40] et al,1985}}. In one of the study by Tsukada et al, epithelialised wounds had a mean pH of 6.0 compared with a mean of 7.8 for

wounds without epithelial tissue, which was shown to be statistically significant ( $p < 0.001$ ) [39]

The pH level of wound environment affects the activity of protease enzymes which is to cleave proteins. This activity is dependent on both the amount of proteases present and on the presence of inhibitors [41]. Every protease shows enzyme activity at certain pH levels mostly at  $pH > 7$  [42]. The presence of necrotic tissue and devitalized tissue in the wound causes an increased metabolic load on the wound resulting in tissue hypoxia [43]. Maintaining acidic environment can reduce the protease activity.

The pH environment also influences oxygen release to the tissues. Oxygen delivery to injured tissue especially in the chronic wound is dependent not only on perfusion but also on diffusion [43]. If pH surrounding the wound is lowered by 0.6 units releases almost 50% more oxygen and a five-fold increase in release of oxygen by a shift of 0.9 pH units [36].

#### **Oxygen Permeability:**

Oxygen is important for cell metabolism, especially energy production by means of ATP, and is critical for nearly all wound healing processes. Increase in oxygen permeability, increases rate of epithelial cell growth. The oxygen permeability must achieve balance; at early stage of wound healing, low oxygen is required for angiogenesis and formation of granulation tissue, whereas in later stage more permeable dressings are essential for epithelial growth and to limit the production of granulation tissue.

Oxygen permeable wound dressing prevents wounds from infection, stimulates angiogenesis, increases keratinocyte differentiation, migration, and re-epithelialization. It

also enhances fibroblast proliferation and collagen synthesis, and promotes wound contraction [44], [45]

### **Moist Environment**

Understanding of the role of occlusion in wound healing has been an important factor in the evolution of modern wound dressings and has created a major shift in wound management. Prior to this, wounds were often kept dry [46]. Winter [15] reported the effect of occlusion on rate of epithelialization in 1962. He compared surgically created wounds under two cases. One of them was left to heal open to air while other was occluded under transparent film. It was observed that the rate of epithelialization of wounds under occlusive dressing was twice that of wounds left to heal in open air. Occlusive dressings can limit the transmission of fluids, water vapor and gases from wounds. MVTR (Moisture vapor transmission rate) should be less than 35g of water vapor transmitted per square meter of dressing per hour. It is low enough to retain a moist environment on wound surface. [47]. A moist environment maintains slightly acidic pH and prevents desiccation, which leads to cell death. Moisture also facilitates epidermal migration, angiogenesis, and connective tissue synthesis [48] [49].

### **Non-Adherence:**

One of the important properties required of the ideal dressing is non-adherence to the wound. A dressing which adheres to the wound may cause the patient pain and removal may damage the regenerating epithelium [15]. Adhesion of dressings to wound is due to exudate which enters the dressing and dries. The dressing should have non adherence. The non-

adherent property can help to reduce pain at dressing changes and associated patient discomfort and anxiety [50].

## **2.4 Types of Wound Dressings**

A number of wound care dressings are now available depending on the characteristics of the wound and the practical needs of the patient. Below is a list of dressings and their characteristics.

### **2.4.1 Calcium alginates**

Calcium alginate can be highly effective for both wounds that have exudate (Incision, Laceration, and Abrasion) as well as deep cavity wounds (puncture) that have to be packed. It helps to keep tissues moist during the healing process. Non-adherent calcium alginate is available in fiber or nonwoven form. It requires tape or secondary dressing to adhere. It can be used in moderate to heavily exuding wounds [51].

### **2.4.2 Hydrofibers**

It is a wound dressing product that can absorb heavy exudates. These dressings does not have adhesive and need to be held in place by a secondary dressing. Hydrofibers keep the wound moist. There is only one manufacturer (ConvaTec) of hydrofibers at the moment [52,53].

### **2.4.3. Hydrogel Impregnated Gauze**

These products should be used in wounds that are mostly free of necrotic tissue and should not be used in wounds that are infected or in wounds that are creating moderate to

heavy exudates. The only disadvantage to the products is that a secondary dressing needs to secure the hydrogel products in place [54].

#### **2.4.4 Hydrogels:**

Hydrogel wound dressings are clear, viscous gels that protect the wound from desiccating. Application of hydrogels is not advisable when the wound is producing moderate to heavy exudates because if the wound is very wet, the presence of the hydrogel would contribute to wound maceration. Since most of the hydrogels do not contain antibacterial agent, application of those does no serve purpose if applied to infected wound. Hydrogels should be used as a primary wound dressing choice in wounds that are substantially or fully granulated. The use of a hydrogel is to keep the granulation tissue moist and help to autolytically debride the scab in the wound bed. It also acts as a barrier against wound contamination from external sources [13, 55, 56].

#### **2.4.5 Foams**

Foam dressings are highly absorbent primary dressings usually made of hydrophilic polyurethane foam. These dressings keep a moist wound environment but absorb the excess exudate sometimes seen in wounds. The foam dressings which are placed in deep wounds can remain for 3-4 days and must be secured in place by a biocclusive type dressing. Some of the foam dressing products has an adhesive backing at the margins of the dressing and therefore these cannot be packed into deep wounds. Foam dressings with adhesive backings are very useful for placing over wounds smaller than the absolute diameter of the dressing. Foams are not used over dry scab and they do not prevent periwound maceration in heavily exudating wounds [6,57].

#### **2.4.6 Transparent films:**

Moisture vapor permeable film dressings are adhesive film dressings that are waterproof but which are also semi-permeable to the passage of oxygen and water vapor to and from the wound site. These dressings prevent the wound from desiccation as well as from contamination by bacteria. They help maintain a moist wound healing environment and retain growth factors next to the wound bed that are in the exudate and transudate. These dressings also promote autolysis of necrotic tissue in the wound bed. These film dressings are translucent or clear and help the wound care clinician to visualize the wound. They can be placed over areas that are somewhat difficult to bandage because they are very thin, flexible and have an adhesive backing [58].

These dressings are good secondary dressings over wounds in areas where there may be a good deal of shear such as the elbows, heels, iliac crest, knees, and wrists. These dressings adhere better to apply over wounds that are producing light to medium exudate.

#### **2.4.7 Hydrocolloids:**

Hydrocolloid dressings contain a dressing matrix which absorbs exudate and creates a gel like dressing. The gel milieu may be retained inside the dressing where the matrix is located or the hydrocolloid gel may be formed in the wound. These dressings help the wound to autolytically debride necrotic tissues. The hydrocolloid dressing is impermeable to water vapor, oxygen and bacteria. These dressings are not adherent to the wound bed and can be removed without tearing the granulation tissue underneath. They are best applied to wounds that produce light to medium exudate. If the wound is not too wet, these primary dressings may remain in place for 3-4 days. These dressings can be placed on wet wounds and wet

surrounding skin and will remain intact because they can adhere to a moist area - a feature called wet tack.

These dressings should not be applied over infected wounds. They should not be applied over wounds that are producing moderately heavy exudate. These dressings can develop a foul odor to them after having been applied for 2-4 days. [59]

## **2.5 Application of Textiles in wound dressings.**

Textiles find an important place in wound healing applications because of their high surface area, absorbency, and variety in product forms. Various fabrics and nonwoven materials form the basis for wound dressings. Fibers used as wound care textiles are classified as biodegradable and non-biodegradable. Biodegradable fibers degrade in vivo within approximately 2-3 months [60]. Examples of such fibers are viscose, alginate, collagen, chitin, chitosan [61]. Synthetic fibers like polyamide, polyester, polypropylene, polytetrafluoroethylene take more than six months to degrade are non-biodegradable fibers [61].

Until relatively recently, there were few types of wound dressings, which mainly consisted of traditional dressings like cotton, lint, and other gauzes. As demands for wound dressings increased and synthetic fibers and films were approved for use in the human body, and new products started launching into the market. Because of their unique structure, biodegradability, biocompatibility and non-toxicity, researchers are concentrating on improving the properties of naturally available cotton, silk, chitosan, flax, hemp using enzymatic and advance biotechnological procedures to overcome their drawbacks. In electrospinning section (section 2.7), it is explained that if these biocompatible and biodegradable polymers

especially chitosan and silk are used in nanofibrous form they can help in improving the wound healing properties of the bandages mentioned. However nanofibers are inherently weak and difficult to handle. Other drawbacks include spinnability, lower mechanical strengths in the form of nanofibers. Being abundantly available in nature, studies on application of these polymers in wound dressing have been an area of focus for past couple of decades.

## **2.6 Polymers used in Wound Dressings**

Traditional cotton and viscose fibers can become entrapped in the wound developing discomfort during dressing removal. As said earlier, researchers are trying to impart novel function into the fibers so that along with their inherent properties they can possess antibacterial properties, better mechanical properties and drug delivery at the same time.

As it is accepted that moist environment improves healing, alginates [55] became one of the prime materials for wound dressings. Alginates can absorb greater amounts of wound exudates than traditional dressings. The gelling of the alginate after absorption of wound exudates maintains wound moisture. Alginate fibers are non-toxic, non-carcinogenic, non-allergic, hemostatic, biocompatible, capable of being sterilized and are of reasonable strength. Calcium alginate [62] fibers can be used as drug carriers in medical wound dressing. Different types of alginate wound dressings material have been manufactured commercially and are being utilized in market. They are as shown in Table 2.2 and have been reviewed widely in literature [63].

Table 2.2 Alginate-based wound dressings commercially available in the market [63]

<b>Product</b>	<b>Manufacturer</b>
AlgiDERM	Bard
AlgiSite	Smith & Nephew, Inc.
Algosteril	Johnson & Johnson
CarraSorb H	Carrington
CURASORB	Kendall
CURASORB Zinc	
Dermacea	Sherwood-Davis & Geck
FyBron	B. Braun
Gentell	Gentell
Hyperion Advanced Alginate Dressing	Hyperion Medical, Inc.
KALTOSTAT	ConvaTec
KALGINATE	DeRoyal
Maxorb	Medline
PolyMem	Ferris Mfg.
Restore	Hollister
SORBSAN	Dow Hickam
SeaSorb	Coloplast Sween Corp.
Tegagen HG	3M Health Care
Tegagen HI	

Unfortunately, these wound dressings are quite costly (e.g. Tegagen HG: \$40.71). Other natural polymers such as chitin, chitosan, silk, Branan ferulate, Hyaluronan, and collagen are also gaining popularity in modern wound dressing.

Hyaluronan is component of extra-cellular matrix such as skin, synovial joints and periodontal tissues. It is also a key component of chronic wounds during each stage of the wound healing process, including the inflammatory, granulation and re-epithelialization stages [64]. However, direct use of hyaluronan has limitations because of solubility, rapid resorption and short tissue residence time. Hyaluronan derivatives including fibers, membranes, sponges, microspheres, show potential in use in medical textiles. Hydrogel films

[56] can be made from hyaluronan and chondroitin sulphate by chemical modification and have an application as bio-interactive dressings.

Proteins such as collagen, gelatin, casein, zein, and elastin are widely used in the production of medical textiles. Collagen is most abundant protein found in mammals, comprising 25% of the total protein and 70% to 80% of skin (dry weight). Collagen has been used for sutures for many years. It can control the biodegradation rate and is also biocompatible and highly pure. Collagen materials [65] are used in scaffolds for tissue culture, wound healing. A hybrid chitosan-collagen matrix [66] may have potential biological and mechanical benefits for use as a cellular scaffold. Collagen is absorbed in tissue through catabolic processes including degradation with extracellular collagenolytic enzymes and phagocytosis. Resorption control of the collagen biomaterial is essential in wound dressing. Synchronization of collagen resorption and tissue regeneration rates is important for obtaining satisfactory regeneration. Introducing cross-linking is effective in the reduction of the resorption rate [67].

Amongst all these polymers, bioactive polymers are receiving more attention. Such bioactive polymers/fibers show great potential in applications such as wound dressings, because of their good biocompatibility and physical properties [68]. Bioactive fibers [60] can be manufactured from synthetic polymers and their properties can be improved by introducing antibacterial properties, biocompatibility, sterilizability to them which can avoid transmission of diseases and infections. Bio-active materials are capable of prompting specific cellular responses and directing new tissue formation mediated by biomolecular recognition. This can be manipulated by altering design parameters of the material [69].

## 2.7 Electrospinning

Electrospinning was first patented by Formhals [70] in 1934. Since then, electrospinning has been widely investigated. Electrospinning is a process in which high voltage is used to produce an interconnected membrane like a web of small fibers [71]. The electrospinning process is used to make fibers with high surface areas and diameters ranging from nanometers to microns.

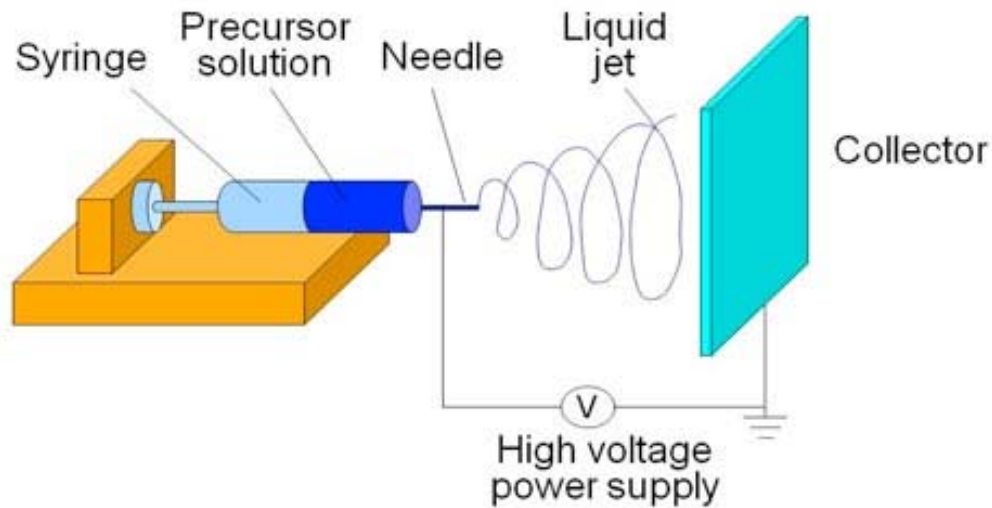


Figure 2.4. Schematic view of a typical electrospinning set-up [72]

An electrospinning system consists of three separate devices; a high voltage supply, an extrusion pump and a collecting device which can be of any shape. A typical electrospinning set-up is shown in Figure 2.4. The extrusion pump consists of a syringe, which holds the polymer solution. One of the metal electrodes from the high voltage supply is in contact with the solution, which serves as the positive terminal. The other end of

electrode, the negative terminal, is fixed to a collector which collects the fibers produced. In this process, the polymer solution is charged to a very high electrical potential. Because of the electric field, charge is induced on the liquid surface. High voltage overcomes the surface tension of the polymeric solution and produces very fine charged jets of liquid which are extruded from the needle tip towards a grounded or negatively charged collector plate. As the electric field increases, the solution at the tip of the capillary tube extends to form a cone like structure, which is also known as the Taylor cone (Figure 2.5) [73].

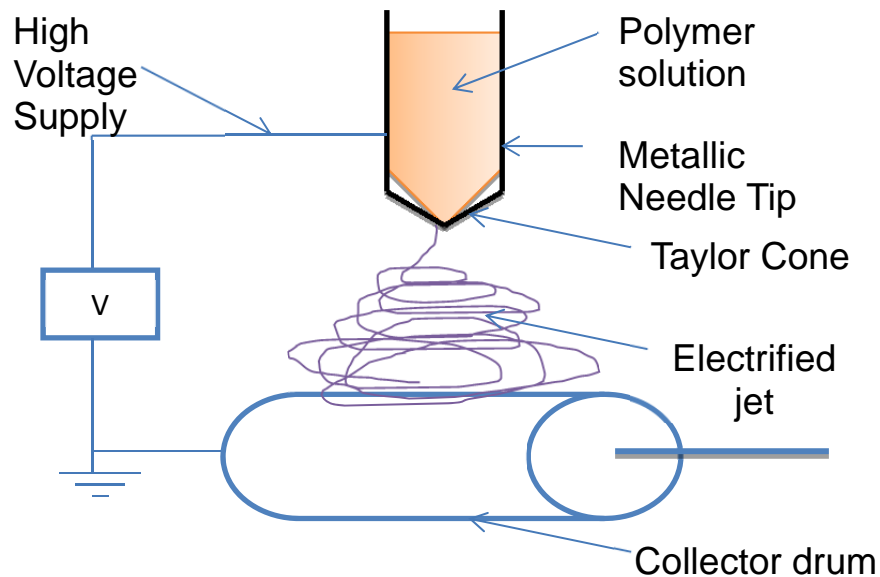


Figure 2.5 .Formation of Taylor Cone and subsequent splaying of fibers

As the intensity of the electric field is further increased, the field reaches a critical point value at which the opposite polarity between the terminals overcomes the surface tension force. At this point a charged jet of the solution is ejected from the tip of the Taylor

cone. Once the force acting on the polymer solution becomes greater than the surface tension, the charged droplet becomes unstable and this instability results in the formation of a charged jet. As this charged jet moves in the air, the solvent evaporates, leaving behind a charged polymer fiber, which lands on a collecting plate [74]. The collection can either be random or oriented depending on the motion of the collector plate. So, fiber formation is due to the instability created by the repulsion between similar charges and continuous fibers are collected as a web or mat. Diameters of these fibers range from nanometers to sub-micron. The nanofibrous web structures have excellent moisture vapor transport, extremely low air permeability, and offer good aerosol particle protection [71]. Material, Process and environmental parameters affect the properties of the resultant nanofiber web. Material parameters include viscosity, conductivity, concentration, solubility, molecular weight and surface tension. Process parameters include high voltage applied between needle and collector plate, distance between them and extrusion rate of solution. Ambient parameters incorporate temperature and relative humidity [75].

### **2.7.1 Applications of Nanofibers in Biomedical/ Biotechnology**

Polymer nanofibers are used in a variety of applications, including filtration, protective clothing, biomedical applications such as wound dressing and drug delivery systems, design of solar sails, light sails and mirrors for use in space, structural elements in artificial organs and in reinforced composites [76]. The progress of research in polymer nanofiber is increasing, because of its use in biomedical and biotechnological applications. Literature shows immense study on the use of polymers nanofibers for application such as Wound Dressing, Medical Implants, and Nanocomposites for Dental restoration, molecular

separation, biosensors and preservation of bioactive agents as shown in Figure 2.6 [5]. In this research, we will be focusing on application of nanofibers in wound dressing.

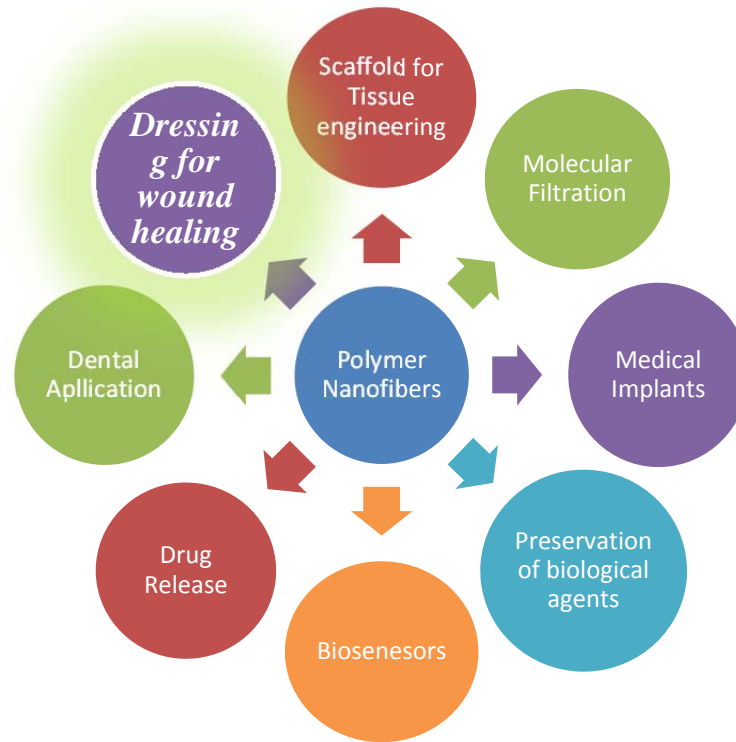


Figure 2.6. Use of polymer nanofibers for biomedical and biotechnological applications.

Though the progress is in early stage, researchers are trying to use polymer nanofibrous membranes for wound dressing. Researchers worked to generate fibrinogen/chitosan/silk/collagen nanofiber mats for potential use as a wound dressing or hemostatic bandage. The collagen nanofibers were characterized by high porosity, excellent mechanical strength, and high surface area-to-volume ratios. These characteristics are favorable parameters for cell attachment, growth, and proliferation [77]. Fibrinogen is a part of blood plasma and plays an important role in wound healing. Bowlin's research groups studied the mechanical

characteristics of electrospun fibrinogen which strongly supported its potential use as scaffold or wound dressing [78]. It was dissolved in 1,1,1,3,3,3-hexafluoro-2-propanol (HFIP) and electrospun into nanofibers of diameters ranging from 80 to 700 nm [79]. Silk fibroin nanofibrous membranes were studied for their cytocompatibility and cell behavior of normal human keratinocytes and fibroblasts cultured onto membranes [80]. In another report, the electrospun nanofibrous polyurethane membranes were studied in-vivo (pig model) as dressings with fiber diameters ranging from 250 to 300 nm [81]. The benefits of using electrospun nanofibrous mat for wound dressing applications are discussed in the following sections.

#### **2.7.1.1 Hemostasis**

Small interstices and high surface areas are characteristics of electrospun nanofibers and can promote hemostasis [79]. Instead of using a hemostatic agent, hemostasis can be achieved from the physical features of the nanofibrous dressings.

#### **2.7.1.2 Absorption of Exudates from Wound**

Because of small interstices and high surface area to volume ratios, nanofibers of particular polymers have demonstrated water absorption of between 17.9 to 213%. If films of the same polymer were used; it showed water absorption of 2.3% [82] [5]. Thus, if nanofibers are employed, the dressings will be able to absorb wound exudates more efficiently than film dressings.

#### **2.7.1.3 Maintaining Moist Environment and Permeability**

The nanofiber mesh-like structure of dressing is porous and good for the respiration of cells making it suitable for cell viability and cell proliferation. Wound dressings made up of

nanofibers can absorb the wound exudates and avoid wound desiccation[81]. This ensures a moist environment for the wound which is favorable for wound healing. Apart from these major functions, the small pore size can of nanofibrous membrane effectively protects the wound from bacterial infection. Electrospun nanofibrous membrane wound dressings can also provide high gas permeation apart from giving effective protection against infection and dehydration [81] .

#### **2.7.1.4 Controlled Drug Release**

Polymer nanofibers can be used for controlled drug release in topical (skin surface) application [83]. Depending on the stage of wound treatment and functionalities required to heal the wound, antiseptics, antifungals, vasodilators which are used to promote epithelialization, growth factors such as fibroblast growth factor (FGF), epithelia growth factor (EGF), etc. and cells like keratinocytes can be added into the polymer nanofibrous structures [84]. If a multilayered nanofibrous structure is used all of these above mentioned functions can be imparted into one wound dressing. This would reduce the damage to newly formed tissue on the wound caused by frequent changing of dressings.

#### **2.7.1.5 Comfort and Flexibility**

Wound dressing if applied on wound should provide a comfort to the patient. Nanofiber being very fine in diameter provides higher flexibility and can adjust on any type of wound. The dressing should have properties of adaptability, compliancy and should be able to conform to the contour of the dressing. Nanofibers wound dressing would be an excellent option to fit to complicated 3-D contours [85]. Therefore, dressing materials made of

ultrafine fibers can provide excellent conformability and thus result in better coverage and protection of the wounds from infection.

## **2.8 Selection of Polymer for Wound Dressings from Various Biocompatible and Biodegradable Polymeric Materials**

Biocompatible and biodegradable polymeric materials are best options to be used in various biomedical applications such as wound dressing, controlled drug delivery, etc. Researchers have used synthetic biomaterials, various non-degradable as well as natural polymers for the same. Synthetic biomaterials include polylactic acid (PLA), Polyglycolic acid (PGA), polylactic-co-glycolic acid (PLAGA), polycaprolactone, polydioxanone and polyphosphazene which are mainly used for scaffold fabrication [86]. Non-biodegradable material includes polyester, polypropylene, polytetrafluoroethylene, polyethylene, polycarbonates [87]. These synthetic polymers have advantages of being available in bulk and having good tailorable properties. On the other hand they lack cell recognition signals and sometime their degraded product may results in toxic substance. Therefore, it is always safe to use natural materials like collagen, elastin, keratin, silk, fibrin clot, chitosan, and mussel protein in biomedical application. They form ideal candidates for use in scaffolds fabrication. Main advantage of using natural polymer over synthetic polymer is that they have favorable cell interaction and non-toxic degradation products. Natural material still have some disadvantages of limited supply and restricted design flexibility [88]. In case of collagen, it was shown that many mouse strains produce a vigorous humoral immune response to type II collagen [89].

In this work, we will focus on polymers addressing bioactivity, barrier properties, tissue scaffolding. Bioactive/healing and tissue scaffolding nanofibers have been created from natural (collagen, fibrinogen, chitosan, silk, gelatin) and synthetic (poly-alpha-hydroxy acids) polymers. Additionally, ceramics or combinations of polymers and ceramics have been shown to be highly effective hemostatic agents. Polyurethanes have been used as barrier enhancing nanofiber layers. After studying the properties of these above mentioned polymers, it was decided to focus on chitosan and silk.

## **2.9 Silk**

Silk is a typical natural macromolecule spun by the silkworm (*Bombyx mori*) or spiders and has remarkable mechanical properties. It consists of primarily two types of proteins, fibroin and sericin [80]. Silk fibers have been used for centuries in the form of sutures. Silk fibroin (SF) can be prepared by removing the outer sericin of silk fibers using anhydrous sodium carbonate solution at an appropriate temperature. Silk has been used in manufacturing of a variety of biomaterials, such as gels, sponges, artificial membranes and films, pharmaceuticals and bio-medicals, healing of wound and post-surgical trauma, anti-oxidative and bio-adhesives, for medical applications. Silk finds use in many biomedical applications and biotechnological fields because of its excellent mechanical strength, biocompatibility, high oxygen, water, and drug permeability and resistance against enzymatic degradation [90]. These properties of silk contribute to its various biomedical applications such as surgical sutures, skin treatments, enzyme immobilization, wound dressing, controlled drug-delivery, and scaffolds for tissue engineering[91][90]. Silk fibroin matrices formed by electrospinning can improve the adhesion, growth and proliferation of the cells [92]. Silk fibroin has been used in-vitro, in-vivo, including wound healing and in tissue engineering of bone, cartilage, tendon, and ligament tissues.

### **2.9.1 Electrospinning of Silk Fibroin (SF)**

Jeong et al. studied the surface characteristics of O<sub>2</sub> or CH<sub>4</sub> plasma treated electrospun SF nanofibers. They observed that hydrophilicity of SF nanofibers was increased significantly when treated with O<sub>2</sub> plasma whereas decreased slightly when treated with CH<sub>4</sub> plasma. Cell culture study showed that the O<sub>2</sub>-treated SF nanofibers had significantly higher

level of cell attachment on days 1 and 3 than the corresponding pure SF and CH<sub>4</sub> plasma-treated SF nanofibers, for both normal human epidermal keratinocytes (NHEK) and normal human epidermal fibroblasts (NHEF) (Figure 2.7). Author believed that this difference in cellular activity might be due to the hydrophilicity of the SF nanofiber surface, especially when treated with O<sub>2</sub> plasma. Controlling the surface properties of nanofibrous structures can be useful in designing novel extracellular matrices for tissue engineering applications [93].

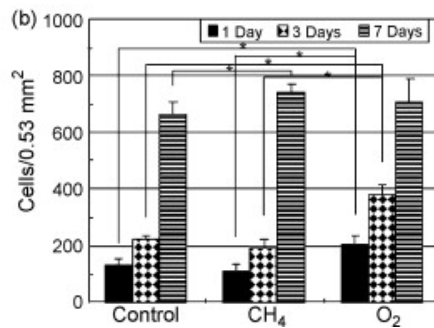
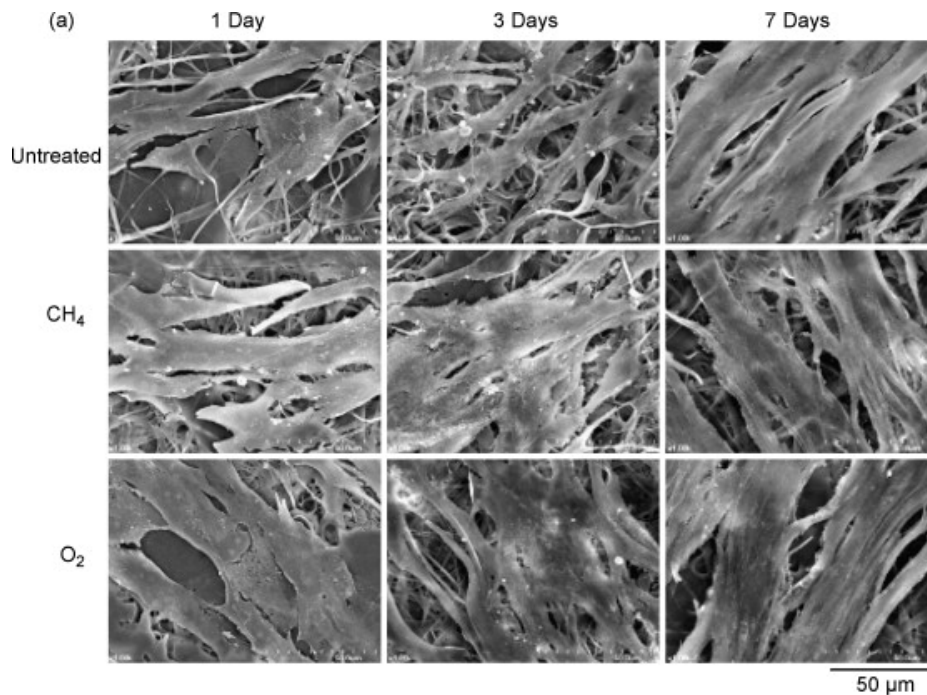


Figure 2.7. Cell attachment and spreading of normal human fibroblasts plated onto SF nanofibers. (a) SEM images of the interaction between the NHEF and SF nanofibers. (b) Level of cell spreading of the NHEF plated onto the SF nanofibers [93].

Researchers electrospun silk fibroin/PEO blended fibers and studied adhesion, spreading and proliferation of human bone marrow stromal cells (BMSCs) on them. Initially, residual PEO inhibited cell adhesion. However, within 1–2 days after PEO extraction, proliferation of BMSCs started. After 14 days of incubation, silk nanofibrous structures supported extensive BMSC proliferation and matrix coverage [90].

In another work by Kim et al., MTT assay was carried on the silk fibroin nanofibrous membrane after 4, 7, and 14 days. As it can be seen in Figure 2.8, the cell numbers were increased with increase in culture periods [94].

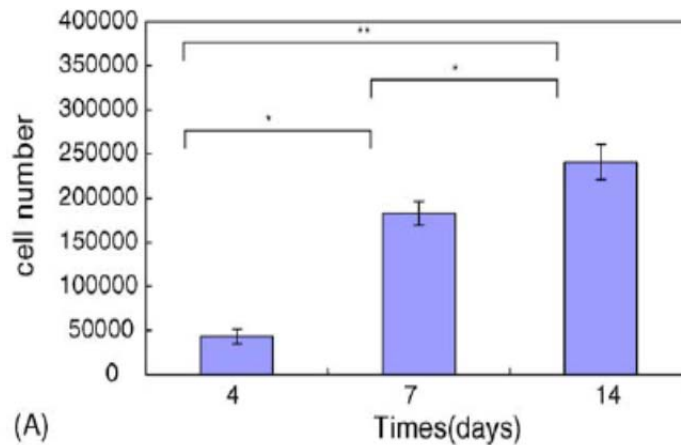


Figure 2.8. The proliferation of cells grown on the SF nanofiber membranes after different culture periods. MTT absorbency at 540 nm of cells on SF nanofibrous membranes were measured and viable cell numbers determined from standard curve [94]

Park et al studied attachment and spreading of NHEK and NHEF on chitin/SF blend nanofibers [95]. They observed that as the silk fibroin content in the blend increased, the attachment of NHEK onto the chitin/SF blend was increased and was almost similar to that of pure SF nanofibers (figure 2.9 A and B). Whereas in case of spreading of NHEF, both the pure chitin and pure SF nanofibrous adhesion was similar to that of polystyrene and the blended structure had little higher amount of cell adhesion than that of pure chitin and pure SF structure. Figure 2.9 C shows that lowest cell spreading for NHEK was observed in case of pure chitin. As SF content increased the cell spreading on blended structure gradually decreased. The one with 75% chitin and 25 % SF blend showed equal cell spreading as that

of pure SF nanofibrous structure and that remained highest in all combinations. In case of NHEF, blend containing 75% chitin and 25% SF nanofibers showed promising and higher cell spreading. The authors also mentioned that this particular blend concentration has a biomimetic three-dimensional structure which resembles collagen-GAG's composite structure in extra cellular matrix and as it can be seen from the graphs that it is an excellent option for cell attachment and spreading for NHEK and NHEF.

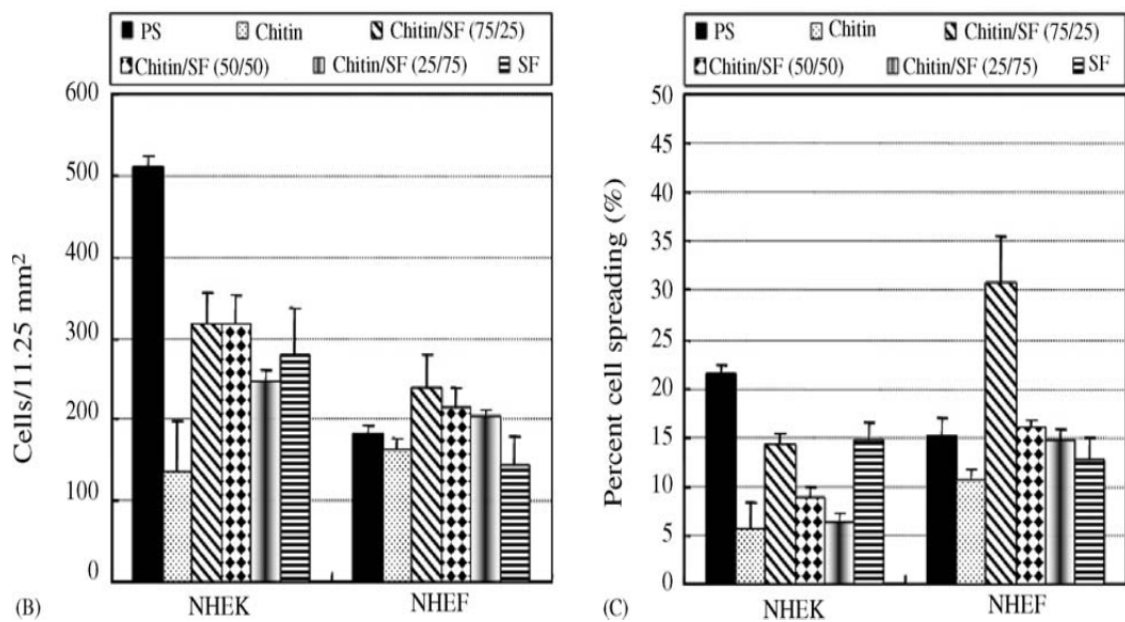
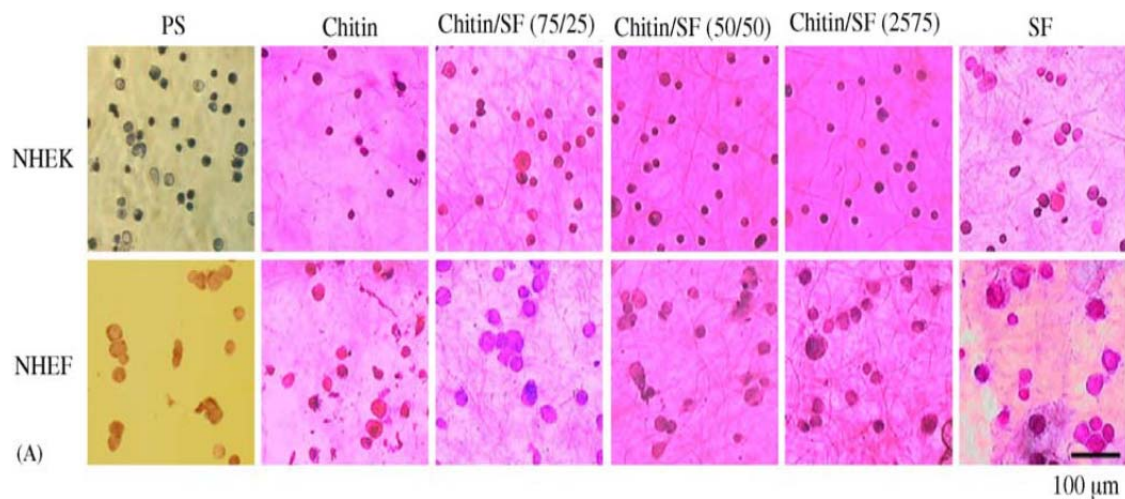


Figure 2.9. (A) Photographs and (B) the numbers of NHEK and NHEF adhered to chitin/SF blend nanofibrous matrices. (C) Percentage of cell spreading for NHEK and NHEF plated onto chitin/SF blend nanofibrous matrices. Data are expressed as mean  $\pm$  S.E. ( $n = 4$ ). PS, polystyrene surface.[95]

## 2.10 Chitosan

Antibacterial nature, biodegradability and biocompatibility make chitosan an interesting polymer for biomedical applications. It is obtained from the chitin, which is second most abundant natural polysaccharide after cellulose. Sources for chitin are shells of crabs, crustaceans, shrimp and lobster, insects, for example the wings of butterflies, also jellyfish, algae, fungi. Chitin products are anti-bacterial, anti-viral, anti-fungal, non-toxic, and non-allergenic [96]. However usage of chitin in medical textile has limitations [97] because it is not readily soluble in common solvents. It is usually converted to its deacetylated derivative i.e. chitosan [97]. Degree of deacetylation (DD) is a percentage measurement of free amine groups along the chitosan backbone [98]. When chitin is deacetylated over about 60% it becomes soluble in dilute aqueous acids and is referred to as chitosan. Chitosan is preferred over chitin in various fields because of its solubility in acidic, neutral and alkaline solutions, (Novel chitin and chitosan nanofibers in biomedical applications). Chitosan has applications in variety of areas, such as pharmaceutical and medical applications, paper production, textile dyeing and finishing, fiber formation, wastewater treatment, biotechnology, cosmetics, food processing, and agriculture [99].

Chitosan-based hemostatic wound dressings have greater advantages over the other commercially available hemostatic dressings because of their inherent properties as mentioned above. The commercially available chitosan hemostatic dressing is relatively expensive (approximately \$50-\$100 per unit) [32].

### **2.10.1 Electrospinning of chitosan**

Chitosan is soluble in most acids. However, electrospinning of chitosan is difficult because protonation of chitosan changes it into a polyelectrolyte in acidic solutions. This is due the repulsive forces between ionic groups within the polymer in an electric field which restricts the formation of continuous uniform nanofiber and can result in formation of beads [80]. There are a few reports on the effects of polyelectrolytes on electrospinning of polymer solutions [100][101].

#### **2.10.1.1 Chitosan blends**

Due to difficulty in electrospinning, chitosan is typically electrospun along with synthetic biodegradable polymers such as polyethylene oxide (PEO), polyvinyl Alcohol (PVA), polyvinylpyrrolidone (PVP), Poly-lactic acid (PLA) and Polyethylene Terephthalate (PET) etc. Additionally, blending chitosan with another polymer was shown to impart improvements in mechanical, biological and other properties to the chitosan nanofibers.

##### **a. Chitosan with Polyvinyl alcohol**

Polyvinyl alcohol (PVA) is used for a variety of biomedical applications such as bone implants and artificial organs [102][103].. Many authors describe electrospinning of composites of chitosan and PVA [104, 105, 106] and their biomedical applications.

Chitosan can be used to reduce the defects in electrospinning such as formation of beads. Since chitosan is a cationic polyelectrolyte in nature, when added to a solution, it increases the conductivity of the solution. thereby reducing the diameter of resulting fibers [107]. It

acts as thickener when added to an aqueous electrospinning solution of polymers such as PVA.

**b. Chitosan with Polyethylene Oxide (PEO)**

PEO is also a biocompatible polymer that has been used as a wound dressing and for cartilage tissue repair [108][109]. Reports indicate [101] that nanofibers obtained by the electrospinning of chitosan/PEO solutions showed decreases in diameter with increases in chitosan concentrations in the blends.

Bhattarai et al. studied electrospinning of Chitosan/PEO blends and cellular compatibility of nanofibers in tissue engineering [109]. At first, a 90/10 ratio of chitosan/PEO did not produce fibers and resulted in short fibers containing a considerable amount of beads. When Triton X-100TM was introduced in electrospinning solution as a surfactant, uniform nanofibers were obtained. Nanofibers obtained from this particular concentration promoted good adhesion of chondrocyte and osteoblast cells.

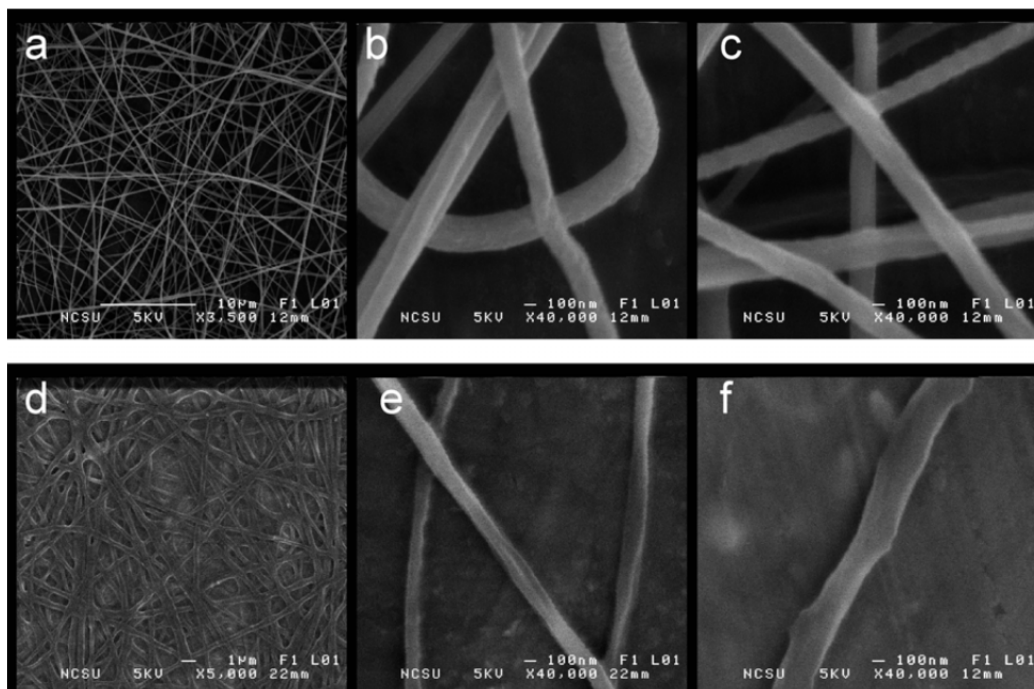


Figure 2.10. SEM images of electrospun chitosan-PEO core-sheath nanofibers. (A-C) Samples before H<sub>2</sub>O rinse and (D-F) samples after H<sub>2</sub>O Rinse [110]

Gorga and Ojha reported sheath-core nanofibrous structures of PEO (sheath) and chitosan (core) [110]. PEO was used as a template to produce chitosan nanofibers by washing the PEO with water. SEM images showed that the overall core and sheath structure before washing had diameters of  $\sim 250$  nm and pure chitosan nanofibers obtained after washing with water had diameters of  $\sim 100$  nm (Figure 2.10).

### c. Chitosan with Polyethylene Terephthalate (PET)

PET is widely used in the textiles and plastics industries. Jung et al. reported electrospinning of a blend of Chitosan/PET and chitin/PET in a Trifluoroacetic acid/Hexafluoro-2-propanol (TFA/ HFIP) solution [111]. After comparing antibacterial

activity studies, it was observed that the chitosan/PET nanofibers inhibited the growth of bacteria much more effectively than both the pure PET and the chitin/PET fibrous mats.

#### **d. Chitosan with Collagen**

Polymers of type I and type III collagen are the main structural elements of extracellular matrix (ECM). Collagen has been used in a variety of tissue engineering applications. Collagen–chitosan complex nanofibers were prepared for the first time using electrospinning[112]. Chen et al used the mixed Hexafluoropropylene/ trifluoroacetic acid (HFP/TFA) (v/v, 90/10) as a solvent for electrospinning. It was found that the diameter of composite nanofibers decreased with increasing chitosan/collagen ratio and vice-versa. In another work by Chen et al.[113] electrospun composite nanofibrous membranes of type I collagen, chitosan, and polyethylene oxide and then cross-linked the fibers using glutaraldehyde vapor. The diameter of composite nanofibers was increased from  $134\pm 42$  nm to  $398\pm 76$  nm after cross-linking. It was found that the Young's modulus of nanofiber was increased after cross-linking, whereas the tensile strength, tensile strain, and water absorption properties were found to be decreased.

#### **e. Chitosan with Silk**

Park et al [91] tried electrospinning of pure chitosan in formic acid. However, electrospinning of pure chitosan was not possible. Electrospinning of silk fibroin/chitosan (SF/CS) blend was carried out using formic acid as a solvent. It was concluded that in order to get continuous fibrous structure, SF/CS blends should contain up to 30% of the CS. . With the addition of chitosan component, the diameter of blended structures gradually decreased

~100nm. Authors attributed this behavior to the increase in solution conductivity by the addition of an ionic CS component

### **2.10.1.2 Pure Chitosan Nanofibers**

Trifluoroacetic acid (TFA) is the main solvent for successful electrospinning of chitosan [114], because the amino groups of the chitosan can form salts with TFA and destroy the rigid interaction between chitosan molecules during electrospinning. Successful electrospinning of chitosan nanofibers was reported by Ohkawa in 2004 [115]. This study focused on the effect of the chitosan concentration on the morphology of the resulting nanofiber structure. A linear relationship between the chitosan concentration and the diameter of the nanofibers was demonstrated. The solvents tested were diluted hydrochloric acid, acetic acid, formic acid and TFA. The morphology of the chitosan nanofibers changed from beaded to interconnected nanofibrous structure with an increase in chitosan concentration. They also mentioned that the addition of dichloromethane to the chitosan/TFA solution improved the homogeneity of the electrospun chitosan fiber. Chitosan fibers with a mean diameter of 330 nm were obtained.

Schiffman and Shauer performed mechanical analyses on glutaraldehyde cross-linked chitosan nanofibers [116]. It was observed that the solubility of chitosan nanofibers was improved whereas the Young's modulus of cross-linked chitosan nanofibers ( $150.8 \pm 43.6$  MPa) was decreased as compared to as-spun fibers ( $154.9 \pm 40.0$  MPa). They also observed increased diameter in the cross-linked chitosan nanofibers.

Other solvents such as trichloromethane and acetic acid have been used to electrospin chitosan [96,117]. Uniform chitosan nanofibers were obtained by electrospinning 7% chitosan in 90% acetic acid solution. However, the nanofibers obtained showed large diameter distribution and presence of beaded structures.

However, studies related to adhesion of chitosan/SF nanofibers to substrate, strength of chitosan nanofibers, effects of plasma treatment on mechanical properties of chitosan/SF nanofibers are not reported yet.

## 2.11 Plasma

Plasma is defined as fourth state of matter. It is an ionized gas consisting of both charged and neutral species including electrons, free radicals, and meta-stable excited species, molecular and polymeric fragments. It is created by applying energy to a gas or mixture of gas to produce excited species and ions. This energy can be thermal, electric current or electromagnetic radiation [118]. Plasma has found applications in different fields including the electronics industry, manufacturing of computer chips, semiconductors, machine tools, medical implants, and integrated circuits [119]. Plasma technology is considered as a solution for environmental problems in textile processing. Rapid development and commercialization of plasma technology has been occurred in past few years. The main advantage of plasma treatment is that it is able to change substrate surface properties at nano-level without affecting the bulk property. Plasma can be used to modify the surface to make it hydrophilic, hydrophobic, charged, etched, grafted or multi-functional [120,121]. Plasma finds many applications in the textile industry such as desizing, flame retardant finish, sterilization, adhesion enhancement, dye-ability enhancement, etc. and significantly reduces toxic-chemical pollution.

Plasma is a gas of charged particles which consists of equal numbers of free positive and negative charge carriers. There are three requirements which a system should fulfill to be classified as “plasma”; 1) the quasi-neutrality, 2) the collective behavior and 3) the motion of the plasma charged particles controlled by electromagnetic forces.

Quasi-neutrality is when an equal number of electrons and ions coexist, which takes place when the gas dissociates and ionizes to give rise to ions and electrons which are equal

in number. Debye shielding gives the plasma its quasi neutrality. In Debye shielding charged particle will attract equal amounts of charged particles of opposite sign. If a positive charge is placed within plasma it becomes surrounded by electrons which form a shield around the positive charge at a certain distance, known as the Debye Length. Because of this shielding the bulk plasma is not affected by the presence of the positive charge. It is necessary that the length of plasma is greater than the length of the Debye shield for Debye shielding to occur.

Collective behavior occurs when the plasma particles are influenced by their immediate surroundings as well as by the regions which are significantly distant [120] [122]. Each particle is attracted or repulsed by surrounding charges, which results in a lot of motion within the plasma. The motion of these particles is controlled by the collisions amongst them and can generate electrical currents and magnetic fields.

Plasma must also have a sufficient degree of ionization. The amount of ionization is a combination of two factors, the collective behavior and the collision times between ionized particles and neutral gas. If  $\omega$  is the frequency of plasma oscillations and  $\tau$  is the time between ion/neutral collisions, then the value of  $\omega\tau$  must be greater than or equal to 1 to classify an ionized gas as plasma [122-124] . The plasma frequency  $\omega$  is a sole function of the plasma number density,

$$\omega = \sqrt{(ne^2/m_e \epsilon_0)}$$

Where  $m_e$  is the mass of the electron where  $\epsilon_0$  is the permittivity of free space,  $k$  is Boltzmann's constant,  $e$  is the unit charge and  $n$  is the plasma quasi-neutral number density.

Plasma can be created by applying high voltage or sufficient energy to gas so as to induce ionization. This energy changes the structure of atoms or molecules to produce

excited ions and species. The energy used to induce plasma formation can be thermal, electrical, or electromagnetic. The plasma generates different properties in terms of electron number density and kinetic temperatures of both electron and ions. When electric energy is applied to working gas, the field breaks down the gas and induces ionization. The electrons then collide with the surrounding neutral species [125] and These collisions can either be elastic or inelastic or a combination of both. In elastic collisions the internal energy of the neutral species does not change and the colliding species maintain their individual identities. Inelastic collisions are more complex and the electronic structure of the neutral species gets modified generating excited species such as ions and free radicals after collision [126]. The colliding species and the individual identities of the species can be altered due to dissociation and recombination processes. The excited species have a very short life and de-excite to the ground state by emitting photons, which appears as optical emission spectra in the visible, ultraviolet and infrared spectra. Some species in meta-stable states may have longer lifetime and thus are maintained active in the plasma.

### **2.11.1 Application of Atmospheric Plasma in Textiles**

Plasma treatment is an economical, eco-friendly and effective method for improving the physical and mechanical properties of fibers and textiles. Treatment or surface modification of the textile surface with plasma requires minimum use of water and other chemicals. Plasma treatment is confined to a depth of few nanometers at the surface. Recently, work has been reported on atmospheric glow discharge plasma for treating polymeric materials in the form of fibers, films, fabrics, etc. The following section discusses the interaction of plasma with the materials.

### **2.11.2 Plasma-Polymer Interactions**

Plasma treatment of polymers may: i) improve surface bonding or adhesive ability,[120,127] ii) increase mechanical strength by cross-linking[127,128], iii) change fiber surface hydrophobicity[128], iv) roughen fiber surfaces [129], v) increase crystallinity [129]. Atmospheric pressure plasma treatments may be used to improve nanofiber mat durability by: i) enhancing the bonding between nanofiber mats and textile substrates through pre-deposition surface activation of textile substrates; and ii) improving the nanofiber strength and bonding through post-deposition cross-linking. We will be mainly focusing on increasing adhesion between nanofiber web and substrate. Earlier work of plasma treatment on fibers and increase in adhesion due to plasma treatment is explained in the following sections.

#### **2.11.2.1 Adhesion**

Adhesion is an important property in most of composite materials. Plasma treatment of polymers can create surface roughness, induce sub-surface cross-linking, or activate the surface available for cross-linking with another polymer. All three effects imparted by plasma treatment can help in increasing the adhesion of one polymer to another polymer substrate or increase the mechanical strength of the polymer itself. It is known that the composite material such as UHMPE (ultrahigh modulus polyethylene), PPTA (poly(p-phenylene terephthalate) and carbon fibers have excellent mechanical properties. However, their chemical inertness and smoothness of surfaces can be a serious problem to apply to resin matrix for composite applications. To remove these disadvantages of high performance fibers, plasma can be used to improve the adhesion between these fibers and resin matrix.

The plasma treatment can create micro-roughness on the surface of UHMPE fibers, resulting in a better mechanical interlocking of the fiber surface to resin matrix. Additionally, plasma treatment can enhance surface functionality, leading to chemical interfacial bonding between the fiber and matrix. Poly *p*-phenylene terephthalamide which is also known as Kevlar® has high stiffness, strength and thermal resistance and finds applications in spacecraft, aircraft, automobiles, military and sport products. However, Kevlar® fiber has restrictions on its uses due to the smooth surface resulting from high crystallinity. Great enhancement of the interfacial strength between Kevlar® and epoxy resin was shown by low-pressure plasma treatments using various gases (NH<sub>3</sub>, H<sub>2</sub>O, O<sub>2</sub>, Air and Ar) [130-133]. The plasma from these gases generated reactive chemical groups (-COOH, -OH, and -NH<sub>2</sub>) with epoxy resin and also created surface roughness to improve the adhesion between matrix and Kevlar®. Similar types of work have been done on carbon fibers with NH<sub>3</sub>, H<sub>2</sub>O, O<sub>2</sub> air and Ar/NH<sub>3</sub> gas plasma treatment. The following are the factors that would assist in adhesion after plasma treatment:

#### **2.11.2.2 Etching**

Etching creates roughness on the surface of the polymer which can increase the frictional forces between adjacent surfaces. Due to increase in frictional forces within the fibers the mechanical properties of the fibers gets improved. Plasma-etching removes organic contaminants such as oils and other production effluents via ablation [134]. These surface contaminants are usually polymers that can undergo abstraction of hydrogen with free radical formation and repetitive chain scissions as shown in Figure 2.11.

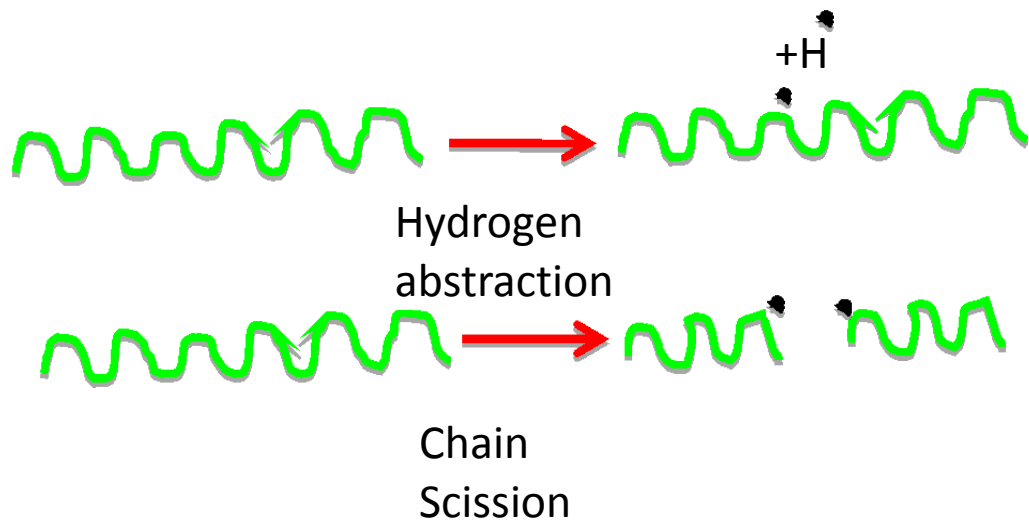


Figure 2.11: Plasma etching: Hydrogen abstraction and Chain Scission

Etching can be compared to an evaporation process, where free radicals, electrons and ions bombard the polymer surface and breaks the covalent bonds of the polymer backbone. This results in formation of lower weight polymer chains. During this conversion of long polymeric chains to short ones, the ablated volatile oligomer and monomer byproducts are swept away by the vacuum pump exhaust or feed gas.

### 2.11.2.3 Cross-linking on Surface

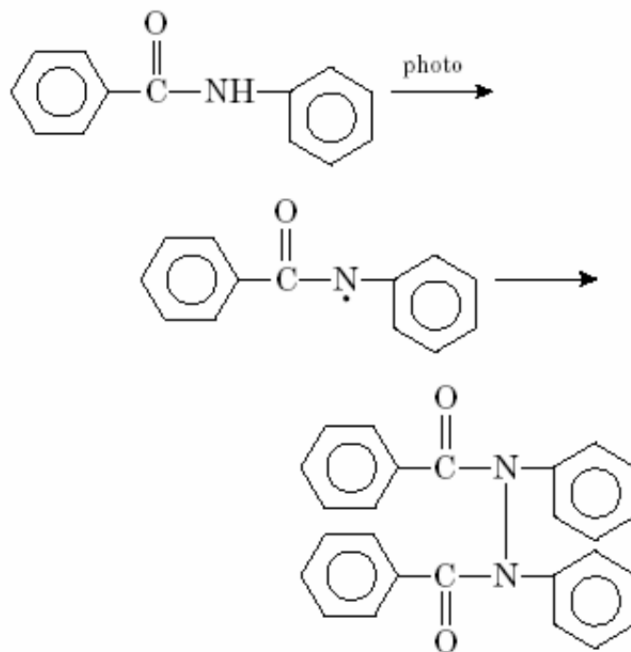


Figure 2.12. Possible Cross-linking Mechanism of Poly(p-phenylene terephthalamide) Film [135]

Wu et al. [135] studied the effect of oxygen plasma on the cross-linking mechanism of poly(p-phenylene terephthalamide) film (Figure 2.12). Author claimed that after treating Poly (p-phenylene terephthalamide) in oxygen plasma, the H in –CONH was substituted by other atoms or groups. After examining the changes of the spectra of ATR-FTIR, the water permeability, as well as the changes of chlorine resistance of the composite membrane, authors concluded that cross-linking between two poly(p-phenylene terephthalamide) occurred at nitrogen as shown in Figure 2.12. .

#### 2.11.2.4 Surface Activation

Surface activation in polymers occurs when they are treated with non-carbon containing gases such as oxygen, air, nitrogen, argon and helium [136-138][139]. The effect of plasma treatment on surface of polymer is the incorporation of different functional group of molecules of the process gas onto the surface. The polyethylene consists mainly of carbon and hydrogen on the surface. Once the surface is treated with plasma it may get activated and may result in formation of functional groups such as hydroxyl, carbonyl, peroxy, carboxylic, amino and/or amines (Figure 2.13). Based on these results it can be concluded that almost any fiber or polymeric surface can be modified to provide chemical functionality, enhancing the adhesion characteristics [139].

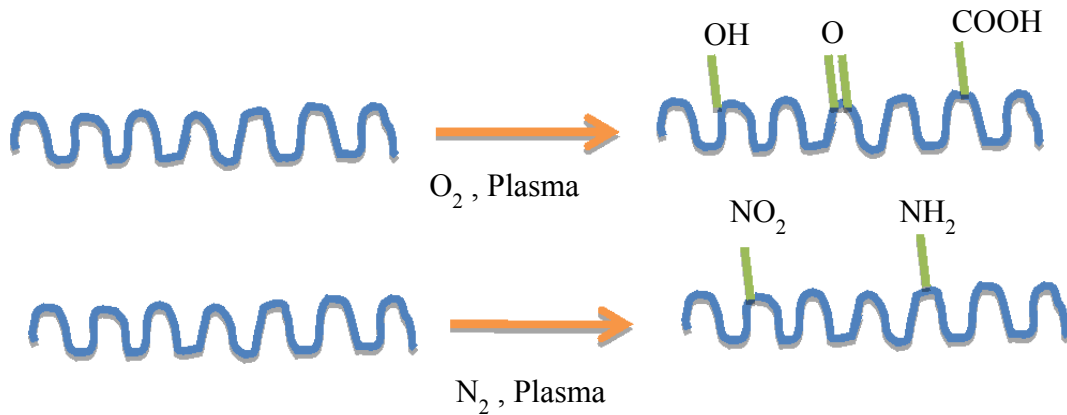


Figure 2.13. Surface activation by oxygen plasma and nitrogen plasma

#### 2.11.2.5 Enhancement in Mechanical Properties and Hydrophilicity

Huang et al reported that after treating the carbon fibers with oxygen plasma, the mechanical properties of their phenolic composition was improved. Also the interfacial

shearing strength (IFSS) of the composites was increased significantly [140]. It is well known that plasma treatment enhances the wettability i.e. hydrophilicity of the textile material. Studies have been carried out on different types of fibers and polymers with varying success. The plasma treatment introduces polar functional groups such as  $-\text{COOH}$ ,  $-\text{OH}$  and  $-\text{NH}_2$ .

Pandiyaraj et al [137] studied surface hydrophilicity and surface energy of grey cotton fabric after treating it in low pressure discharge plasma. It was observed that the surface hydrophilicity and surface energy were increased. The explanation given for this increase in hydrophilicity was due to the formation of polar groups on the surface of the fabrics. The reduction in contact angle was observed to be from  $130^\circ$  to  $0^\circ$ .

## 2.12 References

1. Thomas S. Wound and wound healing. First ed. : Pharmaceuticals Press, London, 1990.
2. Sorbalgon. <http://en.cn.hartmann.info/sorbalgon.php>.
3. MedLine Cotton Woven Gauze. <http://www.shopping.com/Medline-Medline-Cotton-Woven-Gauze-Sponges-Sterile-2-s-3-x-3-12-ply-Qty-of-80-Medline/info>.
4. Sterile wound dressing. <http://www.meghdootpharma.net/sterile-wound-dressings.html>.
5. Zhang Y, Lim C, Ramakrishna S, Huang Z. Recent development of polymer nanofibers for biomedical and biotechnological applications RID A-9865-2008 RID C-9542-2009. Journal of Materials Science-Materials in Medicine 2005;16:933-946.
6. Jørgensen B, Price P, Andersen KE, Gottrup F, Bech-Thomsen N, Scanlon E, Kirsner R, Rheinen H, Roed-Petersen J, Romanelli M, Jemec G. The silver-releasing foam dressing, Contreet Foam, promotes faster healing of critically colonised venous leg ulcers: A randomised, controlled trial. 2005;2:64-73.
7. Razzak MT, Darwis D, Zainuddin, Sukirno. Irradiation of polyvinyl alcohol and polyvinyl pyrrolidone blended hydrogel for wound dressing. Radiat Phys Chem 2001;62:107-113.
8. Jørgensen B, Friis GJ, Gottrup F. Pain and quality of life for patients with venous leg ulcers: proof of concept of the efficacy of Biatain®-Ibu, a new pain reducing wound dressing. Wound Repair and Regeneration 2006;14:233-239.
9. Flanagan M. Barriers to the implementation of best practice in wound care. 2005;1:74-82.
10. Molan P. Clinical usage of honey as a wound dressing: An update. 2004;13:353-356.
11. Pollack SV. Wound healing: a review. II. environmental factors affecting wound healing. 1979;5:477-481.
12. Field CK, Kerstein MD. Overview of wound healing in a moist environment. The American Journal of Surgery 1994;167:S2-S6.
13. Yoshii F, Zhanshan Y, Isobe K, Shinozaki K, Makuuchi K. Electron beam crosslinked PEO and PEO/PVA hydrogels for wound dressing. Radiat Phys Chem 1999;55:133-138.
14. Lionelli GT, Thomas Lawrence W. Wound Dressings. 2003;83:192-195.

15. Winter GD. Formation of the Scab and the Rate of Epithelization of Superficial Wounds in the Skin of the Young Domestic Pig. 1962;193:293-294.
16. Snowden JM, Kennedy DF, Cliff WJ. Wound contraction: the effects of scab formation and the nature of the wound bed. 1982;60:73-82.
17. Luomanen M, Meurman JH, Lehto V-. Extracellular matrix in healing CO2 laser incision wound. Journal of Oral Pathology & Medicine 1987;16:322-331.
18. Horan TC, Gaynes RP, Martone WJ, Jarvis WR, Emori TG. CDC Definitions of Nosocomial Surgical Site Infections, 1992: A Modification of CDC Definitions of Surgical Wound Infections. Infection Control and Hospital Epidemiology 1992;13:pp. 606-608.
19. Kuhn, F., Morris, R., Witherspoon, C.D., Heimann, K., Jeffers, J.B., Treister, G. A standardized classification of ocular trauma . 2007;234:399-403.
20. T. O. Diagnostic value of “superficial” stab wounds in forensic practice. J Clin Forensic Med 2005;12:32-35.
21. Burnsergery.com. [http://www.burnsurgery.org/Modules/BurnWound%201/sect\\_IV.htm](http://www.burnsurgery.org/Modules/BurnWound%201/sect_IV.htm); .
22. American Medical Association, HighWire Press, editor. The journal of the american medical association.
23. Puncture Wound. [http://www.emedicinehealth.com/puncture\\_wound/article\\_em.htm](http://www.emedicinehealth.com/puncture_wound/article_em.htm).
24. Diegelmann RF, Evans MC. Wound healing: an overview of acute, fibrotic and delayed healing. 2004;9:289.
25. Gosain, A., DiPietro, L.A. Aging and Wound Healing. 2004;28:321-326.
26. Broughton G. Wound Healing: An Overview. 2006;117:1e-S-32e-S.
27. Campos, A.C.L., Groth A. K., Branco, A. B. Assessment and nutritional aspects of wound healing. 2008;11:281-288.
28. Meszaros, A.J, Reichner, J.S, Albina, J.E. Macrophage-induced neutrophil apoptosis. 2000;165:435-441.
29. Mosser, D.M, Edwards, J.P,. Exploring the full spectrum of macrophage activation. 2008;8:958-969.

30. Murray MM, Martin SD, Martin TL, Spector M. Histological changes in the human anterior cruciate ligament after rupture.. 2000;82:1387-1397.
31. Hanson SR. Encyclopedia of biomaterials and biomedical engineering. : New York: Dekker Pub, 2004. p. 144-154.
32. Ina M. Develop a More Biodegradable/Biocompatible Hemostatic Fabric for Treatment of Bleeding Wounds. 2009.
33. Cuzzell J. Choosing a wound dressing. Geriatr Nurs 1997;18:260-265.
34. Miscavige M. Considering patient priorities when choosing a dressing. 2005;51:23-24.
35. Okan D, Woo K, Ayello EA. The role of moisture balance in wound healing. 2007;20:39-53.
36. Leveen H, Falk G, Borek B, Diaz C, Lynfield Y, Wynkoop B, Mabunda GA. Chemical acidification of wounds. An adjuvant to healing and the unfavourable action of alkalinity and ammonia. 1973;178:745-750.
37. Roberts, G., Hammad, L., Creevy, J., Shearman, C., and Mani, R. Physical Changes in Dermal Tissues Around Chronic Venous Ulcers. 7th European Conference on Advances in Wound Management. ;18:104-105.
38. Gethin GT, Cowman S, Conroy RM. The impact of Manuka honey dressings on the surface pH of chronic wounds. International Wound Journal 2008;5:185-194.
39. Tsukada, K, Tokunaga, K, Iwama, T, Mishima, Y. The pH changes of pressure ulcers related to the healing process of wounds. 1992;4:16-20.
40. Kaufman, T, Eichenlaub, E.H., Angel, M.F., Levin, M., Futrell, J.W. Topical acidification promotes healing of experimental deep partial thickness skin burns: a randomised double-blind preliminary study. 1985;12:84-90.
41. Hoffman, R, Noble, J, Eagle, M. The use of proteases as prognostic markers for the healing of venous leg ulcers. 1999;8:272-276.
42. Greener, B,, Hughes, A,, Bannister, N,, Douglass, J,. Proteases and pH in chronic wounds. 2005;14:59-61.
43. Hunt, T.K, Beckert, S. Therapeutical and practical aspects of oxygen in wound healing. 2005.

44. Bishop A. Role of oxygen in wound healing. 2008:399-402.
45. Rodriguez PG, Felix FN, Woodley DT, Shim EK. The Role of Oxygen in Wound Healing: A Review of the Literature. *Dermatologic Surgery* 2008;34:1159-1169.
46. Bradley M, Cullum N, Nelson EA, Petticrew M, Sheldon T, Torgerson D. Systematic reviews of wound care management: (2) Dressings and topical agents used in the healing of chronic wounds. 1999;3:1-35.
47. Bolton L, Pirone L, Chen J. Dressings' effects on wound healing. 1990;2:134.
48. Alvarez O. Moist environment for healing: Matching the dressing to the wound. 1988;21:64-83.
49. Barnett A, Berkowitz RL, Mills R, Vistnes LM. Comparison of synthetic adhesive moisture vapor permeable and fine mesh gauze dressings for split-thickness skin graft donor sites. *The American Journal of Surgery* 1983;145:379-381.
50. Clark R BS. SILVERCEL® Non-Adherent Made Easy. 2010;1:1-6.
51. Sorbson. <http://www.healthykin.com/p-3024-sorbsan-calcium-alginate-topical-wound-dressing.aspx>.
52. Coutts P, Sibbald RG. The effect of a silver-containing Hydrofiber® dressing on superficial wound bed and bacterial balance of chronic wounds. 2005;2:348-356.
53. Convatec Hydrofiber. <http://www.shopping.com/Convatec-Convatec-Aquacel-Ag-Hydrofiber-Dressing-With-Ionic-8-X-12-Pack-Of-5/info>.
54. Hydrogel Impregnated Gauze. [http://www.google.com/products/catalog?pq=3.%09hydrogel+impregnated+gauze&hl=en&ugexp=kjrmc&cp=0&gs\\_id=h&xhr=t&q=hydrogel+impregnated+gauze&tok=WxZ9L9yd2AvcFEzp4cUWOW&client=firefox-a&hs=Jin&rls=org.mozilla:en-US:official&gs\\_upl=&bav=on.2,or.r\\_gc.r\\_pw.r\\_cp.cf.osb&biw=924&bih=928&bs=1&um=1&ie=UTF-8&tbm=shop&cid=17613781017112569010&sa=X&ei=-5m1ToHKJ6Lm2AXinL3MDQ&sqi=2&ved=0CGAQ8wIwBQ](http://www.google.com/products/catalog?pq=3.%09hydrogel+impregnated+gauze&hl=en&ugexp=kjrmc&cp=0&gs_id=h&xhr=t&q=hydrogel+impregnated+gauze&tok=WxZ9L9yd2AvcFEzp4cUWOW&client=firefox-a&hs=Jin&rls=org.mozilla:en-US:official&gs_upl=&bav=on.2,or.r_gc.r_pw.r_cp.cf.osb&biw=924&bih=928&bs=1&um=1&ie=UTF-8&tbm=shop&cid=17613781017112569010&sa=X&ei=-5m1ToHKJ6Lm2AXinL3MDQ&sqi=2&ved=0CGAQ8wIwBQ).
55. Balakrishnan B, Mohanty M, Umashankar PR, Jayakrishnan A. Evaluation of an in situ forming hydrogel wound dressing based on oxidized alginate and gelatin. *Biomaterials* 2005;26:6335-6342.
56. Kirker KR, Luo Y, Nielson JH, Shelby J, Prestwich GD. Glycosaminoglycan hydrogel films as bio-interactive dressings for wound healing. *Biomaterials* 2002;23:3661-3671.

57. Flexzan Dressings. [http://www.google.com/products/catalog?hl=en&q=Foam+dressings+Dow+Hickam%27s+Flexan&gs\\_upl=271551278901012834512101010101152126810.21210&bav=on.2.or.r\\_gc.r\\_pw..cf\\_osb&biw=1920&bih=976&um=1&ie=UTF-8&tbm=shop&cid=9240769028143188779&sa=X&ei=c5y1TpDFCtS2twf88rjkAw&ved=0CE4Q8wIwAA](http://www.google.com/products/catalog?hl=en&q=Foam+dressings+Dow+Hickam%27s+Flexan&gs_upl=271551278901012834512101010101152126810.21210&bav=on.2.or.r_gc.r_pw..cf_osb&biw=1920&bih=976&um=1&ie=UTF-8&tbm=shop&cid=9240769028143188779&sa=X&ei=c5y1TpDFCtS2twf88rjkAw&ved=0CE4Q8wIwAA).
58. Biocclusive Dressings by J&J. <http://www.vitalitymedical.com/johnson-and-johnson-biocclusive-transparent-dressing.html>.
59. 3M Tegaderm - Hydrocolloid Wound Dressing. <http://www.exmed.net/p-1189-3m-tegaderm-hydrocolloid-wound-dressing.aspx>.
60. Petrulyte S. Advanced textile materials and biopolymers in wound management.. 2008;55:72-77.
61. Horrocks r, Anand S. Medical textile. , 2000. p. 407-423.
62. Attwood AI. Calcium alginate dressing accelerates split skin graft donor site healing. Br J Plast Surg 1989;42:373-379.
63. Willi P, Sharma C. Chitosan and Alginate Wound Dressings: A Short Review. 2004;18:18-23.
64. Moseley R, Walker M, Waddington RJ, Chen WYJ. Comparison of the antioxidant properties of wound dressing materials—carboxymethylcellulose, hyaluronan benzyl ester and hyaluronan, towards polymorphonuclear leukocyte-derived reactive oxygen species. Biomaterials 2003;24:1549-1557.
65. Montesano R, Orci L. Transforming growth factor beta stimulates collagen-matrix contraction by fibroblasts: implications for wound healing. Proceedings of the National Academy of Sciences 1988;85:4894-4897.
66. Tan W, Krishnaraj R, Desai T. Evaluation of Nanostructured Composite Collagen–Chitosan Matrices for Tissue Engineering. 2001;7:203-210.
67. Miyata, T, Taira, T, Noishiki,Y. Collagen engineering for biomaterial use. 1992;9:139-148.
68. Man G, Lei R, Ting W, Li-Ping S, Ling-Rong L, Qi-Qing Z. Potential wound dressing with improved antimicrobial property. J Appl Polym Sci 2007;105:1679-1686.

69. Shin H, Jo S, Mikos AG. Biomimetic materials for tissue engineering. *Biomaterials* 2003;24:4353-4364.
70. Formhals A. Process and apparatus for preparing artificial threads. US Patent No. 1,975,504, 1934.
71. Gibson P, Schreuder-Gibson H, Rivin D. Transport properties of porous membranes based on electrospun nanofibers. *Colloids Surf Physicochem Eng Aspects* 2001;187-188:469-481.
72. <http://nanotechweb.org/cws/article/lab/38728/1/image2>.
73. Wilm MS, Mann M. Electrospray and Taylor-Cone theory, Dole's beam of macromolecules at last? *International Journal of Mass Spectrometry and Ion Processes* 1994;136:167-180.
74. Doshi J, Reneker DH. Electrospinning process and applications of electrospun fibers. *J Electrostatics* 1995;35:151-160.
75. Deitzel JM, Kleinmeyer J, Harris D, Beck Tan NC. The effect of processing variables on the morphology of electrospun nanofibers and textiles. *Polymer* 2001;42:261-272.
76. Moon S, Farris RJ. How is it possible to produce highly oriented yarns of electrospun fibers? *Polymer Engineering & Science* 2007;47:1530-1535.
77. Rho KS, Jeong L, Lee G, Seo B, Park YJ, Hong S, Roh S, Cho JJ, Park WH, Min B. Electrospinning of collagen nanofibers: Effects on the behavior of normal human keratinocytes and early-stage wound healing. *Biomaterials* 2006;27:1452-1461.
78. McManus MC, Boland ED, Koo HP, Barnes CP, Pawlowski KJ, Wnek GE, Simpson DG, Bowlin GL. Mechanical properties of electrospun fibrinogen structures. *Acta Biomaterialia* 2006;2:19-28.
79. Wnek G, Carr M, Simpson DG, Bowlin G. Electrospinning of Nanofiber Fibrinogen Structures. 2003;3:213-216.
80. Min BM, Lee G, Kim SH, Nam YS, Lee TS, Parl WH. Electrospinning of silk fibroin nanofibers and its effect on the adhesion and spreading of normal human keratinocytes and fibroblasts in vitro. 2004;25:1289-1297.
81. Khil MS, Cha D, Kim HY, Kim IS, Bhattarai N. Electrospun Nanofibrous Polyurethane Membraneas Wound Dressing. 2003;67B:675-679.

82. Dabney SE. The use of Electrospinning technology to produce wound dressings. 2002.
83. Verreck G, Chun I, Rosenblatt J, Peeters J, Dijck AV, Mensch J, Noppe M, Brewster ME. Incorporation of drugs in an amorphous state into electrospun nanofibers composed of a water-insoluble, nonbiodegradable polymer. *J Controlled Release* 2003;92:349-360.
84. Zahedi P, Rezaeian I, Ranaei-siadat SO, Jafari SH, Supaphol P. A review on wound dressings with an emphasis on electrospun nanofibrous polymeric bandages. 2010;21:77-95.
85. Dutta PK, Rinki K, Dutta J. Chitosan: A Promising Biomaterial for Tissue Engineering Scaffolds. 2011:1-35.
86. Ambrosio AMA, Allcock HR, Katti DS, Laurencin CT. Degradable polyphosphazene/poly( $\alpha$ -hydroxyester) blends: degradation studies. *Biomaterials* 2002;23:1667-1672.
87. Toms D, Wnuk A. Disposable absorbent articles with biodegradable backsheets. US Patent No. 5417679, 1995.
88. Gandhi M, Heejae Y, Frank K. regeneration of bombyx mori silk by Electrospinning: A comparative study of biocompatibility of natural and synthetic polymers for tissue engineering applications. 2007;1:274-281.
89. Nagler-Anderson C, Bober LA, Robinson ME, Siskind GW, Thorbecke GJ. Suppression of type II collagen-induced arthritis by intragastric administration of soluble type II collagen. *Proceedings of the National Academy of Sciences* 1986;83:7443-7446.
90. Jin H, Chen J, Karageorgiou V, Altman GH, Kaplan DL. Human bone marrow stromal cell responses on electrospun silk fibroin mats. *Biomaterials* 2004;25:1039-1047.
91. Park WH, Jeong L, Yoo DI, Hudson S. Effect of chitosan on morphology and conformation of electrospun silk fibroin nanofibers. *Polymer* 2004;45:7151-7157.
92. Min B, Jeong L, Nam YS, Kim J, Kim JY, Park WH. Formation of silk fibroin matrices with different texture and its cellular response to normal human keratinocytes. *Int J Biol Macromol* 2004;34:223-230.
93. Jeong L, Yeo I, Kim HN, Yoon YI, Jang DH, Jung SY, Min B, Park WH. Plasma-treated silk fibroin nanofibers for skin regeneration. *Int J Biol Macromol* 2009;44:222-228.
94. Kim K, Jeong L, Park H, Shin S, Park W, Lee S, Kim T, Park Y, Seol Y, Lee Y, Ku Y, Rhyu I, Han S, Chung C. Biological efficacy of silk fibroin nanofiber membranes for guided bone regeneration. *J Biotechnol* 2005;120:327-339.

95. Park KE, Jung SY, Lee SJ, Min B, Park WH. Biomimetic nanofibrous scaffolds: Preparation and characterization of chitin/silk fibroin blend nanofibers. *Int J Biol Macromol* 2006;38:165-173.
96. Geng X, Kwon O, Jang J. Electrospinning of chitosan dissolved in concentrated acetic acid solution. *Biomaterials* 2005;26:5427-5432.
97. Pillai CKS, Paul W, Sharma CP. Chitin and chitosan polymers: Chemistry, solubility and fiber formation. *Progress in Polymer Science* 2009;34:641-678.
98. Baxter A, Dillon M, Anthony Taylor KD, Roberts GAF. Improved method for i.r. determination of the degree of N-acetylation of chitosan. *Int J Biol Macromol* 1992;14:166-169.
99. Abdel-Halim ES, Abdel-Mohdy FA, Al-Deyab SS, El-Newehy MH. Chitosan and monochlorotriazinyl- $\beta$ -cyclodextrin finishes improve antistatic properties of cotton/polyester blend and polyester fabrics. *Carbohydr Polym* 2010;82:202-208.
100. Son WK, Youk JH, Lee TS, Park WH. The effects of solution properties and polyelectrolyte on electrospinning of ultrafine poly(ethylene oxide) fibers. *Polymer* 2004;45:2959-2966.
101. Duan B, Dong C, Yuan X, Yao K. Electrospinning of chitosan solutions in acetic acid with poly(ethylene oxide). 2004;15:797-811.
102. Chen K, Lin Y. Immobilization of microorganisms with phosphorylated polyvinyl alcohol (PVA) gel. *Enzyme Microb Technol* 1994;16:79-83.
103. Zhang Y, Huang X, Duan B, Wu L, Li S, Yuan X. Preparation of electrospun chitosan/poly(vinyl alcohol) membranes. ;285:855-863.
104. Li L, Hsieh Y. Chitosan bicomponent nanofibers and nanoporous fibers. *Carbohydr Res* 2006;341:374-381.
105. Zhou Y, Yang D, Nie J. Electrospinning of chitosan/poly(vinyl alcohol)/acrylic acid aqueous solutions. *J Appl Polym Sci* 2006;102:5692-5697.
106. Huang X, Ge D, Xu Z. Preparation and characterization of stable chitosan nanofibrous membrane for lipase immobilization. *European Polymer Journal* 2007;43:3710-3718.
107. Lin T, Fang J, Wang H, Cheng T, Wang X. Using chitosan as a thickener for electrospinning dilute PVA solutions to improve fibre uniformity. 2006;17:3718-3723.

108. Subramanian A, Vu D, Larsen GF, Lin H. Preparation and evaluation of the electrospun chitosan/PEO fibers for potential applications in cartilage tissue engineering. 2005;16:861-873.
109. Bhattarai N, Edmondson D, Veiseh O, Matsen FA, Zhang M. Electrospun chitosan-based nanofibers and their cellular compatibility. *Biomaterials* 2005;26:6176-6184.
110. Ojha S, Stevens D, Hoffman T, Stano K, Klossner R, Scott M, Krause W, Clarke L, Gorga R. Fabrication and Characterization of Electrospun Chitosan Nanofibers Formed via Templating with Polyethylene Oxide. 2008;9:2523-2529.
111. Jung K, Huh M, Meng W, Yuan J, Hyun SH, Bae J, Hudson SM, Kang I. Preparation and antibacterial activity of PET/chitosan nanofibrous mats using an electrospinning technique. *J Appl Polym Sci* 2007;105:2816-2823.
112. Chen Z, Mo X, Qing F. Electrospinning of collagen–chitosan complex. *Mater Lett* 2007;61:3490-3494.
113. Chen J, Chang G, Chen J. Electrospun collagen/chitosan nanofibrous membrane as wound dressing. *Colloids Surf Physicochem Eng Aspects* 2008;313-314:183-188.
114. Hasegawa M, Isogai A, Onabe F, Usuda M. Dissolving states of cellulose and chitosan in trifluoroacetic acid. *J Appl Polym Sci* 1992;45:1857-1863.
115. Ohkawa K, Cha D, Kim H, Nishida A, Yamamoto H. Electrospinning of Chitosan. *Macromolecular Rapid Communications* 2004;25:1600-1605.
116. Schiffman J, Shauer C. Cross-linking of chitosan Nanofibers. 2007;8:594-601.
117. Torres-Giner S, Ocio M?, Lagaron J?. Development of Active Antimicrobial Fiber-Based Chitosan Polysaccharide Nanostructures using Electrospinning. *Engineering in Life Sciences* 2008;8:303-314.
118. Lieberman MA, Lichtenberg AJ. Frontmatter. *Principles of Plasma Discharges and Materials Processing*: John Wiley & Sons, Inc., 2005; 2005. p. i-xxxv.
119. Canup LK. Non aqueous treatment of fabrics utilizing plasmas. 2000.
120. Hwang YJ, McCord MG. Surface modification of organicpolymer films treated in atmospheric Plasmas. 2004;151:495-501.

121. Shin Y, Son K, Yoo DI, Hudson S, McCord M, Matthews S, Whang Y. Functional finishing of nonwoven fabrics. I. Accessibility of surface modified PET spunbond by atmospheric pressure He/O<sub>2</sub> plasma treatment. *J Appl Polym Sci* 2006;100:4306-4310.
122. Chen FF. Introduction to plasma physics and controlled fusion, volume I: Plasma physics. New York and London: Plenum Press, 1988.
123. Cornelius C. Atmospheric Plasma Characterization and Mechanism of Substrate Surface Modification. 2006.
124. Geyter N, Morent R. Surface Modification of Polyester Non-woven with a dielectric barrier Discharge in Air at Medium Pressure. 2006:2460-2466.
125. Lieberman M, Lichtenberg A. Principles of plasma discharges and material processing. 2nd ed. New York: John Wiley and Sons, 2005.
126. Fridman AAK, L.A., editor. Plasma physics and engineering. : Taylor & Francis, 2004.
127. Hwang YJ, Mccord MG, An JS, Kang BC, Park SW. Effects of Helium Atmospheric Pressure Plasma Treatment on Low-Stress Mechanical Properties of Polypropylene Nonwoven Fabrics. *Textile Research Journal* 2005;75:771-778.
128. McCord MG, Hwang YJ, Qui Y, Hughes LK, Bourham MA. Surface Analysis of Cotton Fabrics Fluorinated in RadioFrequency Plasma. 2003;88:2038-2047.
129. Matthews SR. Plasma aided finishing of textile materials. 2005.
130. Biro D, Pleizier G, Deslandes Y. Application of the Microbond Technique. IV. Improved Fiber-Matrix Adhesion by RF Plasma Treatment of Organic Fibers. 1993;47:894.
131. Wertheimer M, Schreiber H. Surface Property Modification of AromaticPolyamides by Microwave Plasmas. 1981;26:2087-2096.
132. Wu S, Sheu G, Shyu S. Kevlar Fiber-Epoxy Adhesion and Its Effect onComposite Mechanical and Fracture Properties by Plasma and Chemical Treatment. 1996;62:1347-1360.
133. Qiu Y, Zhang C, Hwang YJ, Bures BL, McCord M. The effect of atmospheric pressure helium plasma treatment on the surface and mechanical properties of ultrahigh-modulus polyethylene fibers. 2002;16:99-107.
134. Hippler R, Schmidt M, Schoenbach KH. Low temperature plasma fundamentals, technologies, and techniques. : Wiley-VCH, 2008.

135. Wu S, Xing J, Zheng C, Xu G, Zheng G, Xu J. Plasma modification of aromatic polyamide reverse osmosis composite membrane surface. *J Appl Polym Sci* 1997;64:1923-1926.
136. Liao. *Plasma chemistry and plasma processing*. 2005;25:255.
137. Pandiyaraj KN, Selvarajan V. Non-thermal plasma treatment for hydrophilicity improvement of grey cotton fabrics. *J Mater Process Technol* 2008;199:130-139.
138. Hong SM, Kim SH, Kim JH, Hwang HI. Hydrophilic Surface Modification of PDMS Using Atmospheric RF Plasma. 2006;34:656-661.
139. Mittal K. *Development of Dual Functional Polymeric Textile Materials Using Atmospheric Plasma Treatments*. 2009.
140. Huang YD, Qiu JH, Liu LX, Zhang ZQ. The uniform treatment of carbon fiber surface in three-directional orthogonal fabric by oxygen-plasma. 2003;38:759-766.

CHAPTER 3  
Motivation and Objective

### **3.1 Motivation**

Evolving technology in polymers, electrospinning, etc. has introduced a wide range of applications in medical textile/bio-textiles. Since last couple of decades, human life has been affected by some major factors such as frequent casualties from traffic accidents, increasing number of sufferers from natural calamities, wars, chronic deceases/wounds, etc. Wounds are commonly observed in all these cases and therefore wound dressing is one of the main areas under research. Conventional textile-based wound dressings are cheap and highly absorbent, but cannot provide optimal wound healing conditions (hemostasis, non-adherence, maintenance of a moist wound bed, etc.), whereas modern wound dressings which are usually non-textile components such as films, gels, antimicrobials, and biological, provide advanced functionalities at a significantly higher cost.

Literature provides extensive information on use of different types of polymers in wound dressing wound dressing manufactured from different types of polymers. Amongst these polymers, natural materials like collagen, elastin, keratin, silk, fibrin clot, chitosan, mussel protein are preferred in biomedical application. Advantage of using natural polymers over synthetic polymers is that they have favorable cell interaction and non-toxic degradation products. This research will be focusing on natural polymers i.e. chitosan and silk. Chitosan is biologically renewable, biodegradable, antifungal, bactericidal, non-antigenic, and biocompatible, and used in wound dressing, wound healing, controlled drug delivery, and various tissue engineering applications whereas silk fibroin (SF) has good biocompatibility, good oxygen and water vapor permeability, biodegradability, and minimal inflammatory

reaction and has applications in cosmetics, medical materials for human health, and food additives.

Research on use of nanofibers in wound dressing is gaining popularity in last couple of decades. Nanofibers have versatility in wound healing functions which includes desirable wound adherence, absorption, oxygen permeability, resorbability, and occlusivity. Because of their highly porous nature, nanofiber webs form highly effective filters for contaminants, particulates, and microorganisms. Nanofibers also play important role in controlled drug release, hemostasis, cell proliferation, keeping wound scar-free, and maintaining moist environment. However, widespread use of nanofiber webs in wound dressings has been limited by the challenges such as poor mechanical properties and difficulty in handling.

These shortcomings of nanofibers can be overcome by the treatment of substrate by atmospheric plasma. Atmospheric pressure plasma technology helps to modify the structures and properties of various materials, especially textile materials. Plasma can etch the polymer surface increasing the frictional forces between the adjacent layers which increase the adhesive force between the layers. It can also enhance the bonding between nanofiber mats and textile substrates through pre-deposition surface activation of textile substrates. However, plasma post treatment of composite bandages would improve the nanofiber strength and bonding between them. Thus mechanical properties and durability of composite bandages can be increased by electrospinning nanofibers onto plasma treated gauze substrate.

The novelty of this research lies in the fact that no study has been carried out on the application of plasma in the manufacture of electrospun nanofiber wound dressings, particularly using chitosan nanofibers. The use of atmospheric plasma to improve the

adhesion between nanofiber mat and substrate, for wound dressing application has not been explored as yet by researchers. Pre-treating a substrate with atmospheric plasma can improve the adhesion between substrate and nanofibers by generating the reactions between polymers and plasma species that cannot be achieved in conventional methods. Combination of atmospheric plasma and electrospinning leads to a viable, rapid, safe, eco-friendly and economical nanofiber and mat production system that can be scaled up to nanofiber mass production line. This combined process of atmospheric plasma treatment on substrate and electrospinning of chitosan nanofibers offers mechanically strong, antibacterial, biocompatible, inexpensive wound dressing.

In summary, the motivations behind this research are 1) to improve the properties of conventional textile based wound dressing, 2) To reduce the cost of wound dressing without compromising properties essential for the quick wound healing, and 3) make it available to more number of people. To achieve these goals following objectives will be taken into considerations.

## Objectives

The objective of this research is to develop durable high-performance nanofiber/textile wound dressings, and the research activities include the following three tasks:

### **1: Selection of Appropriate Substrate and Nanofiber Combinations**

Nanofibers under investigation for wound dressings can be broken into three general categories:

1. Bioactive/healing
2. Barrier
3. Tissue Scaffolds

While selecting the polymer for electrospinning, it should address all three categories. Substrate materials for the nanofiber coatings will be chosen from existing commercially available textile gauzes.

### **2: Electrospin Selected Polymer onto Substrates.**

Study the processing-structure-property relationship in order to obtain excellent coverage, uniformity, moisture vapor transmission rate, oxygen permeability by controlling electrospinning parameters such as polymer type, solution concentration, voltage, solution flow rate, needle tip to collector distance, motion of collector drum, and addition of nanoparticles. Based on the results, the electrospinning process will be optimized to obtain electrospun nanofiber-deposited textile bandages with ideal wound dressing properties.

The ability of atmospheric plasma treatment to enhance adhesion and durability of the coating and to sterilize the composite bandage will be investigated by characterization of four sample sets:

- ❖ No plasma treatment
- ❖ Pre-treat substrate with plasma
- ❖ Post-treat electrospun coating with plasma
- ❖ Pre-treat and post-treat

### **3: Characterization of Uncoated and Nanofiber Coated Textile Bandage Materials**

Study the performance of the resultant nanofiber mats, and establish integrated processing-structure-performance relationships, which will guide to understand desired structures and performance for nanofiber mats deposited on textile wound dressing materials. All characterization studies will use uncoated fabrics as controls. Characterization of Plasma treated substrate as well as nanofibers will be investigated.

## CHAPTER 4

Novel Atmospheric Plasma Enhanced Chitosan Nanofiber/Gauze Composite Wound

Dressings

**Novel Atmospheric Plasma Enhanced Chitosan Nanofiber/Gauze Composite Wound Dressings**

**Rupesh Nawalakhe,<sup>1</sup> Narendiran Vitthuli,<sup>1</sup> Quan Shi,<sup>1</sup> Jessie Noar,<sup>4</sup> Jane M. Caldwell,<sup>3</sup> Frederick Breidt,<sup>3</sup> Mohamed A. Bourham,<sup>2,\*</sup> Xiangwu Zhang,<sup>1,\*</sup> and Marian G. McCord<sup>1,5,\*</sup>**

<sup>1</sup> *Fiber and Polymer Science Program, Department of Textile Engineering, Chemistry and Science, North Carolina State University, Raleigh, NC 27695-8301, USA*

<sup>2</sup> *Department of Nuclear Engineering, North Carolina State University, Raleigh, NC 27695-7909, USA*

<sup>3</sup> *U.S. Department of Agriculture, Agricultural Research Service, Department of Food, Bioprocessing and Nutrition Sciences, North Carolina State University, Raleigh, North Carolina 27695-7624*

<sup>4</sup> *Department of Microbiology, North Carolina Agricultural Research Service, North Carolina State University, Raleigh, North Carolina 27695-7615*

<sup>5</sup> *Joint Department of Biomedical Engineering, North Carolina State University, Raleigh, NC 27695-7115, USA, and University of North Carolina, Chapel Hill, NC, 27599, USA*

#### **4.1 Abstract**

Electrospun chitosan nanofibers were deposited onto atmospheric plasma treated cotton gauze to create a novel composite bandage with higher adhesion, better handling properties, enhanced bioactivity, and moisture management. Plasma treatment of the gauze substrate was performed to improve the durability of the nanofiber/gauze interface. The chitosan nanofibers were electrospun at 3-7% concentration in trifluoroacetic acid (TFA). The composite bandages were analyzed using peel, gelbo flex, antimicrobial assay, moisture vapor transmission rate (MVTR), X-ray photoelectron spectroscopy (XPS), absorbency, and air permeability tests. The peel test showed that plasma treatment of the substrate increased the adhesion between nanofiber layers and gauze substrate by up to 4 times. Atmospheric plasma pretreatment of the gauze fabric prior to electrospinning significantly reduced degradation of the nanofiber layer due to repetitive flexing. The chitosan nanofiber layer contributes significantly to the antimicrobial properties of the bandage. Air permeability and moisture vapor transport were reduced due to the presence of a nanofiber layer upon the substrate. X-ray photoelectron spectroscopy ( XPS) of the plasma treated cotton substrate showed formation of active sites on the surface, decrease in carbon content and increase in oxygen content as compared to the untreated gauze. Deposition of chitosan nanofibers also increased the absorbency of gauze substrate.

**Keywords: Plasma, Electrospinning, Wound Dressing, Chitosan, Adhesion, Antibacterial.**

## 4.2 Introduction

Traditional textile-based wound dressings fail to provide optimal wound healing conditions (hemostasis, non-adherence, maintenance of a moist wound bed, etc.) [1-2]. Recently, many advanced wound dressings have been developed to provide enhanced functionalities and help to maintain an appropriate healing environment around wounds, but also led to higher cost and difficulty in handling [3-4]. The goal of this research is to create chitosan nanofiber/gauze composite bandages that combine the desirable properties each component, and to characterize the physical and mechanical properties of these materials in order to predict the performance of these novel materials for wound care applications.

Among various wound dressing materials, chitosan has been extensively investigated due to its inherent biocompatibility, biodegradability, antimicrobial activity, wound healing property, and antitumor effect [5]. Chitosan has previously been used for other related biomedical applications, including drug delivery and bone healing [8-10]. Aoyagi et al. [6] formulated wound dressing films made of chitosan, minocycline hydrochloride and Tegaderm™ as backing materials for the treatment of severe burns. Wound protection and controlled drug release were achieved using these chitosan containing films. Studies on sponge-like asymmetric chitosan membranes by Fwu-Long Mi et al. [7] demonstrated the oxygen permeability, as well as hemostatic and antibacterial properties of chitosan.

In the context of wound dressings, nanofibers have been shown to have functional versatility, including desirable wound adherence, absorption, oxygen permeability, resorbability, and occlusivity [11-13]. Their high specific surfaces make them superlative matrices for controlled drug release. Nanofiber webs form highly effective filters for the

contaminants, particulates, and microorganisms without sacrificing air and moisture permeability [11-13].

Owing to the antibacterial properties of chitosan and the advantages of electrospun nanofibers, several attempts were made by researchers to electrospin chitosan nanofiber webs. However, electrospinning of pure chitosan was problematic due to its highly crystalline nature and inability to dissolve in solvents; instead, many previous studies relied on blends of chitosan/PVA [14] and chitosan derivatives [15]. Subsequently, successful electrospinning of pure chitosan in TFA was reported by Ohkawa, et al. [16]. They derived a linear relationship between nanofiber diameter and electrospinning solution concentration. In other work, electrospinning of pure chitosan was carried out in aqueous 90% acetic acid at 7% concentration [17]. However, characterization of mechanical strength, antibacterial properties, and absorbency of chitosan nanofibers was not reported.

Nanofiber webs are inherently weak and difficult to handle [18-19]. Deposition of nanofiber coatings onto conventional textile bandages addresses the need for structural support [19], but the challenge of delamination due to compliance mismatch or poor adhesion remains. While numerous studies of chitosan based nanofibers as components of wound dressings have shown promise, properties of pure chitosan nanofibers in wound dressings have not yet been completely characterized. Additionally, the adhesion of primary wound dressing layer of chitosan nanofibers electrospun onto a secondary cotton wound dressing substrate layer is a critical issue that has not been fully addressed in published work.

In our previous studies, atmospheric pressure plasma technology has been used to modify the structures and properties of various materials (especially textile materials). We

have shown that plasma treatment can: i) improve surface bonding or adhesive ability [20-22], ii) increase mechanical strength by crosslinking [21-25], iii) change fiber surface hydrophobicity [26], iv) roughen fiber surfaces [27], v) increase crystallinity [27, 28]. Recently, Vitchuli et al. [18] successfully employed atmospheric plasma treatment to improve the adhesion between nylon nanofibers and nylon/cotton fabric substrates.

In this study, pure chitosan nanofiber webs were electrospun onto plasma-treated 100% cotton (gauze) substrates to produce mechanically strong, highly absorbent, antibacterial, biocompatible, composite wound dressings. The composite materials were characterized to determine:

- Effects of plasma pre-treatment of the substrate on the bonding between nanofiber mats and textile substrates, ,
- Absorbency,
- Air permeability
- Moisture Vapor Transport Rate
- Antimicrobial activity.

## **4.3 Materials and Methods**

### **4.3.1 Materials**

Chitosan (Sigma Aldrich, Molecular Weight: 190kDa-375kDa, Degree of Deacetylation: 85%) was used for electrospinning onto a 100% cotton gauze substrate (Carolina Narrow Fabric Co. Inc.). Trifluoroacetic acid (Sigma Aldrich) was selected as the solvent.

### **4.3.2 Electrospinning of nanofiber webs onto substrates**

The electrospinning equipment consisted of an extrusion system (syringe pump), fiber collection system (rotating drum), and high voltage power supply. The syringe was fixed onto the extrusion system and was filled with chitosan solution to produce the desired spinning yield. A positive charge was applied to polymer solution via high voltage power supply. Chitosan nanofibers were electrospun in the range of 2 - 7% concentration in trifluoroacetic acid (TFA) with an extrusion rate of 1.5 ml/hr for 2 hrs., applied voltage of 25 kV and distance of 15 cm in between rotating drum and needle tip.

The collection system for nanofibers includes a cylindrical polyvinyl chloride (PVC) drum with a grounded metal ring at one end. A metal rod is attached to the ring and runs along the length of the cylinder. In order to make the surface conductive, aluminum foil was wound over the drum in contact with the metal rod. The textile substrate was then wrapped around the aluminum foil to enable deposition of electrospun nanofibers onto it. The speed of the drum was maintained at 20 rpm using a motor.

### **4.3.3 Plasma pre-treatment of substrate**

The atmospheric pressure audio frequency glow discharge system was designed and developed at North Carolina State University. The capacitively-coupled dielectric-barrier-discharge (DBD) consists of two parallel copper electrodes, each embedded within a Lexan polycarbonate insulator as shown in Figure 4.1. Stable and uniform plasma was achieved at a low (audible) frequency of 1.373 kHz during the operation. The voltage across the plates was ~6.3 kVrms and 7.6 kVmax for 100% He plasma and ~6.6 kVrms and 7.85 kVmax for 99% He plus 1% O<sub>2</sub>. Gas flow rates were 20 lit/min for helium gas and 0.3 lit/min for oxygen gas.

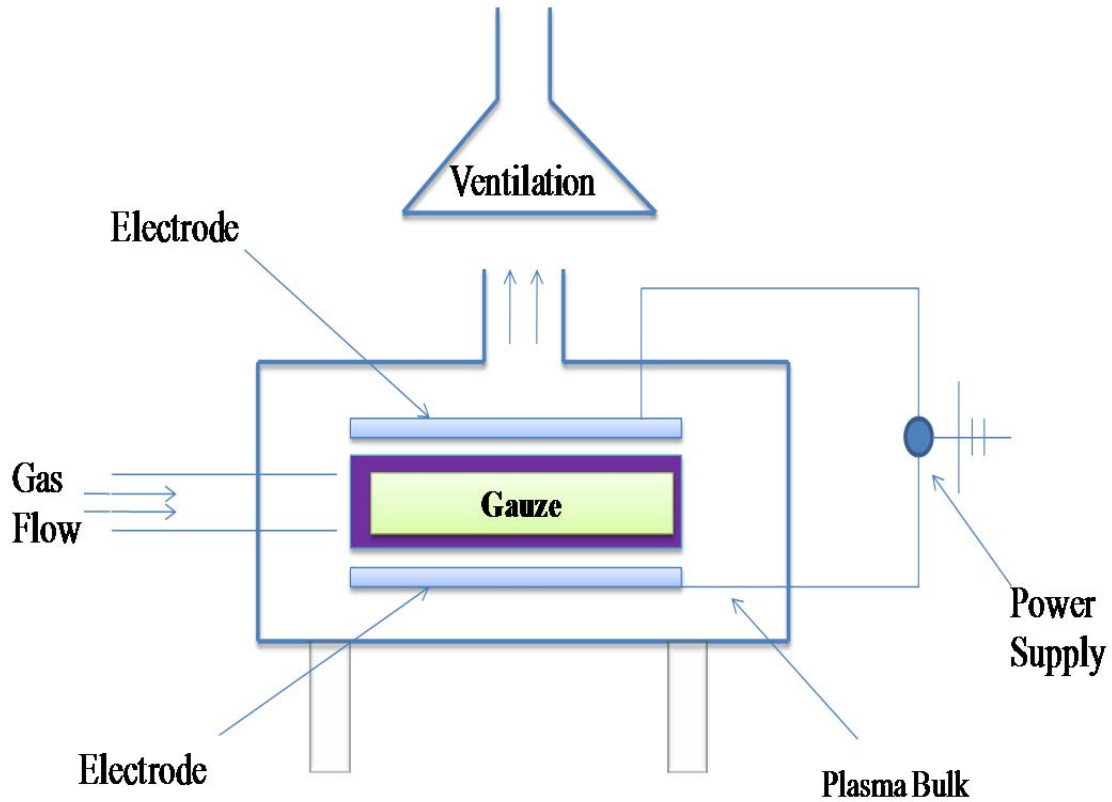


Figure 4.1. Schematic diagram of atmospheric pressure plasma system

The gauze substrates were placed on a nylon grid suspended in the middle of the plasma chamber to enable complete and uniform plasma exposure from all sides. The fabrics were treated with 100% He-plasma or 99%He/1%O<sub>2</sub> plasma prior to nanofiber deposition. After nanofiber deposition, the samples were conditioned at standard temperature of  $20 \pm 1^\circ\text{C}$  and relative humidity of  $65 \pm 2\%$  for at least 8 hours before they were tested for adhesion, antibacterial properties, moisture vapor transmission rate, air permeability, and surface chemical composition (via X-Ray photoelectron Microscopy).

#### **4.3.4 Adhesion between nanofiber mats and supporting fabrics**

##### **Peel Test**

A peel test method was devised for evaluating the adhesion between the nanofiber mat and the fabric substrate based on ASTM D2261-*Tearing strength of woven fabrics by tongue (Single Rip) method* [29] using an Instron Tensile Tester. The 90° peel test was used (Figure 2). This method allows the user to control the rate of delamination and the locus of failure. Substrate samples (5 cm × 1 cm) with chitosan nanofibers deposited on them were tested. Pieces of masking tape were used to couple the two layers, *i.e.*, substrate (fabric) and nanofiber mat, to the lower and upper jaws, respectively. The speed of the upper jaw was kept constant at 50 mm/min. A 50 gm load cell with a gauge length of 1.27 cm was used to measure the force of adhesion. For each sample, 6-8 specimens were tested on an Instron® Tensile Tester and the average force to peel off the nanofiber layer off the substrate was recorded.

##### **Gelbo Flex Tester**

In order to assess the ability of nanofiber mats electrospun onto the substrate to withstand repetitive strain, Gelbo Flex testing was employed using a modification of ASTM F 392-93, *Standard Test Method For Flex Durability Of Flexible Barrier Materials* [30]. Nanofiber-deposited fabric samples of size 5 cm × 1 cm were attached to two circular clamping disks, via hose clamps, and the samples were twisted and flexed for 1000 cycles. Results of Gelbo Flex testing provided a visual adhesion assessment which was observed under scanning electron microscopy (JEOL 6400F Field Emission SEM).

#### 4.3.5 Antibacterial Tests

Antibacterial testing was performed on plasma treated cotton gauze with and without chitosan nanofibers. Cultures used for the antibacterial tests were *Escherichia coli* O157 strain B179 and *Bacillus cereus* strain B2, obtained from the USDA/ARS Food Science Research Unit culture collection, Raleigh, NC. Five ml of broth culture was prepared for each organism, *E. coli* in Luria Broth (LB broth, BD Diagnostic Systems, Sparks, MD) at 37°C, and *B. cereus* in Tryptic Soy Broth (TSB, BD Diagnostic Systems) at 30°C, with shaking for aeration at 200 rpm in a 15 ml centrifuge tube (Corning®). In a biological safety cabinet, pieces of fabric ~5 mm square were aseptically cut and placed in 1.5 ml tubes. Broth cultures were harvested at 5000 rpm for 10 minutes, and resuspended in an equal volume of saline to give approximately 10<sup>9</sup> CFU/ml. Three concentrations of the cell suspensions were subsequently used: undiluted, 10<sup>-3</sup>, and 10<sup>-5</sup> CFU/ml. An aliquot (200 ul) of each cell suspension was added to the tubes with fabric: *B. cereus* with chitosan-free fabric, *B. cereus* with chitosan-treated fabric, *E. coli* with chitosan-free fabric, and *E. coli* with chitosan-treated fabric. After incubation of *E. coli* at 37 °C and *B. cereus* at 30 °C with shaking at 200 - 300 rpm, the surviving cells were appropriately diluted and plated on LB (*E. coli*), or TSA (*B. cereus*) using a spiral plater (Autoplate 4000®, Spiral Biotech, Inc. Norwood, MA). Plates were incubated for 24 hours at 37 °C for *E. coli* and 30 °C for control and *B. cereus*, and the colonies were counted using an automated plate reader (Qcount®, Spiral Biotech).

#### 4.6.6 Air Permeability

The air permeability of electrospun fiber-deposited fabrics was measured using a Frazier air permeability testing instrument (Frazier Precision Instrument Co., MD). The

measurement was carried out according to ASTM D737-04 *Standard Test Method for Air Permeability of Textile Fabrics* [31], with 1 mm and 1.4 mm orifices for composite bandages and an 8 mm orifice for cotton gauze (since it has a more open structure than composite bandages), 6.45 cm<sup>2</sup> test area, at 760 mm mercury pressure, 21° C, and 65% RH. An average of 10 readings of air permeability from different parts of the composite bandages was recorded.

#### **4.3.7 Moisture Vapor Transmission Rate (MVTR)**

Measurements for MVTR of the samples (100% gauze with and without chitosan nanofibers) were made in at the standard atmosphere laboratory temperature and humidity (70 ± 2°F and 65% RH). The rate of moisture vapor diffusion through the material was determined according to the Simple Dish Method similar to ASTM E96-80, *Standard Test Method for Water Vapor Transmission of Materials* [32]. A sample was placed on a water dish (82 mm in diameter and 19 mm in depth) with a 9 mm air space between the water surface and specimen. A vibration free turntable with 8 dishes, rotating at a uniform speed of 5 m/min was used to ensure that all dishes were exposed to the same average ambient conditions during the test. The specimen dishes were allowed to stabilize for two hours before taking the initial weight. The final weight was measured after a 24 hour interval. The MVTR was calculated in units of g/m<sup>2</sup>-24 hours. The experiment was repeated 5 times for each sample.

#### **4.3.8 XPS Analysis**

X-ray photoelectron spectroscopy (XPS) was carried out to investigate the changes in the surface chemical composition of 100% cotton gauze substrate as a result of changes in

plasma parameters (percentage of Helium and oxygen). Spectra were obtained using a Riber LAS-3000 with MgK $\alpha$  excitation (1254 eV). Energy calibration was established by referencing to adventitious Carbon (C1s line at 284.5 eV binding energy). A takeoff angle of  $\sim 75^\circ$  from surface was used with an x-Ray incidence angle of  $\sim 20^\circ$  and an x-ray source to analyzer angle of  $\sim 55^\circ$ . Base pressure in the analysis chamber was in  $10^{-10}$  Torr range. CASA XPS software was used for data reduction.

#### **4.3.9 Absorbency**

An absorbency test was carried out on the composite wound dressing and gauze fabric in accordance with BS EN 13726-1: 2002 *Test methods for primary wound dressings, - Part 1: Aspects of absorbency, Section 3.2 – Free Swell Absorptive Capacity* [33]. The composite dressing was cut into  $4 \times 4$  cm pieces and was weighed ( $W_0$ ). A solution consisting of 142 mmol Na ions and 2.5 mmol Ca ions was first pre-warmed to  $37^\circ\text{C}$ . The composite nanofiber dressing was placed in a Petri dish and treated with the above mentioned solution (weight of solution being at least 40 times the weight of sample) and incubated at  $37^\circ\text{C}$  for 30 minutes. After 30 minute's incubation the Petri dish was removed from the incubator, and was suspended for 30 seconds on paper towel [34] before being reweighed ( $W_{30}$ ) so as to allow the excessive solution to run off. The procedure was repeated 5 times. The absorbency of the dressing was expressed as amount of solution absorbed per square centimeter dressing ( $[W_{30} - W_0]/\text{area}$ ). The absorbency can be expressed in terms of  $\text{g}/\text{cm}^2$  ( $[W_{30} - W_0] / \text{area}$ ) or percentage ( $[W_{30} - W_0] \times 100 / W_0$ ).

## 4.4 Results and Discussion

### 4.4.1 Electrospinning of chitosan nanofibers

Chitosan nanofibers were electrospun in the range of 2 – 7% concentration in trifluoroacetic acid (TFA) (Figure 4.2).

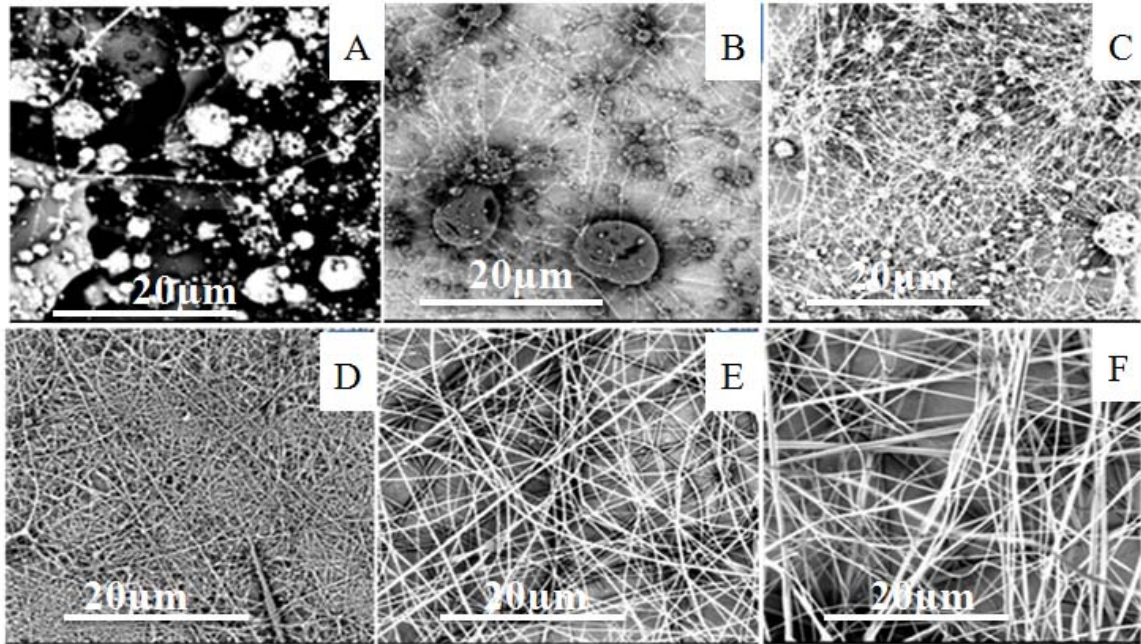


Figure 4.2. SEM images of Chitosan nanofibers Concentration: A)2%, B)3%, C)4%, D)5%, E)6%, and F)7% in TFA. Extrusion rate: 1.5ml/hr, Applied voltage: 25kV, Distance: 15cm. (20µm)

Electrospinning of 2% concentration of chitosan in TFA showed bead formation with no fiber formation. However, as the concentration increased from 3 to 7%, an obvious reduction in number of beads, with an increase in fiber forming tendency was observed. A 1% increment in concentration from 3 to 7% yielded increasing average diameters of 97, 105, 116, 165, and 252 nm, respectively. Concentrations above 7% are not considered because the

increase in average diameter will significantly decrease the specific surface area and porosity of the nanofiber web. All further experiments were performed at 7% concentration.

#### 4.4.2 Adhesion between nanofiber mats and supporting fabrics

The peel test results showed that after treating the substrate with 100% helium plasma and 99% helium/1% oxygen plasma, the force required to peel off the nanofiber layer from substrate was increased by up to approximately 4 times (Table 4.1).

Table 4.1. Measurement of adhesion between nanofiber mats and supporting fabrics.

<b>Treatment on substrate</b>	<b>Control</b>	<b>He (Pre-treatment)</b>	<b>He + 1% O<sub>2</sub> (Pre-treatment)</b>
Mean (gf)	11.05	42.28	31.23
Standard deviation	1.95	6.12	1.24

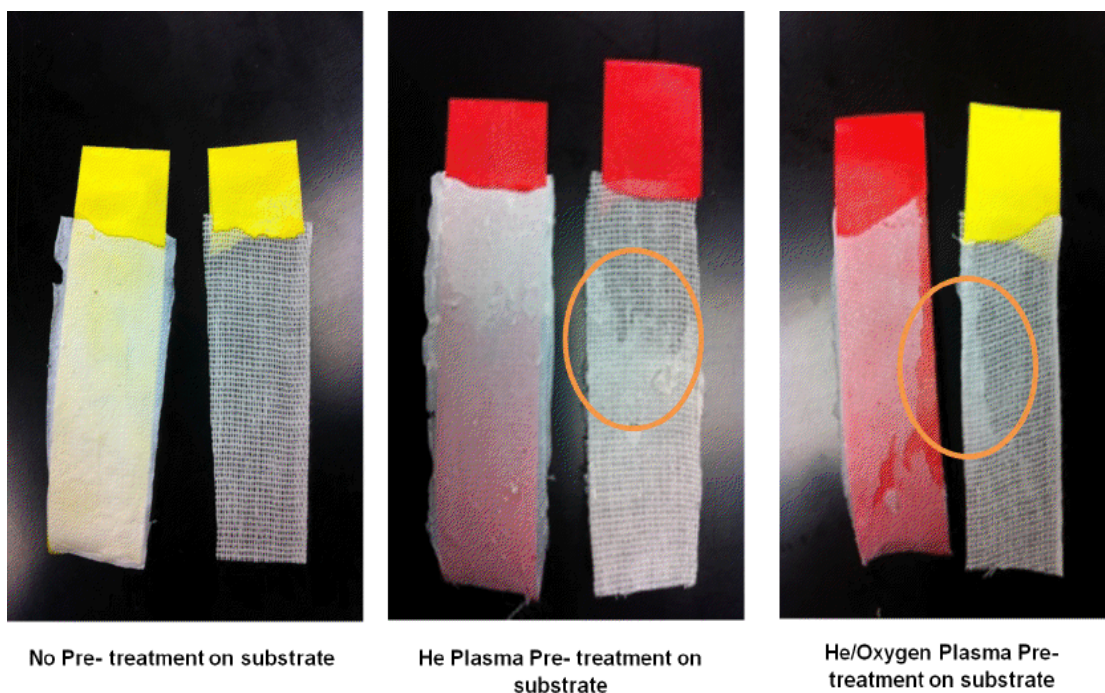


Figure 4.3 Evaluation of nanofiber-fabric adhesion using the 90 degree peel test.

While control sample nanofiber webs were removed intact, tearing of the nanofiber web was observed (Figure 4.3) during the peel tests on plasma treated substrates, indicating improved adhesion between nanofiber layers and the substrates.

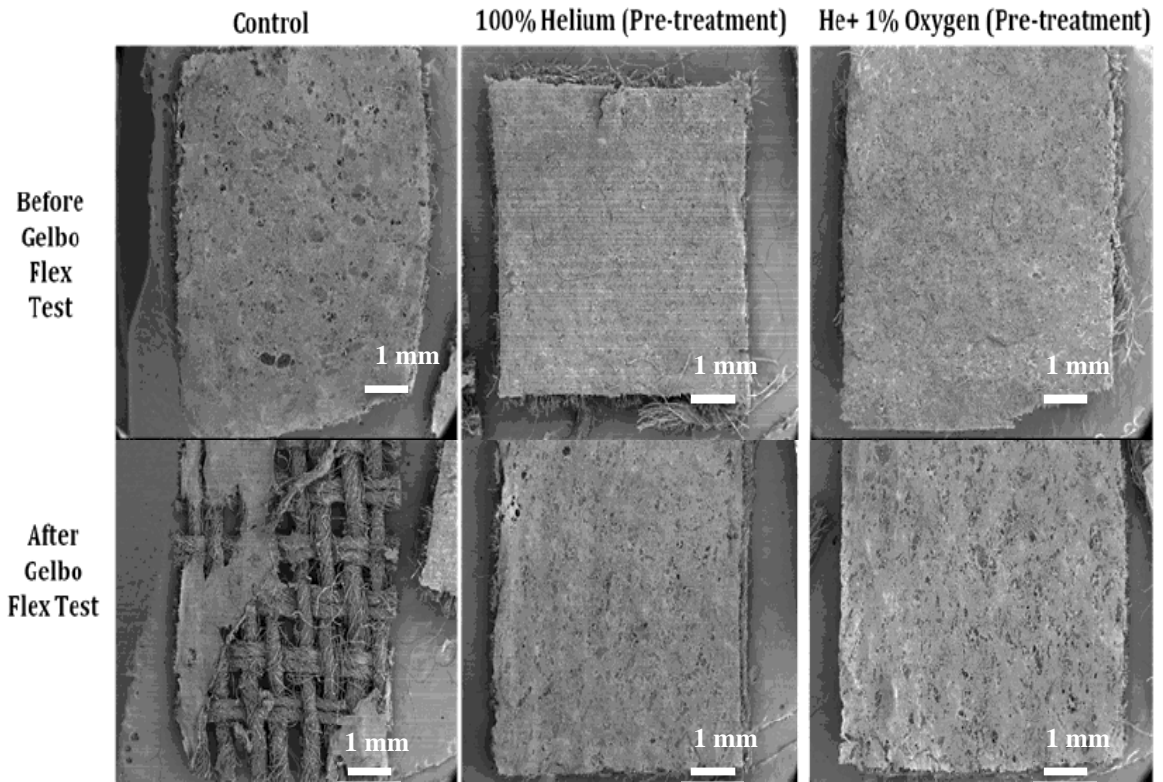


Figure 4.4. SEM images of composite bandages, before Gelbo testing and after 1000 cycles of Gelbo flex testing with no pre-treatment, 100% He, 99%He/1%O<sub>2</sub> plasma pre-treatment on substrate.

Gelbo Flex testing was performed on the samples and their morphologies were observed in SEM at  $15 \times$  magnification as shown in Figure 4.4. It was observed that the nanofiber layer was badly damaged after 1000 cycles in the case of untreated substrate, whereas it showed much better durability when the substrate was pre-treated by plasma. In the latter case, the nanofiber layer was intact and firmly adhered to the substrate as a whole layer.

#### 4.4.3 Antibacterial Test

An open wound is highly susceptible to infectious bacteria [35]. Once the wound becomes infected, it requires additional treatments that are painful and result in delayed healing. The use of antimicrobial materials in wound dressings in a non-occlusive dressing provides enhanced protection while maintaining good moisture management properties. The addition of chitosan nanofibers to the substrate gauze significantly increases the antimicrobial activity of the bandage, and is expected to aid in infection prevention via contact with bacteria in or surrounding the wound.

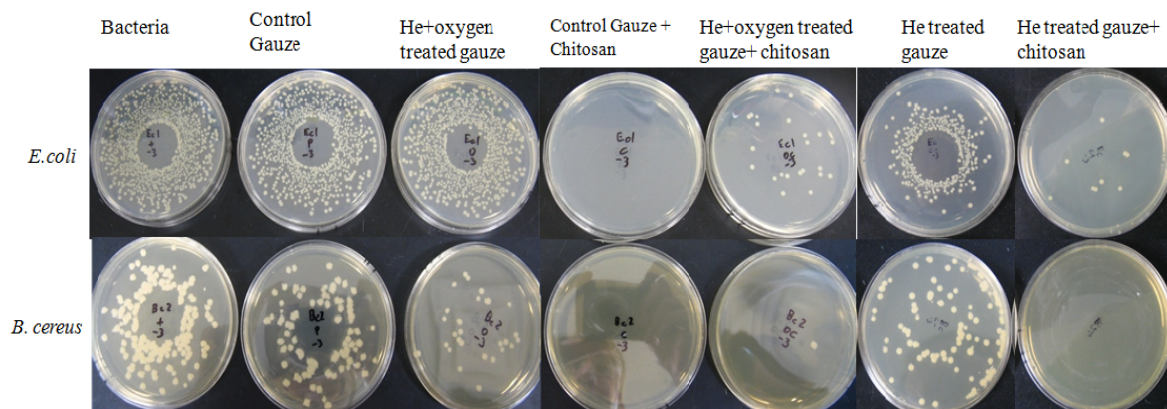


Figure 4.5 Antibacterial testing on control (untreated) gauze, He and He/O<sub>2</sub> treated substrate with and without chitosan nanofibers.

Table 4.2 Antibacterial activities of Chitosan nanofiber coated gauze fabric against only gauze.

Samples	<i>E. coli</i> [log(CFU/ml)]	<i>B. cereus</i> [log(CFU/ml)]
Only Bacteria	7.52 ± 0.01	6.55 ± 0.08
Gauze	7.47 ± 0.09	6.14 ± 0.14
He Treated Gauze	7.01 ± 0.36	5.73 ± 0.25
He/O <sub>2</sub> treated gauze	7.51 ± 0.14	5.69 ± 0.03
Gauze + chitosan	3.65 ± 0.02	2.98 ± 0.1
He-treated gauze + Chitosan	5.09 ± 0.53	4.18 ± 0.81
He/O <sub>2</sub> treated gauze + chitosan	4.82 ± 0.06	2.80 ± 0.06

Results of antimicrobial tests are shown in Table 4.2. The control gauze substrate showed no antimicrobial activity, while the chitosan-gauze composites showed antimicrobial activity against both *E. coli* and *B. cereus*. It is clear from Table 2 that untreated gauze fabric with chitosan nanofibers showed log reduction of 4 as compared to that of untreated gauze for both *E.coli.* and *B. cereus*. The cationic amide group in chitosan is responsible for its antibacterial activity. Figure 4.5 and Table 4.2 show that the antibacterial activity of the chitosan nanofiber webs were retained after treating the substrate with He- and He/O<sub>2</sub>-plasma. While He-plasma pre-treated gauze fabric with chitosan nanofibers showed 2.5 and 2.5 log reductions, respectively, He/O<sub>2</sub> plasma pre-treated gauze fabric with chitosan nanofibers showed 2.5 and 3.5 log reduction for both *E.coli.* and *B. cereus* respectively. From the above results, we can conclude that the plasma pre-treatment did not change the antibacterial properties of the cotton gauze fabric, while the introduction of the chitosan nanofiber layer significantly improved the antibacterial properties (Figure 4.5 and Table 4.2).

#### **4.4.4 Air Permeability**

Moisture management is critical to wound healing, and is governed by factors including air permeability, moisture vapor transmission and fluid absorbency. While too much moisture in the bandage microclimate results in maceration, too little moisture results in wound desiccation; both conditions have been demonstrated to delay wound healing [36]. Compared to a wound left open to heal in air, a wound occluded under a transparent film has a higher rate of epithelialization [37]. Gupta et al. [38] studied the air permeability of cotton fabric and cotton fabric covered with chitosan film. It was observed that air permeability of

approximately  $8.6 \text{ cm}^3/\text{cm}^2/\text{sec}$  would help in maintaining the wound moist without inducing maceration.

Table 4.3. Average Air Permeability and moisture vapor transmission rate (MVTR) of the composite wound dressing i.e. Chitosan nanofiber electrospun on untreated, He plasma treated and He-O<sub>2</sub> plasma treated cotton substrate

<b>Samples</b>	<b>Air permeability <math>\text{cm}^3/\text{cm}^2/\text{sec}</math></b>	<b>MVTR <math>\text{g}/\text{m}^2/\text{day}</math></b>
Gauze	$265.68 \pm 7.87$	$885.36 \pm 18$
Gauze + chitosan	$3.38 \pm 0.11$	$744.94 \pm 12$
Gauze (He pretreated) + Chitosan	$4.88 \pm 0.07$	$754.46 \pm 17$
Gauze (He/O <sub>2</sub> pretreated) + Chitosan	$8.76 \pm 0.20$	$766.36 \pm 19$

Gauze with no chitosan nanofibers showed an average air permeability of  $265.68 \text{ cm}^3/\text{cm}^2/\text{sec}$ . Untreated, He and He/O<sub>2</sub> plasma treated substrates with chitosan nanofibers showed reduced average air permeabilities of 3.38, 4.88, and  $8.76 \text{ cm}^3/\text{cm}^2/\text{sec}$  respectively (Table 4.3). As all the values of air permeabilities obtained after deposition of nanofibers onto the substrate have values close to the  $8.6 \text{ cm}^3/\text{cm}^2/\text{sec}$  recommended by Gupta et al.[38], the composite bandages would help in maintaining the appropriate wound moisture. Thus, use of chitosan nanofiber coated gauze bandages should result in faster wound healing. It is

expected that the air permeability would be affected by the thickness of nanofibers deposited on to the gauze fabric. Higher thicknesses of nanofibers will result in lower air permeabilities due to the greater number of nanofiber layers making the composite bandage a more compact structure.

#### **4.4.5 Moisture Vapor Transmission Rate (MVTR)**

Bolton et al. [39] studied a variety of dressings and determined that an MVTR of less than 840g/m<sup>2</sup>/day is required to maintain a moist wound surface. MVTRs for gauze with no nanofibers, and untreated gauze and plasma pre-treated gauze with chitosan nanofibers are shown in Table 4.3. A higher MVTR (885.36 g/m<sup>2</sup>/day) was obtained in case of substrate with no chitosan nanofibers than for the untreated as well as the He, He/O<sub>2</sub> plasma treated gauzes with chitosan nanofibers deposited on them (744.94, 754.46, 766.36 g/m<sup>2</sup>/day respectively). The decrease in the MVTR after deposition of the chitosan nanofiber layer as compared with the gauze alone indicates that the composite bandage is likely to provide better wound moisture retention than the untreated gauze.

#### **4.4.6 XPS Analysis of Substrate after Plasma Treatment**

The carbon content in the control sample was 84.88 % as shown in Table 4.4. Typical cellulose would have a carbon content of 66.9 % [40]. This atypical cellulose composition may be due to the presence of residual long chains of hydrocarbons [41] on the cotton fiber surface which remain even after aqueous processing, or may be due to the composition of the cotton fiber outer wall which consists of mixture of fats, waxes and resin [42]. XPS analysis of control gauze, He- and He/O<sub>2</sub> - plasma treated gauze was carried out to study the plasma effect on surface chemistry of the treated substrates. Previous studies in our lab showed

Table 4.4 Results of surface elemental analysis for plasma treated and untreated Cotton substrate with Atmospheric Pressure Plasmas

<b>100% cotton Substrate</b>	<b>C-spectra</b>			<b>Overall</b>	
	C-C (%)	C-O (%)	COO-(%)	O (%)	C(%)
<b>No treatment</b>	85	14	1	15.12	84.88
<b>He Plasma treated</b>	82	9	9	22.38	77.62
<b>He-O<sub>2</sub> plasma treated</b>	82	8	10	18.82	81.18

possible radical formation on the surface of cotton fabric due to fluorinated radio frequency plasma [40]. Table 4.4 shows a reduction in the carbon content of the cotton substrate from 84.88% to 77.62% and 81.18% after He- and He/O<sub>2</sub> -plasma treatment. This effect was more pronounced for the He treated substrate than for the He/O<sub>2</sub> plasma treated substrate. Reduction in surface carbon content is due to the etching of some of the long chain hydrocarbons from the surface as a result of plasma treatment which results in roughness of the surface. Oxygen contents of the cotton substrate were increased from 15.12 % to 22.38 % and 18.82 % after He- and He/O<sub>2</sub> plasma treatments respectively. Higher oxygen content can be explained by the scission at site 'B' from the cellulosic ring as shown in Figure 4.6.

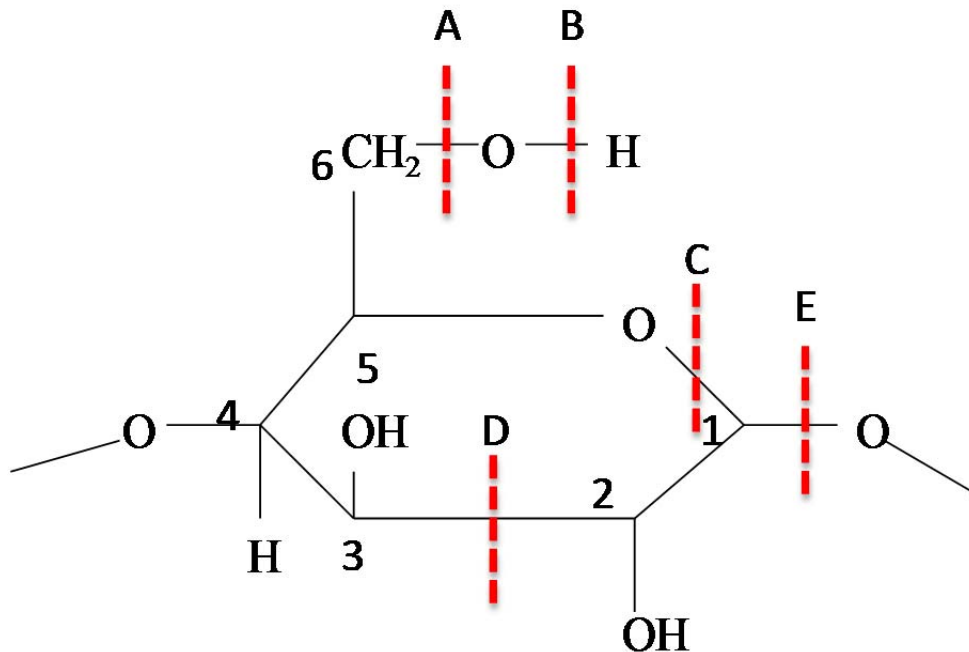


Figure 4.6. Possible sites for scission of cotton substrate after plasma treatment (A) Dehydroxylation, B) Dehydrogenation, C) scission between C1 and ring oxygen, D) dehydrogenation/dehydroxylation, E) scission between C1 and glycosidic oxygen

Scission at sites 'C' and 'E' would produce radicals that could react with active groups of the chitosan nanofibers. In addition, dehydrogenation or dehydroxylation at site 'B' and 'A' in -C-O-H groups (figure 4.6) on cellulose can make the cotton substrate susceptible to reaction with chitosan nanofibers at C6. Due to the abundance of hydroxyl groups on chitosan as well as on cotton substrate, there are high chances of hydrogen bonding at the nanofiber- substrate interface.

C1s spectral analysis showed that there was formation of new functional groups on the cotton substrates after treating them with He- or He/O<sub>2</sub>-plasma. Increases in COO<sup>-</sup> (289.1eV) indicate formation of polar groups available for cross-linking with hydroxyl or cationic amide groups of chitosan nanofibers. After treating the cotton substrate with plasma,

breaking of cellulose ring can occur resulting from scission at sites 'C' and 'E'. This scission can be explained by the reduced intensities of C-C and C-O bonds in C1 spectra and can be responsible for crosslinking between the substrate and nanofibers to be deposited on it. Considering all these factors, it is likely that increased functionality and surface roughness as a result of plasma treatment are responsible for the increased adhesion. Qualitative assessment of the surface roughness of nanofibers is technically challenging and was not characterized in this study.

#### **4.4.7 Absorbency**

Adding a nanofiber layer onto the conventional cotton gauze is expected to result in an increase in the liquid absorbency. Due to the high surface area to volume ratio of the nanofibers, they exhibit water absorptions in the range of 17.9–213% [43]. Absorbency of gauze and composite bandages is shown in Table 4.5. The chitosan nanofibers composite wound dressing showed an average of 68% - 82% higher absorbency than the gauze fabric alone. Though it was expected that plasma treatment would make the cotton substrate more hydrophilic, there was no significant dependence of absorbency on the type of plasma used to treat the composite bandages.

Table 4.5 Absorbency of Gauze and Composite wound dressing.

<b>Samples</b>	Average Absorbency, g	Absorbency, %
Gauze	0.12 ± 0.01	91 ± 6
Gauze + chitosan	0.22 ± 0.01	153 ± 10
Gauze (He pretreated) + Chitosan	0.22 ± 0.01	164 ± 7
Gauze (He/O <sub>2</sub> pretreated) + Chitosan	0.23 ± 0.01	166 ± 9

These composite wound dressings of cotton gauze and chitosan nanofibers could potentially help resolve excessive hydration and wound maceration by reducing swelling and inflammation through higher absorbency. Chitosan nanofiber coated composite wound dressings showed absorbencies of 0.22g -0.23g as shown in Table 4.5. These results are comparable to those of commercial dressings, e.g., Arglaes and Acticoat7 [44], which have absorbencies of 0.5 and 0.6g, respectively. It is expected that the absorbency can also be manipulated by the thickness of nanofiber layer. If a thicker layer of nanofiber is deposited on the substrate, the absorbency of composite wound dressings can be increased.

#### **4.5 Conclusions**

Chitosan nanofibers were electrospun onto 100% cotton gauze substrates to form composite bandages. Atmospheric pressure plasma technology was utilized to improve the adhesion and durability of the nanofiber coating. Peel tests showed that treatment of the substrate with 100% He plasma and 99% He/1% O<sub>2</sub> plasmas increased the adhesion between nanofiber layers and substrates by up to 4 times. Also, plasma pretreatment of the gauze fabric prior to electrospinning significantly reduced degradation of the nanofiber layer due to

repetitive flexing. Antibacterial results showed that with plasma pre-treatment of the substrate, the antibacterial properties of chitosan were retained against Gram positive (*Bacillus cereus*) and Gram negative bacteria (*Escherichia coli*). Air permeability and moisture vapor transport were reduced due to the presence of a nanofiber layer upon the substrate, which is expected to aid in keeping the wound moist, resulting in better wound healing. XPS analysis showed that after the substrate was treated by plasma, the surface carbon content (C1s) was decreased and oxygen content was increased. Also, plasma treatment created surface oxidation, which was responsible for the increased adhesion between the substrate and chitosan nanofibers through crosslinking between the active sites. As compared to uncoated gauze alone, gauze coated with chitosan nanofibers had on average a 68-82% higher absorbency, which is likely to enhance absorption of wound exudates and blood.

#### **4.6 Acknowledgements**

The authors wish to acknowledge the National Textiles Center for funding this research. Facilities and resources at the NCSU College of Textiles, the Department of Nuclear Engineering and USDA ARS Food Science Research Unit were utilized to complete this research.

#### 4.7 References

1. Baranoski S 2008 Wound and Skin Care. January p 60-61.
2. Mlekusch W, Dick P, Haumer M, Sabeti S, Minar E, Schillinger M. 2006 J Endovasc Ther. 13 1 p 23-31.
3. Baranoski S, 2008 Wound and Skin Care. February p 14-15.
4. <http://jan.ucc.nau.edu/~daa/woundproducts/products.html>
5. Hudson SM, Lim S 2003 J. of Macromol. Sci. 43 2 p 223-269.
6. Aoyagi S, Onishi H, Machida Y 2007 International Journal of Pharmaceutics. 330 1 2 p 138–145.
7. Mi FL, Shyu SS, Wu YB, Lee ST, Shyong JY, Huang RN 2001 Biomaterials. 22 2 p 165-173.
8. Biagini G, Bertani A, Muzzarelli R, Damadei A, DiBenedetto G, Belligolli A, Riccotti G, Zucchini C, Rizzoli C 1991 Biomaterials. 12 3 p 281-286.
9. Abhay SP 1998 United States Patent No. 5836970.
10. Su CH, Sun CS, Juan SW, Hu CH., Ke WT, Sheu MT 1997 Biomaterials 18 p 1169-1174.
11. Duan YY, Jia J, Wang SH, Yan W, Jin L, Wang ZY 2007 J. Appl. Polym. Sci. 106 p 1208-1214.
12. Venugopal J, Ramakrishna S 2005 Appl. Biochem. Biotechnol. 125 p 147-157.

13. Jia J, Duan YY, Wang SH, Zhang SF, Wang ZY 2007 J. US-China Med. Sci. 4 2 p 52-54.
14. Duan B, Dong C, Yuan X, Yao, K 2006 European Polymer Journal. 42 p 2013-2022.
15. Jiang H, Fang D, Hsiao B, Chu B, Chen W 2004 Journal of Biomaterials Science. 15 3 p 279-296.
16. Ohkawa K, Minato KI, Kumagai G, Hayashi S, Yamamoto H, 2006. Biomacromolecules. 7 11 p 3291–3294.
17. Geng X, Kwon O, Jang J 2005 Biomaterials 26 27 p 5427-5432.
18. Vitchuli N, Shi Q, Nowak J, Nawalakhe R., Sieber M, Bourham M, McCord M, Zhang X 2011 Plasma Chemistry and Plasma Processing 32 2 p 275-291.
19. Graham K, Gogins M, Schreuder-Gibson H 2004 INTC 2003, Technical Association of the Pulp & Paper Industry, September 15-18, 2003, Baltimore, MD.
20. Hwang YJ, Qiu Y, McCord MG 2006 Indian J. Fibre Text. Res.
21. Hwang YJ, An JS, McCord MG, Park SW, Kang BC 2005 Fabrics. Text. Res. J.75 11 p 771-778.
22. McCord MG, Qiu Y, Zhang C, Hwang YJ, Bures B 2002 Adhes. Sci. Technol. 16 1 p 99-107.
23. McCord MG, Hwang YJ, Kang BC 2005 Fiber and Polym. 6 2 p 113 - 120.
24. Cai Z, Qiu Y, Hwang Y, Zhang C, McCord MG 2003 J. Indust. Text. 32 3 p 223-232.

25. Hwang YJ, McCord MG, Kang BC 2005 Fiber Polym 6 2 p 113-120.
26. McCord MG, Hwang YJ, An JS, Park SW, Kang BC 2005 Textile Res. J. 75 p 771 - 778.
27. McCord MG, Hwang YJ, Qiu Y, Canup LK, Bourham MA 2003 J. Appl. Polym. Sci. 88 8 p 2038-2047.
28. Matthews SR, Hwang YJ, McCord MG, Bourham MA 2004 J. Appl. Polymer. Sci. 94 6 p 2383-2389.
29. ASTM D2261-Tearing strength of woven fabrics by tongue (Single Rip) Procedure (Constant-Rate-of-Extension Tensile Testing Machine).
30. ASTM F 392-93 2004 Standard Test Method for Flex Durability of Flexible Barrier Materials.
31. ASTM D737 - 04e1 2008 Standard Test Method for Air Permeability of Textile Fabrics.
32. ASTM E 96-80, Standard Test Methods for Water Vapor Transmission of Materials.
33. EN 13726:2002, Test methods for primary wound dressings-Part 1: Aspects of absorbency.
34. Reneker DH, Smith DJ 2006 United States Patent No. 0246798.

35. Mi FL, Wu YB, Shyu SS, Chao, AC, Lai, JY, Su, CC 2003 Journal of Membrane Science 212 p 237-254.
36. Coutts P, Sibbald, RG 2005 International wound Journal. 2 4 p 348-356.
37. Lionelli G, Thomas W 2003 Surg. Clin. N. Am. 83 3 p 617-638.
38. Gupta B, Arora A, Saxena S, Alam MS 2009 Polym. Adv. Technol., 20 p 58-65.
39. Bolton LL 2007 JWOCN 34 1 p 23-29..
40. McCord MG, Hwang, YJ, Qiu Y, Hughes LK, Bourham MA 2003 J. Appl. Polymer. Sci. 88 8 p 2038-2047.
41. Mitchell R, Carr CM 2005 Cellulose 12 6 p 629-639.
42. Narjès R, Michel N, Jean-Yves D, Richard F 2010 Chemistry and Materials Science. 17 1 p 25-32.
43. Dabney SE 2002 PhD Dissertation, The University of Akron, May, 2002.
44. Nametka M and Gibbins B 2002 presented at 17<sup>th</sup> ann. Clin. Symp. on adv. in skin and wound care, Dallas, TX, Sept 21-24.

## CHAPTER 5

### Novel Atmospheric Plasma Enhanced Silk Fibroin Nanofiber/Gauze Composite Wound Dressings

## 5.1 Abstract

Electrospun nanofiber dressings have demonstrated the potential to revolutionize wound care by providing significantly enhanced moisture management, barrier properties, and bioactivity. However, nanofiber webs are inherently weak and difficult to handle. Deposition of electrospun nanofiber coatings on conventional textile bandages addresses the need for structural support, but faces challenges of delamination due to compliance mismatch or poor adhesion. In this work, silk fibroin (SF) nanofibers were electrospun onto plasma-treated 100% cotton gauze bandages to form a novel silk-gauze composite wound dressing. Atmospheric pressure plasma treatment was used to increase the adhesion between the SF nanofibers and cotton substrates. The adhesion of the nanofibers to the substrates was assessed by qualitative and quantitative techniques. Moisture vapor transmission rate, X-ray photoelectron spectroscopy and air permeability tests were also conducted. Along with the plasma pre-treatment of substrate, effect of post-treatment on the composite bandages was also studied. Plasma pre-treatment of the substrate with 100% helium and 99% helium/1% oxygen plasmas showed up to a 50% increase in the force required to peel off the nanofiber layer. This force was further increased up to 75% after pre- as well as post-treatment of the composite bandages. Plasma pre-treatment of the gauze fabric prior to nanofiber deposition and post-treatment to the composite bandages significantly reduced degradation of the nanofiber layer during repetitive flexing. Air permeability and moisture vapor transport were significantly reduced due to the presence of a nanofiber layer upon the substrate. The results of surface elemental analysis showed that the adhesion and durability increase are mainly due

to the active species generated by plasma on the surface of cotton substrate as well as on the surface of the silk fibroin nanofibers.

**Keywords:** wound healing, adhesion, silk fibroin, nanofibers, wound dressings, bandages, atmospheric pressure plasma

## 5.2 Introduction

An ideal wound dressing should provide an environment in which healing and regeneration of tissues can take place at the fastest rate with an acceptable cosmetic appearance [1]. Traditional textile-based wound dressings are cost-effective and highly absorbent, but usually unable to provide optimal wound healing conditions such as hemostasis, non-adherence, maintenance of a moist wound bed, etc [1-2]. Advanced wound dressings, which have received great research interest in recent years, often incorporate multiple non-textile components including film, hydrocolloid, calcium alginate, foam wound dressing, etc that provide enhanced functionalities at a significantly higher cost [3-4]. The goal of this research is to combine the advantage of biopolymer nanofibers and traditional wound dressing fabrics to build novel composite wound dressing systems with desirable wound care abilities and mechanical properties. Polymers based on protein are of specific interest in healthcare applications because of their biocompatibility, combined strength and toughness. Silk fibroin (SF) is a natural protein, mainly consisting of amino acids with small side groups, such as glycine, alanine and serine. Previous studies on silk fibroin have shown excellent biocompatibility, biodegradability [6-13], high oxygen and water permeability [14-15], desirable drug permeability [16] and effective resistance against enzymatic degradation [17]. These properties make SF useful for a broad range of biomedical applications, including surgical sutures [18], skin treatments [19-20], wound dressing materials [21], cell culture substrates [13], controlled drug-delivery, cosmetics, and food additives [21-22]. In recent research on wound dressings, nanofibers demonstrated functional versatility, including desirable wound adherence, absorption, oxygen permeability, resorbability, and occlusivity

[23-25]. Nanofiber webs have high surface-area-to-volume ratios, which render them effective as filters of contaminants, particulates, and microorganisms, and as matrices for controlled drug release. Due to their small interstices and high surface area, nanofibers can assist in hemostasis [26-27]. As compared with conventional fibers, the high specific surface area of nanofibers has been shown to increase fluid absorption by up to 213% [28]. High porosity nanofiber wound dressings are ideal for respiration of cells and at the same time prevent wound desiccation [29]. According to Martindale [30], electrospun wound dressings can reduce scarring and encourage normal skin growth. However, widespread use of nanofiber webs in wound dressings has been limited by the challenges such as poor mechanical properties and difficulty in handling [31-32].

Researchers have studied processing parameters and morphology of SF nanofibers [33-35] electrospun using hexafluoroacetone, hexafluoro-2-propanol and formic acid as solvents. SF nanofibers have been shown to be excellent substrates for cell growth [36]. Xia et al. [37] have tried to improve the antibacterial properties by blending SF with other materials such as titanium dioxide. DermaSilk<sup>®</sup>, is a commercially available sericin-free silk fabric treated with an antibacterial finish, AEGIS AEM5772/5. This product has been used in the treatment of Atopic Dermatitis [38]. The effects of O<sub>2</sub> and methane plasmas on cell viability and water contact angle of silk nanofiber webs have been investigated [39]. However, studies on electrospinning of SF nanofibers on gauze fabric, adhesion between nanofibers and substrate, and mechanical properties of the nanofiber web have not been reported.

Atmospheric pressure plasma technology has been widely used to modify the structures and properties of various materials, especially textile materials. Previous studies in our

atmospheric plasma lab have shown that plasma treatment can i) improve surface bonding or adhesive ability [40-42], ii) increase mechanical strength by crosslinking [41-46], iii) change fiber surface hydrophobicity [47], iv) roughen fiber surfaces [48], and v) increase crystallinity [48]. Recently, Vitchuli et al. [31] successfully utilized the plasma technology to increase the adhesion between nylon nanofibers and substrates. Plasma treatment proved to be able to enhance the bonding between nanofiber mats and textile substrates through the pre-deposition surface activation of textile substrates, and improve the nanofiber strength and bonding through post-deposition crosslinking, thereby imparting increased mechanical strength and durability to the nanofiber mat.

The aim of this research is to produce mechanically strong, highly absorbent, biocompatible composite wound dressings. In this study, the composite bandages were created by electrospinning SF nanofiber webs onto plasma-treated 100% cotton gauze substrates. In addition, plasma post-treatment was applied to the composite bandages, i.e., nanofibers electrospun onto plasma pre-treated/untreated cotton substrate. The composite materials were characterized to determine:

- Effects of plasma pre-treatment of the substrate and effect of plasma post-treatment of the composite bandages on the bonding between nanofiber mats and textile substrates,
- Air permeability,
- Moisture Vapor Transport Rate, and
- Surface chemistry of the plasma treated SF nanofibers and the cotton substrate.

## **5.3 Materials and Methods**

### **5.3.1 Materials**

Raw silk (Grade 5A produced in Brazil) was degummed before electrospinning. Sericin was removed from raw silk in boiling water with 0.25 % (w/v) sodium lauryl sulfate and 0.25% (w/v) sodium carbonate, bath ratio of 1:100 (w/v), for 1 hour. Fibroin obtained after this treatment was washed in boiling water for 1 hour to remove leftover sericin and surfactants, and then rinsed with distilled water. Degummed silk was used for electrospinning onto a 100% cotton gauze substrate (Carolina Narrow Fabric Co. Inc.) cut into dimensions of 5cm × 1cm. Trifluoroacetic acid (Sigma Aldrich) was selected as the solvent.

### **5.3.2 Electrospinning of nanofiber webs onto substrates**

Electrospinning of SF nanofibers was carried out using the electrospinning setup with collecting rotating drum as shown in the picture of Figure 5.1. The setup consisted of a syringe pump (New Era Pump System, Inc.), collecting rotating drum, and a high voltage power supply (Gamma High voltage Res. Inc.). Syringe was filled with the solution of SF in TFA and was fixed to the extrusion system. Extrusion system was used to control the feed rate of the spinning solution and was maintained at 1 ml/hr. A positive charge was applied to the tip of the needle by fixing a high voltage power supply of 25 kV. The collection system for the nanofibers included a cylindrical polyvinyl chloride (PVC) drum (5.2 cm in diameter and 16.3 cm in circumference) with a grounded metal ring at one end. The speed of the drum was maintained at 20 rpm, i.e., surface speed of 3.3 m/min using a motor. Because PVC is a non-conducting material, a metal rod was attached to the ring and ran along the length of the cylinder. In order to make the rotating drum surface conductive, aluminium foil was wound

over the drum in contact with the metal rod. The textile substrate was then wrapped around the aluminium foil to enable deposition of electrospun nanofibers onto it.

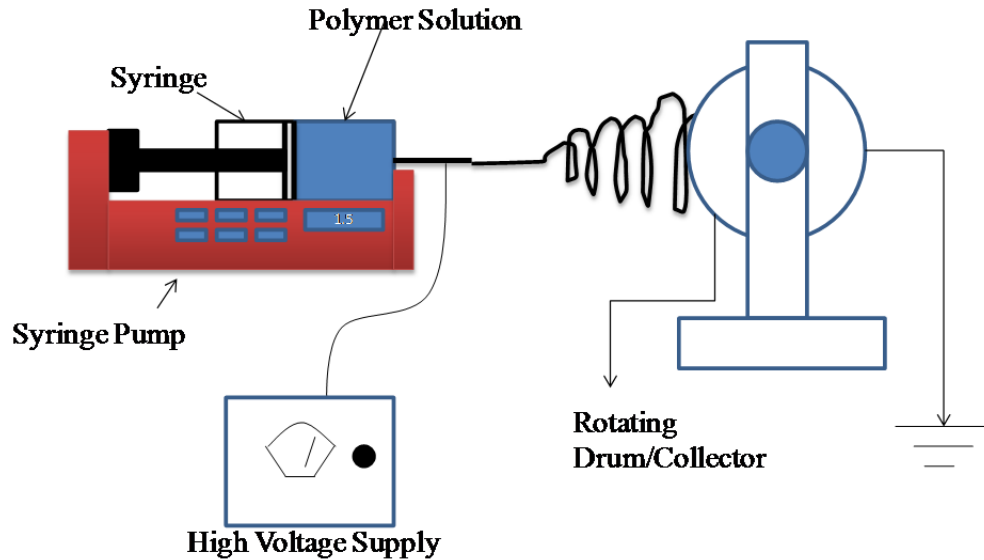


Figure 5.1 Depositing nanofibers onto the fabric by rotating collector.

### 5.3.3 Plasma pre-treatment of Substrate and post-treatment of composite bandages

The atmospheric pressure audio frequency glow discharge system (NCAPS) was designed and developed at North Carolina State University. The capacitively-coupled dielectric-barrier-discharge (DBD) consists of two parallel copper electrodes, each embedded within a Lexan polycarbonate insulator as shown in Figure 1. The device has an active exposure area of approximately  $60 \times 60 \text{ cm}^2$  between two copper electrodes with an adjustable 5 cm gap separation. The dielectric-barrier non-equilibrium discharge generates a low-temperature (1-2 eV), low electron number density ( $10^{14}$ - $10^{16} / \text{m}^3$ ) pseudo-glow discharge plasma, which is

typical for dielectric-barrier discharges at atmospheric pressure. Stable and uniform plasma was achieved at low (audible) frequency, 1.373 kHz during the operation. The voltage across the plates was ~6.3 kVrms and 7.6 kVmax for 100% He plasma and ~6.6 kVrms and 7.85 kVmax for 99% He plus 1% O<sub>2</sub>. A gas flow of 20 lit/min for helium gas and 0.3 lit/min for oxygen gas was used.

Two types of protocol were followed. In the first case, the fabrics were pre-treated with 100% He- plasma or 99%He/1%O<sub>2</sub> plasma prior to electrospinning. The gauze substrates were placed on a nylon grid suspended in the middle of the test cell to enable complete and uniform plasma exposure from all sides. In the second case, plasma pre-treated/untreated gauze fabric coated with SF nanofiber web was treated in the plasma chamber. These samples will be referred to as plasma post-treated samples. The ability of atmospheric plasma treatment to enhance adhesion and durability of the composite bandage was investigated by characterization of four sample sets:

- 1) No plasma pre-treatment of the substrate and no plasma post-treatment of the composite bandages,
- 2) Plasma pre-treatment of the substrate and no plasma post-treatment of the composite bandages,
- 3) No plasma pre-treatment of the substrate and plasma post-treatment of the composite bandages, and

4) Plasma pre-treatment of the substrate and plasma post-treatment of the composite bandages.

The adhesion force between nanofibers and substrates, moisture vapor transmission rates, air permeabilities, and surface chemical composition (via XPS) were subsequently evaluated for each group of materials.

#### **5.3.4 Adhesion between Nanofiber Mats and Supporting Fabrics**

A quantitative method (90° peel test) was devised to study the effect of atmospheric pressure plasma on adhesion between SF nanofibers and gauze fabrics. The peel test method was based on ASTM D2261-*Tearing strength of woven fabrics by tongue (Single Rip) method* [49] using an Instron Tensile Tester, which allows the user to control the rate of delamination and the locus of failure. The SF nanofiber mat sample, dimension: 50 mm × 10 mm, was held by the movable grip of the Tensile Tester and the fabric substrate held by the stationary grip. To facilitate proper peeling and avoid grip slippage, short tapes were attached to the nanofiber mat and fabric substrate. These tapes were held by Instron tensile tester grips. The speed of the upper jaw was kept constant at 50 mm/min. A 50 gm load cell with a gauge length of 1.27 cm was used to measure the force of adhesion. Prior to testing, the composite bandages were conditioned at standard temperature of  $20 \pm 1$  °C and relative humidity (RH) of  $65 \pm 2$  % for at least 8 hours. For each sample, 6-8 specimens were tested on Instron Tensile Tester and the average force to peel the nanofiber layer away from the substrate was recorded.

In order to assess the ability of nanofiber mats electrospun on the substrate to withstand repetitive strain, Gelbo Flex testing was employed (modification of ASTM F 392-93, *Standard Test Method for Flex Durability of Flexible Barrier Materials* [50]). Nanofiber-deposited fabric samples of size 5 cm × 1 cm were attached to two circular clamping disks, via hose clamps, and the samples were twisted and flexed for 1000 cycles. Results of Gelbo Flex testing provided a visual adhesion assessment which was observed under (JEOL 6400F Field Emission SEM). Prior to testing, the nanofiber-deposited fabric samples were conditioned at standard temperature of  $20 \pm 1$  °C and RH of  $65 \pm 2$  % for at least 8 hours.

### **5.3.5 Air Permeability**

Air permeability plays an important role in keeping the wound moist and its healing. The air permeability of electrospun fiber-deposited fabrics was measured using a Frazier air permeability testing instrument (Frazier Precision Instr Co. MD). The measurement was carried out according to ASTM D737-04 *Standard Test Method for Air Permeability of Textile Fabrics* [51], with a 1.4 mm and 2 mm orifices for composite bandages, an 8 mm orifice for cotton gauze (since it has a more open structure than composite bandages), 6.45 cm<sup>2</sup> test area, at 760 mm mercury pressure, 21° C, and 65% RH. An average of 10 readings of differential pressure from different parts of the composite bandages was recorded from the vertical manometer. Final results of air permeability of gauze fabric and composite wound dressing were obtained by matching the tabular values of orifice diameter in mm and differential pressures from the vertical manometer.

### 5.3.6 XPS Analysis of Substrate and SF Nanofibers after Plasma Treatment

X-ray photoelectron spectroscopy (XPS) was carried out to investigate the changes in the surface chemical composition of 100% cotton gauze substrate and SF nanofibers as a result of plasma treatment and changes in plasma parameters (percentage of helium and oxygen). XPS data were taken using a Riber LAS-3000 with MgK $\alpha$  excitation (1254 eV). Energy calibration was established by referencing to adventitious Carbon (C1s line at 284.5 eV binding energy). A take-off angle of  $\sim 75^\circ$  from the surface was used with an X-Ray incidence angle of  $\sim 20^\circ$  and an x-ray source to analyzer angle of  $\sim 55^\circ$ . Base pressure in the analysis chamber was in  $10^{-10}$  Torr range. CASA XPS software was used for data reduction.

### 5.3.7 Moisture Vapor Transmission Rate

Moisture vapor transmission rates (MVTR) for the samples (100% gauze with and without silk nanofibers) were measured at the standard temperature and humidity ( $20 \pm 1^\circ\text{C}$  and 65% RH). The rate of moisture vapor diffusion through the material was determined according to the Simple Dish Method, similar to ASTM E96-80, *Standard Test Method for Water Vapor Transmission of Materials* [52]. A sample was placed on a water dish (82 mm in diameter and 19 mm in depth) with a 9 mm air space between the water surface and specimen. A vibration free turntable with 8 dishes, rotating at a uniform speed of 5 m/min was used to ensure that all dishes were exposed to the same average ambient conditions during the test. The specimen dishes were allowed to stabilize for two hours before taking the initial weight. The final weight was measured after a 24 hour interval. The MVTR values were calculated in units of  $\text{g/m}^2\text{-24 hours}$ . The experiment was repeated 5 times for each sample.

## 5.4 Results and Discussion

### 5.4.1 Electrospinning of SF nanofibers

Silk nanofibers were electrospun in trifluoroacetic acid (TFA) for 2 hrs with an extrusion rate of 1 ml/hr, applied voltage of 25 kV, and distance of 15 cm between the rotating drum and the needle tip. The concentration varied from 5 to 10 wt%. The average diameters of nanofibers obtained in the range of 5 - 10% concentrations were 95, 220, 560, 620, 1270, and 1760 nm, respectively, as shown in Figure 5.2. In order to create a robust nanofiber layer, 9% concentration was selected for the further experiments to get sturdy structure and higher production of nanofibers. All further experiments were performed at that concentration. Concentrations above 9% were not considered because the increase of average diameter will significantly decrease the specific surface area and porosity of the nanofiber web.

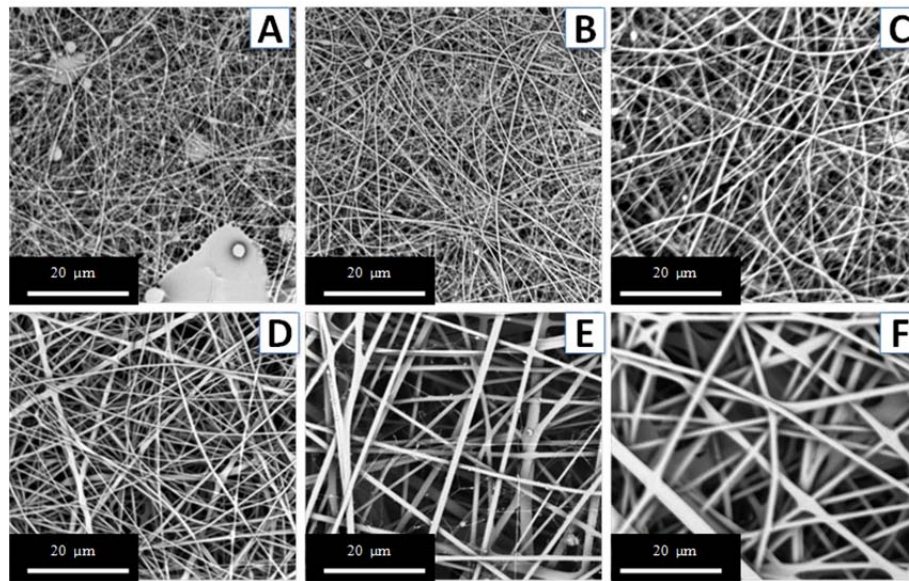


Figure 5.2 SEM images of SF nanofibers electrospun at concentrations of A) 5%, B) 6%, C) 7%, D) 8%, E) 9%, F) 10% in TFA. Magnification: 2500 ×.

### 5.4.2 Peel test

Table 5.1 shows the average adhesion strengths between SF nanofiber mats and cotton gauze fabric substrates. It was observed that after treating the substrates with 100% helium plasma and 99% helium/1% oxygen plasma, the forces required to peel off the nanofiber layers from the substrates increased by up to approximately 50% as compared to untreated controls. In this case, there was no post-treatment of the composite. The increase in interfacial adhesion can be attributed to the formation of free radicals and active species at the surface of cotton substrate. These active sites are available for the crosslinking between the cotton fibres and the SF nanofibers.

As shown in Table 5.1, He-plasma post-treatment showed an approximately 75% increase in adhesion as compared with the composite bandages without any plasma pre- or post-treatment. This can be explained by the fact that more active sites were found on both the cotton substrate as well as on the silk fibroin nanofibers when composite bandages were exposed to He-plasma (see XPS section below). He/O<sub>2</sub> plasma post-treatment also showed better adhesion as compared to the control sample. A detailed mechanism is proposed below (see sections 5.4.6 and 5.4.7).

Table 5.1. Load (gf) required to peel the SF nanofiber layer off the substrate.

	<b>No post-treatment (gf)</b>	<b>He post-treatment (gf)</b>	<b>He/O<sub>2</sub> post-treatment (gf)</b>
<b>No pre-treatment</b>	29.2 ± 4.2	52.37 ± 5.5	37.53 ± 4.9
<b>He pre-treatment</b>	39.47 ± 2.1	41.33 ± 5.5	42.43 ± 6.0
<b>He/O<sub>2</sub> pre-treatment</b>	41.94 ± 3.0	48.65 ± 6.3	44.25 ± 8.8

For the case of both pre-treatment of substrate and post-treatment of composite bandages, the increase in adhesion was greater than the adhesion increase observed for the case of pre-treatment of the substrate without post-treatment of the composite. Applying both pre- and post-treatment on composite bandages should lead to greater exposure to atmospheric pressure plasma, hence more radicals and chemical species interacting with the fabric substrate as well as with the SF nanofibers to generate more active surface sites. This combination of plasma-induced surface activities on nanofibers and substrates helps to improve the interfacial bonding between them through formation of covalent bonds. Increased adhesion after plasma treatment may also be explained by the increased frictional force between two layers due to increased surface roughness, although this was not assessed in this study. Amongst all the treatments, it was found that He-plasma post-treatment in combination with pre-treatment with He or He/O<sub>2</sub> plasma was most effective in increasing the interfacial adhesion.

### 5.4.3 Gelbo Flex Test

To evaluate the ability of SF nanofiber layer on the composite bandage to withstand repetitive flex forces, gelbo flex testing was performed on the samples and their morphology after testing was observed in SEM at 15× magnification as shown in Figure 5.3.

It was observed that the nanofiber layer was badly damaged after 1000 cycles in the case of untreated substrate (Figure 5.3 A), whereas it showed much better durability when the substrate was pre-treated by plasma (Figures 5.3 D and G). For the case of no pre-treatment with plasma post-treatment of composite bandages, durability also improved (Figures 5.3 B and C). The best results were obtained with a combination of plasma pre-treatment and post-treatment (Figures 5.3 E, F, H and I). When the composite bandages were given a pre-treatment to the substrate and post-treatment to the composite bandages, it was observed that the nanofiber layer was least damaged. The rolling off of the nanofibers from the top layer showed that in spite of having vigorous flexing of 1000 cycles, the bottom of the layer was still intact and firmly adhered to the substrate.

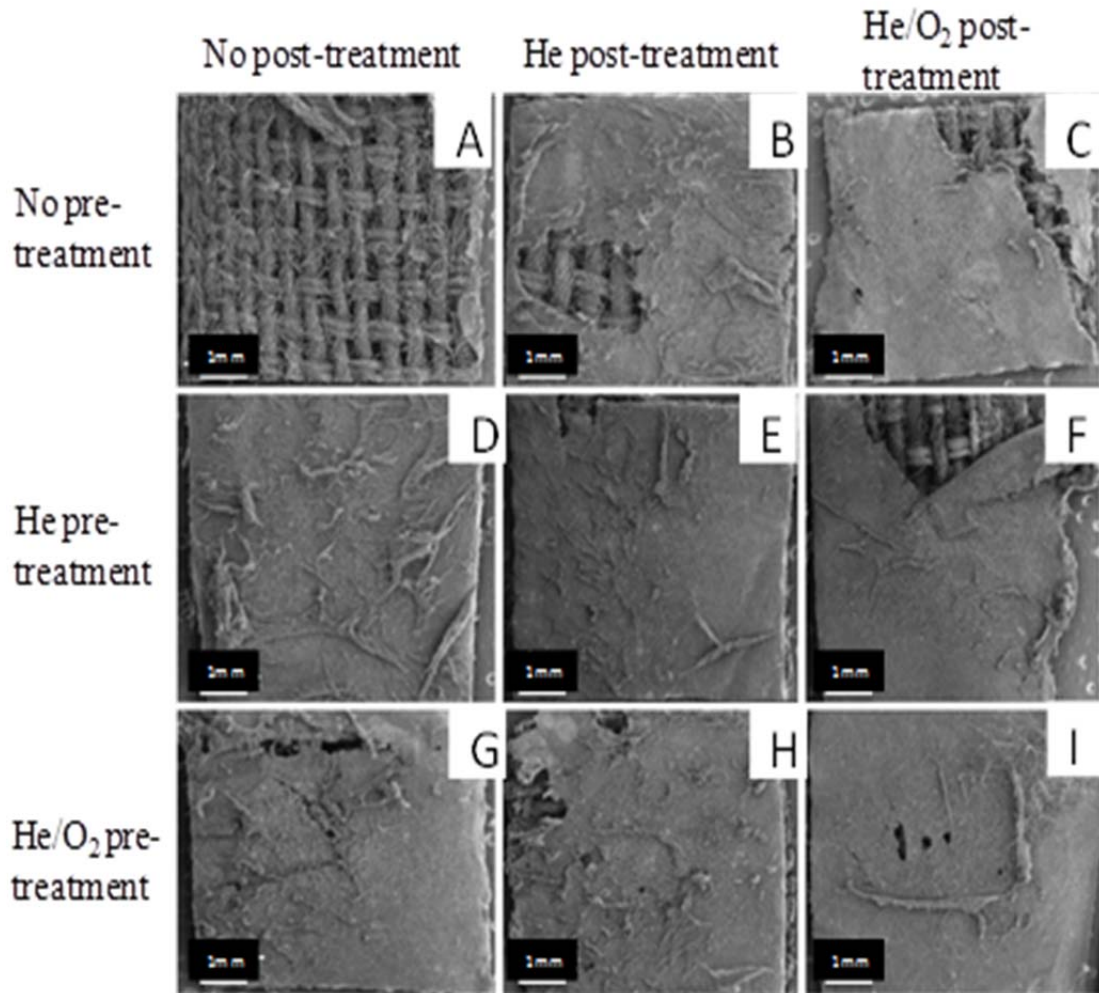


Figure 5.3. Distortion of SF nanofibers after 1000 cycles of Gelbo flex test, electrospun on 100% cotton gauze. First row: no plasma pre-treatment, second row: He plasma pre-treatment, third row: He/O<sub>2</sub> plasma pre-treatment. First column: no plasma post-treatment, second column: He plasma post-treatment, third column: He/O<sub>2</sub> plasma post-treatment.

It can be concluded from both the quantitative (peel test) and qualitative (gelbo flex test) analysis that the plasma pre-treatment of the substrate significantly increased the adhesion between the nanofibers and substrate gauze. This effect was further enhanced after the post-treatment of the composite bandages. The increase in adhesion between nanofibers and

substrates can be attributed to possible crosslinking between them, via surface free radicals or functional groups, and to mechanical interactions resulting from increased surface roughness.

#### **5.4.4 Air Permeability**

Moisture management is critical to wound healing, and is governed by factors including air permeability, moisture vapor transmission and fluid absorbency. While too much moisture in the bandage microclimate results in maceration, too little moisture results in wound desiccation. Both conditions have been demonstrated to delay wound healing. Compared to a wound left open to heal in air, a wound occluded under a transparent film has a higher rate of epithelialization [1, 53].

Gupta et al. [54] studied the air permeability of cotton fabric and cotton fabric covered with chitosan film. It was reported that, air permeability of approximately  $8.6 \text{ cm}^3/\text{cm}^2/\text{sec}$  would help in maintaining the wound moist without getting it macerated. Air permeability of substrate with and without SF nanofibers was measured.

Plain gauze fabric with no SF nanofibers showed a high air permeability of  $265.68 \text{ cm}^3/\text{cm}^2/\text{sec}$  (Table 5.2), whereas the air permeability of untreated ( $8.8 \text{ cm}^3/\text{cm}^2/\text{sec}$ ), He ( $16.2 \text{ cm}^3/\text{cm}^2/\text{sec}$ ) and He/O<sub>2</sub> ( $17.2 \text{ cm}^3/\text{cm}^2/\text{sec}$ ) plasma treated substrates with SF nanofibers showed decreased air permeabilities. The decrease in air permeability is expected to aid in keeping the wound moist and result in better wound healing.

#### **5.4.5 Moisture Vapor Transmission Rate (MVTR)**

MVTR is a key property of wound dressings that directly affects the maintenance of an appropriately moist wound bed. A higher MVTR indicates a high rate of evaporation through

the composite wound dressing, which could result in drying of the wound. Bolton et al. [55] studied a variety of dressings and determined that an MVTR of less than 840 g/m<sup>2</sup>/day is required to maintain a moist wound surface. MVTR's of plain gauze, untreated gauze with SF nanofibers, and plasma pre-treated gauze with SF nanofibers are listed in Table 5.2.

Table 5.2. Average Air Permeability and Moisture Vapor Transmission Rate (MVTR) of the composite wound dressing: SF nanofibers electrospun on untreated, He-plasma treated and He-O<sub>2</sub> plasma treated cotton substrate.

<b>Sample</b>	<b>Air permeability ( cm<sup>3</sup>/cm<sup>2</sup>/sec )</b>	<b>MVTR g/m<sup>2</sup>/day</b>
Only Gauze	265.68 ± 7.87	885.36 ± 18
Gauze + SF nanofibers	8.8 ± 0.23	735.42 ± 17
He-Plasma pre-treated gauze + SF nanofibers	16.2 ± 0.61	752.08 ± 16
He/O <sub>2</sub> plasma pre-treated gauze + SF nanofibers	17.2 ± 0.57	711.62 ± 22

Plain gauze had a significantly higher MVTR than plasma treated or untreated composite materials. Due to additional layer of SF nanofibers on the top of gauze fabric and SF being hydrophilic it restricts the moisture transfer from the composite bandages. Therefore presence of nanofibers would reduce the MVTR of gauze fabric. Plasma treatment of the substrate did not appear to affect the MVTR. It is expected that decreased moisture vapor transmission will be helpful in maintaining wound moisture and preventing dehydration.

#### **5.4.6 XPS Analysis of Substrate after Plasma Treatment**

XPS spectroscopy was used to study the chemical composition of the cotton gauze (with or without plasma treatment) which was used as the substrate in the composite wound dressing.

Pure cellulose has a carbon content of 66.9 % [47]. Table 5.3 shows the carbon content of cotton fiber to be 84.88%. This atypical cellulose composition may be due to the presence of residual long chains of hydrocarbons [56] on the cotton fiber surface which remain even after aqueous processing or may be due to the composition of the cotton fiber outer wall which consists of mixture of fats, waxes and resin [57]. As indicated by the XPS result, carbon content (C1s) decreased after plasma treatment (Table 5.3). This is likely due to the removal of some of the long chain hydrocarbons from the surface as the result of plasma treatment, which is more pronounced for the He treated substrate than for the He/O<sub>2</sub> plasma treated sample. This process is likely to generate roughness on the surface of cotton, which is expected to increase frictional forces between cotton fabric and nanofibers to be deposited on them.

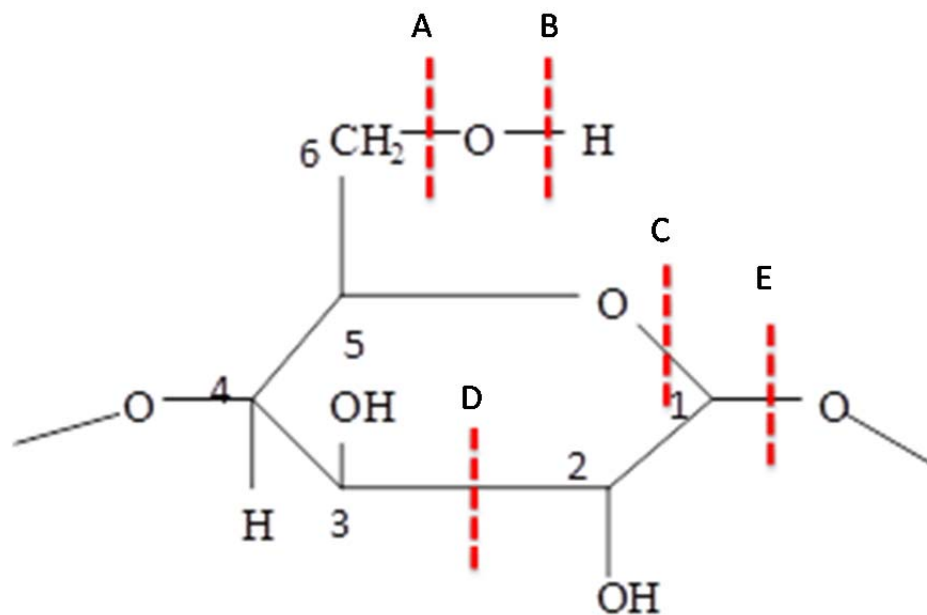


Figure 5.4. Possible sites for scission of cotton substrate after plasma treatment A) Dehydroxylation, B) Dehydrogenation, C) scission between C1 and ring oxygen, D) dehydrogenation/dehydroxylation, E) scission between C1 and glycosidic oxygen.

Oxygen content of the cotton substrate was increased from 15.12 % to 22.38 % and 18.82 % after He- and He/O<sub>2</sub> plasma treatment, respectively. Higher oxygen content can be explained by the scission at site 'B' from the cellulosic ring as shown in Figure 5.4. The scission at sites 'C' and 'E' produced radicals that could react with active groups of the SF nanofibers. In addition, dehydrogenation or dehydroxylation at site 'B' and 'A' in -C-O-H groups (Figure 5.4) on cellulose can make cotton substrate susceptible to react with SF nanofibers at C6. Due to abundance of hydroxyl groups on SF as well as on cotton substrate generated by plasma, there are high chances of hydrogen bonding at the nanofiber- substrate interface.

Table 5.3 Elemental and chemical composition of substrate with and without plasma treatment.

100% cotton Substrate	Overall Elemental analysis (%)		C-spectra (%)		
	O	C	C-C	C-O	COO-
No treatment	15.12	84.88	85	14	1
He Plasma	22.38	77.62	82	9	9
He-O <sub>2</sub> plasma	18.82	81.18	82	8	10

The increase in oxygen content was more significant for the He plasma treated substrates than for the He/O<sub>2</sub> plasma treated samples. C1s spectral analysis showed an increase in substrate COO- groups (289.1eV) which would be available for reaction with -OH and -NH groups of SF nanofibers.

#### 5.4.7 XPS analyses of silk fibroin nanofibers

To study the effect of plasma post-treatment, SF nanofibers were also analyzed using XPS spectroscopy to study the surface chemical structure before and after plasma treatment.

Table 5.4 shows the surface chemical composition of untreated, He and He/O<sub>2</sub> plasma treated SF nanofibers. The XPS spectra of the SF nanofibers after the plasma treatment showed three strong peaks in the region of 200–600 eV. The first (290 eV), second (400 eV) and third peaks (530 eV) were assigned to C1 s, N1 s and O1 s, respectively. Table 5.4 shows C1 spectra, N1 spectra and overall elemental composition of SF nanofibers with and without plasma treatment. C1s spectral analysis showed formation of new groups. The intensities of C-C (285.0 eV) and C-N bonds decreased with both the plasma treatments. This is probably due to the creation of free radicals on the surface of SF nanofibers (Figure 5.5). The percentage of N-C=O (288 eV) bonds increased due to plasma treatment, as shown in Table 5.4. The increases in N-C=O and N-H bonds after plasma treatment are likely due to scission of the C-C linkage (Figure 5.6) from -HN-C-CO-NH- group. Etching of the surface of silk nanofiber may also play a role in increasing the frictional force between SF nanofibers and cotton substrate; however, this was not assessed in this study.

Table 5.4 Results of chemical composition of C1s, N1 peaks and overall elemental analysis for treated and untreated SF nanofibers with atmospheric pressure plasmas.

SF Nano-fibers	C1 - spectra (%)				N1 - spectra (%)		Overall Elemental analysis (%)		
	C-O/C-N	C-C/C-H	N-C=O	C=O	N-H	N-C	O	C	N
<b>Un-treated</b>	20.57	32.66	10.73	36.04	82.87	17.13	21.26	61.28	17.45
<b>He Plasma</b>	21.63	27.05	11.70	39.62	85.38	14.62	26.71	57.45	15.83
<b>He-O<sub>2</sub> plasma</b>	15.40	24.40	28.41	31.80	93.06	6.94	22.67	61.23	16.06

N1 spectra of untreated and plasma treated SF nanofibers showed increased percentages of N-H groups (85.38% and 93.06 %) and decreased percentages of N-C (14.62% and 6.94% ) groups when treated with He and He/O<sub>2</sub> plasma. This clearly indicates scission of C-N bond from -HN-C-CO- linkage and formation of free radicals on the surface of SF nanofibers. Both of these effects will result in possible crosslinking/covalent bonding between active groups of SF (-NH and -OH groups) and the cotton substrate (C6, C1, C2, C3 or oxygen ring).

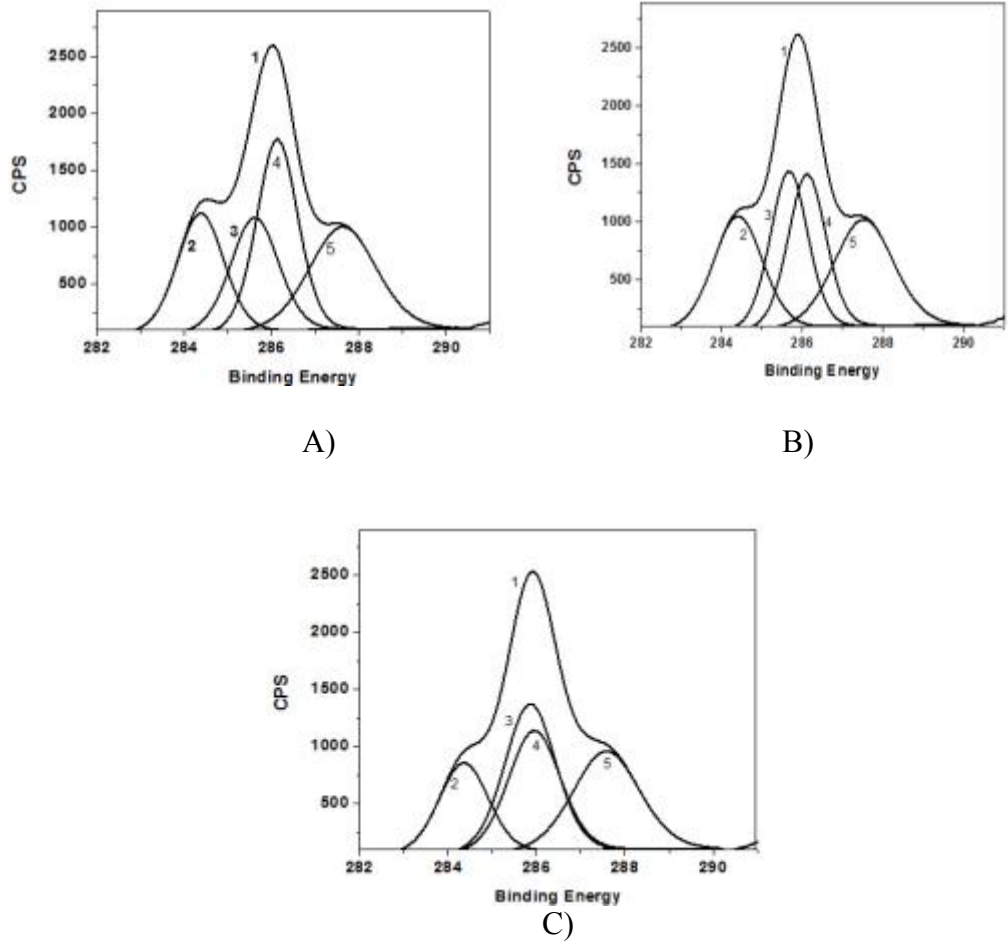


Figure 5.5. Chemical composition of plasma-treated and untreated silk fibroin nanofibers with Atmospheric A) Untreated, B) He-plasma treated and C) He/O<sub>2</sub> plasma treated SF nanofibers .1: Envelope, 2: C=O, 3: C=O/N-C=O, 4: C-O/C-N, 5: C-C/C-H.

In addition, SF nanofibers treated by He- and He/O<sub>2</sub>- plasmas exhibited relatively higher amounts of oxygen-containing chemical groups than those untreated with plasma. Oxygen content is higher for He- plasma treated nanofibers than for He/O<sub>2</sub> plasma treated nanofibers, which indicates higher number of active site on the surface of nanofibers available for cross-linking with nanofibers. This is reflected in the higher force is required to peel the nanofibers from the substrate in case of the He-plasma post-treated composite bandages.

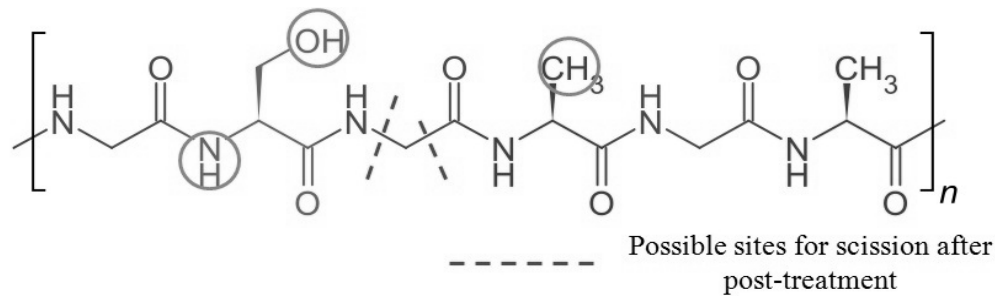


Figure 5.6. Possible sites for scission after plasma treatment of SF nanofibers.

Encircled regions in Figure 5.6 show the available sites for cross-linking and hydrogen bonding between SF nanofibers and cotton substrate. The surface activation of SF nanofibers by post plasma treatment can lead to the hydrogen bonding between  $-OH$  and  $-NH$  groups of SF nanofibers and  $-OH$  groups of the cotton substrate. As it can be seen in Table 5.4, the percentage of C-H groups was reduced from 32.66% to 27.05% and 24.40% after treating the composite bandages with He-plasma and He/O<sub>2</sub> plasma, respectively. Reduction in C-H groups is expected to lead to the formation of free radicals which are available for cross-linking with the cotton substrates.

Thus, formation of active sites on the surfaces of the SF nanofibers and substrates, chain scission, hydrogen and covalent bonding, creating of roughness on the surface and interfacial cross-linking between SF nanofibers and cotton substrates are responsible for increased interfacial adhesion after pre-treatment of substrates and post-treatment of composite bandages.

## 5.5 Conclusion

In this work, we prepared an effective novel composite wound dressing by enhancing gauze fabric with a layer of SF nanofiber, and improved the durability of the composite via plasma pretreatment of the gauze substrate prior to electrospinning and plasma post-treatment after electrospinning. SF nanofibers were electrospun onto 100% cotton gauze substrates to form composite bandages. Atmospheric pressure plasma treatment was utilized to improve the adhesion and durability of the nanofiber coating. Substrates were pre-treated with atmospheric plasma prior to electrospinning of SF nanofibers to study the effect of pre-treatment and plasma post-treatment was performed on composite bandages to study effect of plasma post-treatment. The durability and adhesion of the nanofibers to the substrates was investigated using peel tests and Gelbo Flex tests. Other properties evaluated included MVTR, surface chemical composition via XPS (X-ray photoelectron spectroscopy), absorbency and air permeability. The peel test showed that plasma pre-treatment of the substrates and plasma post-treatment of composites with 100% He-plasma and 99% He/1% O<sub>2</sub>-plasma increased the forces required to peel off the nanofiber layer. This confirmed that the pre-treatment of the substrate with atmospheric plasma followed by electrospinning of SF nanofiber produced durable composite bandages. The peel force required to peel the nanofibers off the pre-treated substrate was further increased after post treatment of the composite bandages. These results were supported by the Gelbo flex testing carried out on the composite bandages. Air permeability and moisture vapor transport were reduced due to the presence of a nanofiber layer upon the substrate which is expected to aid in keeping the wound moist, resulting in better wound healing. The results of surface elemental analysis of

the cotton substrate showed formation of oxygen rich active sites on the surface after plasma treatment. Plasma treatment creates surface oxidation, which may be responsible for the crosslinking and formation of covalent bonds between the substrate and SF nanofibers. Surface analysis of SF nanofibers showed that SF nanofibers treated by He- and He-O<sub>2</sub> plasma contained higher amounts of oxygen-containing chemical groups than untreated substrates. Study of C1 spectra and N1-spectra of SF nanofibers showed scission of C-C and C-N linkages which indicates the formation of radicals on the surface and etching of the surfaces of SF nanofibers.

## **5.6 Acknowledgement**

The authors wish to acknowledge the National Textiles Center for funding this research. Facilities and resources at the NCSU College of Textiles and the Department of Nuclear Engineering were utilized to complete this research.

## 5.7 References

- 1) Thomas S. "Wound Management and Dressings," Pharmaceutical Press, London. 1990.
- 2) Baranoski S. Choosing a wound dressing, part 2, Wound and Skin Care. 2008; January: 60-61.
- 3) Mlekusch W, Dick P, Haumer M, Sabeti S, Minar E, Schillinger M. J Endovasc Ther. Arterial Puncture Site Management After Percutaneous Transluminal Procedures Using a Hemostatic Wound Dressing (Clo-Sur P.A.D.) Versus Conventional Manual Compression: A Randomized Controlled Trial, 2006; 13, 1: 23-31.
- 4) Baranoski S. Choosing a wound dressing, part 2, Wound and Skin Care. 2008; February: 14-15.
- 5) <http://jan.ucc.nau.edu/~daa/woundproducts/products.html>
- 6) Ha, Sung-Won, Structural Study of Bombyx mori Silk Fibroin during Processing for Regeneration, Ph. D dissertation at North Carolina State University, 2004.
- 7) Sofia S, McCarthy MB, Gronowicz G, Kaplan DL. Functionalized Silk based Biomaterials for Bone Formation. Biomed Mater Res, 2001, 54: 139-148.
- 8) Bunning TJ, Jiang H, Wade Adams W, Crane RL, Farmer B, Kaplan DL. Applications of Silk. Mat. Sci. and Biotechnol. ACS Symp Series 544 Washington D.C., 1994, 353-358.
- 9) Liu Y, Zhang X, Liu H, Yu T, Deng J. Immobilization of Glucose Oxidase onto the Blend Membrane of poly(vinyl alcohol) and Regenerated Silk Fibroin: Morphology and Application to Glucose Biosensor. J Biotechnol, 1996, 46: 131-138.
- 10) Tsukada M, Freddi G, Minoura N, Allara G. Preparation and Application of Porous Silk Fibroin Materials. J Appl Polym Sci, 1994; 54: 507-514.

- 11) Gil ES. Stimuli-Responsive Protein-Based Hydrogels by Utilizing  $\beta$ -Sheet Conformation of Silk Fibroin as Cross-Links. Ph.D dissertation at North Carolina State University, 2004.
- 12) Nazarov R, Jin H, Kaplan D. Porous 3-D Scaffolds from Regenerated Silk Fibroin. *Biomacromol.* 2004, 5: 718-726.
- 13) Gotoh Y, Tsukada M, Minoura N, Imai Y. Synthesis of poly(ethylene glycol)-silk fibroin conjugates and surface interaction between L-929 cells and the conjugates. *Biomaterials* 1997, 18: 267-271.
- 14) Minoura N, Tsukada M, Nagura M. Fine Structure and Oxygen Permeability of Silk Fibroin Membrane Treated with Methanol. *Polymer* 1990, 31: 265- 269.
- 15) Minoura N, Tsukada M, Nagura M. Physico-chemical properties of silk fibroin membrane as a biomaterial. *Biomaterials* 1990, 11, 6: 430-434.
- 16) Chen J, Minoura N, Tanioka A. Transport of pharmaceuticals through silk fibroin membrane. *Polymer* 1994, 35: 2853–2856.
- 17) Gu J, Yang X, Zhu H. Surface sulfonation of silk fibroin film by plasma treatment and in vitro antithrombogenicity study. *Mat Sci and Eng C* 2002, 20: 199-202.
- 18) Vonfraunhofer JA, Sichina WJ. Characterization of surgical suture materials using dynamic mechanical analysis. *Biomaterials* 1992, 13: 715-720.
- 19) Padamwar MN, Pawar AP. Silk sericin and its applications: A review. *J Sci and Ind Res*, 2004, 63: 323-329.
- 20) Zhang YQ. Natural silk fibroin as a support for enzyme immobilization. *Biotechnol. Advances*, 1998, 16: 961-971.

- 21) Santin M, Motta A, Freddi G, Cannas M. In vitro evaluation of the inflammatory potential of the silk fibroin. *J Biomed Mat Res Part A*, 1999, 46: 382-389.
- 22) Effects of Some Electrospinning Parameters on Morphology of Natural Silk-Based Nanofibers *J Appl Polym Sci*, 2009, 113: 226–234.
- 23) Duan YY, Jia J, Wang SH, Yan W, Jin L, Wang ZY. Preparation of Antimicrobial Poly( $\epsilon$ -caprolactone) Electrospun Nanofibers Containing Silver-Loaded Zirconium Phosphate Nanoparticles, *J Appl Polym Sci*, 2007, 106: 1208-1214 .
- 24) Venugopal J & Ramakrishna S. Application of Polymer Nanofibers in Biomedicine and Biotechnology. *Appl Biochem Biotechnol*, 2005, 125: 147-157.
- 25) Jia J, Duan YY, Wang SH, Zhang SF & Wang ZY. Preparation and Characterization of Antibacterial Silver-Containing Nanofibers for Wound Dressing Applications. *J. US-China Med Sci*, 2007, 4, 2: 52-54.
- 26) Wnek GE, Carr ME, Simpson DG, Bowlin GL. Electrospinning of Nanofiber Fibrinogen Structures Gary E. Wnek,, Marcus E. Carr,, David G. Simpson, and, Gary L. Bowlin: *Nano Letters*, **2003**, 3, 2: 213-216
- 27) Martin GE and Cockshott ID. Fibrillar Product of Electrostatically Spun Organic Material, US Patent 4043331, 1977.
- 28) Dabney SE. The Use of Electrospinning Technology to Produce Wound Dressings, PhD Dissertation, The University of Akron, May, 2002.
- 29) Khil M, Cha D, Kim H, Kim I, Bhattarai N. Electrospun nanofibrous polyurethane membrane as wound dressing. *J Biomed Mat Res Part B: App Biomat*, 2003, 67, B: 675-679.

- 30) Martindale D, *Sci. Amer.* July 2000: 34–36.
- 31) Vitchuli N, Shi Q, Nowak J, Nawalakhe R., Sieber M, Bourham M, McCord M, Zhang X  
2011 *Plasma Chemistry and Plasma Processing* 32 2 275-291.
- 32) Graham K, Gogins M, Schreuder-Gibson H 2004 *INTC 2003*, Technical Association of  
the Pulp & Paper Industry, September 15-18, 2003, Baltimore, MD.
- 33) Zarkoob S, Eby RK, Reneker DH, Hudson SD, Ertley D, Adams WW. Structure and  
morphology of electrospun silk nanofibers. *Polymer* 2004, 45: 3973-3977.
- 34) Ohgo K, Zhao C, Kobayashi M, Asakura T. Preparation of non-woven nanofibers of  
*Bombyx mori* silk, *Samia cynthia ricini* silk and recombinant hybrid silk with  
electrospinning method. *Polymer* 2003, 44: 841-846.
- 35) Min B, Lee G, Kim SH, Nam YS, Lee TS, Park WH. Electrospinning of silk fibroin  
nanofibers and its effect on the adhesion and spreading of normal human keratinocytes  
and fibroblasts in vitro. *Biomaterials* 2004, 25: 1289-1297.
- 36) Minoura N, Aiba S, Gotoh Y, Tsukada M, Imai Y. Attachment and growth of cultured  
fibroblast cells on silk protein matrices. *J Biomed Mater Res* 1995, 29: 1215-1221.
- 37) Xia Y, Gao G, Li Y. Preparation and properties of nanometer titanium dioxide/silk  
fibroin blend membrane. *J Biomed Mater Res Part B: App Biomater* 2009, 90, B: 653-658.
- 38) Vlachou C, Thomas KS, Williams HC. A case report and critical appraisal of the  
literature on the use of DermaSilk® in children with atopic dermatitis. *Clin Exp Dermatol*  
2009, 34: e901-e903.
- 39) Jeong L, Yeo I, Kim HN, Yoon YI, Jang DH, Jung SY, Min B, Park WH. Plasma-treated  
silk fibroin nanofibers for skin regeneration. *Int J Biol Macromol* 2009, 44: 222-228.

- 40) Hwang YJ, Qiu Y, McCord MG. Adhesion Enhancement of Aramid Fiber using Atmospheric Pressure Plasma, *Indian J. Fibre Text. Res.* 2006
- 41) Hwang YJ, An JS, McCord MG, Park SW, Kang BC. The Effects of Helium Atmospheric Pressure Plasma Treatment on Low-stress Mechanical Properties of Polypropylene Nonwoven Fabrics, *Text. Res. J.* 2005; 75, 11: 771-778.
- 42) McCord MG, Qiu Y, Zhang C, Hwang YJ, Bures, B. The Effect of Atmospheric Pressure Helium Plasma Treatment on Surface and Mechanical Properties of Ultrahigh Modulus Polyethylene Fibers, *Adhes. Sci. Technol.* 2002;. 16, 1: 99-107.
- 43) McCord MG, Hwang YJ, Kang BC. Helium/Oxygen Atmospheric Pressure Plasma Treatment on Poly(Ethylene Terephthalate) and Poly(Trimethylene Terephthalate) Fabrics: Comparison of Low-Stress Mechanical Properties, *2005 Fiber and Polym.* 6, 2: 113 - 120.
- 44) Cai Z, Qiu Y, Hwang Y, Zhang C, McCord MG. The Use of Atmospheric Pressure Plasma Treatment in Desizing PVA on Viscose Fabrics, *J. Indust. Text.* 2003; 32, 3: 223-232.
- 45) Hwang YJ, McCord MG, Kang BC. Helium/Oxygen Atmospheric Pressure Plasma Treatment on Poly(Ethylene Terephthalate) and Poly(Trimethylene Terephthalate) Knitted Fabrics: Comparison of Low-Stress Mechanical/Surface Chemical Properties, *Fiber Polym* 2005; 6, 2: 113-120.
- 46) McCord MG, Hwang YJ, An JS, Park SW, Kang BC. The Effects of Helium Atmospheric Pressure Plasma Treatment on Low-Stress Mechanical Properties of Polypropylene Nonwoven Fabrics, *Textile Res. J.* 2005; 75: 771 - 778.

- 47) McCord MG, Hwang YJ, Qiu Y, Canup LK, Bourham MA. Surface Analysis of Cotton Fabrics Fluorinated in Radio-Frequency Plasma, *J. Appl. Polym. Sci.* 2003; 88, 8: 2038-2047.
- 48) Matthews SR, Hwang YJ, McCord MG, Bourham MA. Investigation into Etching Mechanism of Polyethylene Terephthalate (PET) Films Treated in Helium and Oxygenated-Helium Atmospheric Plasmas, *J. Appl. Polymer. Sci.* 2004; 94, 6: 2383-2389.
- 49) ASTM D2261-Tearing strength of woven fabrics by tongue (Single Rip) Procedure (Constant-Rate-of-Extension Tensile Testing Machine)
- 50) ASTM F 392-93, Standard Test Method for Flex Durability of Flexible Barrier Materials, 2004.
- 51) ASTM D737 - 04e1, Standard Test Method for Air Permeability of Textile Fabrics, 2008.
- 52) ASTM E 96-80, Standard Test Methods for Water Vapor Transmission of Materials.
- 53) Lionelli G, Thomas W. Lawrence, Wound Dressing, *Surg. Clin. N. Am.* 2003; 83, 3: 617–638.
- 54) Gupta B, Arora, A, Saxena S, Alam, MS. Preparation of chitosan–polyethylene glycol coated cotton membranes for wound dressings: preparation and characterization, *Polym Adv Technol*, 2009, 20: 58–65.
- 55) Bolton LL. Evidence-based Report Card: Operational definition of moist wound healing, *JWOCN* 2007; 34, 1: 23–29
- 56) Mitchell R, Carr CM. Surface chemical analysis of raw cotton fibers and associated materials, *Cellulose*, 2005, 12, 6: 629–639.

57) Narjès R, Michel N, Jean-Yves D, Richard F. Comparison of surfaces properties of different types of cotton fibers by inverse gas chromatography, Chem and Mat Sci, 2010, 17, 1: 25-32.

## Chapter 6

Electrospinning of Chitosan Nanofibers: Improving its Mechanical Properties and Adhesion  
with the Cotton Gauze with the help of Atmospheric Pressure Plasma

**Electrospinning of Chitosan Nanofibers: Improving its Mechanical Properties and Adhesion with the Cotton Gauze with the help of Atmospheric Pressure Plasma**

Rupesh Nawalakhe,<sup>1</sup> Narendiran Vitchuli,<sup>1</sup> Quan Shi,<sup>1</sup> Mohamed A. Bourham,<sup>2,\*</sup> Xiangwu Zhang,<sup>1,\*</sup> and Marian G. McCord<sup>1,3,\*</sup>

<sup>1</sup> *Fiber and Polymer Science Program, Department of Textile Engineering, Chemistry and Science, North Carolina State University, Raleigh, NC 27695-8301, USA*

<sup>2</sup> *Department of Nuclear Engineering, North Carolina State University, Raleigh, NC 27695-7909, USA*

<sup>3</sup> *Joint Department of Biomedical Engineering, North Carolina State University, Raleigh, NC 27695-7115, USA, and University of North Carolina, Chapel Hill, NC, 27599, USA*

\* Corresponding author:

E-mail address: bourham@ncsu.edu (Mohamed A. Bourham);

E-mail address: xiangwu\_zhang@ncsu.edu (Xiangwu Zhang);

E-mail address: mmccord@ncsu.edu (Marian G. McCord).

## 6.1 Abstract

In this work, novel composite bandages were produced by electrospinning chitosan nanofibers on 100 % cotton gauze fabric. The idea behind preparation of composite bandages is that chitosan nanofiber web can act as a primary wound dressing whereas cotton gauze substrate can act as a backing material. However, nanofiber webs are inherently weak and difficult to handle and it is necessary to improve their mechanical properties. In composite bandages, deposition of electrospun nanofiber coatings on cotton gauze addresses the need for structural support, but faces the challenge of delamination due to compliance mismatch or poor adhesion. To improve the durability of composite bandages and adhesion between nanofiber layer and cotton gauze, cotton gauze was given plasma pre-treatment and composite bandages were given plasma post-treatment. The adhesion of the nanofibers to the substrates was assessed by qualitative and quantitative techniques. Plasma pre-treatment of the substrate with 100% helium and 99% helium/1% oxygen plasmas showed up to 4 times increase in force required to peel off the nanofiber layer. This force was further increased when composite bandages were given plasma pre-treatment to substrate as well as post-treatment to composite bandages. Storage modulus, glass transition temperature and crystallinity of untreated, He and He/O<sub>2</sub> plasma treated chitosan nanofiber web were studied to observe the effect of plasma treatment on the chitosan nanofibers using dynamic mechanical analysis (DMA), differential scanning calorimetry (DSC) and wide angle X-ray diffraction (WAXD) respectively. To understand the mechanism of improved adhesion, surface elemental analysis of plasma treated chitosan nanofibers and cotton substrate was carried out using X-ray photoelectron spectroscopy.

## 6.2 Introduction

Electrospinning has been recognized as an efficient technique for the fabrication of polymer nanofibers. Electrospun nanofibers have broad application in tissue engineering, controlled drug release, wound dressings, medical implants, nanocomposites for dental restoration, molecular separation, biosensors, and preservation of bioactive agents where their unique properties contribute to product functionality [1-5]. Researchers are trying to revolutionize the wound management by introducing nanofibers as a part of wound dressing. Nanofiber, if used in wound dressings are shown to demonstrate functional versatility which includes desirable wound adherence, absorption, oxygen permeability, resorbability, and occlusivity [6]. Their high specific surface makes them effective matrices for controlled drug release [7]. Nanofiber webs form highly effective filters for contaminants, particulates, and microorganisms. Due to advantage of small interstices and high surface area, nanofibers can assist in hemostasis [8, 9]. Due to high surface area to volume ratio, nanofibers of the same polymer give much higher absorption as compared to film [9].

Chitosan is an N-deacetylated product of chitin, the second-most abundant natural polysaccharide next to cellulose, which is embedded in a protein matrix of a crustacean shell or a squid pen [1,10]. Because of its abundant production in nature, excellent biocompatibility, biodegradability, commercial availability at relatively low cost, it has been widely used as biomaterials in pharmaceuticals, wound dressings, etc. [5, 11-13]. Aoyagi et al. [14] has formulated wound dressing films made of chitosan, with minocycline hydrochloride and Tegaderm™ as a backing for the treatment of severe burns. Wound protection and controlled drug release were achieved using these chitosan containing films.

Studies on sponge-like asymmetric chitosan membranes by Fwu-Long Mi et al. [15] demonstrated the oxygen permeability, hemostatic and antibacterial properties of chitosan.

Considering advantages of nanofibers and chitosan in wound healing, studies on chitosan nanofibers is gaining an attention in medical textile field. However, electrospinning of chitosan is difficult; because protonation of chitosan changes it into a polyelectrolyte in acidic solutions. This is due to the repulsive forces between ionic groups within the polymer in an electric field which restricts the formation of continuous uniform nanofiber and can result in formation of beads [16]. Due to difficulty in electrospinning, chitosan is typically electrospun along with synthetic biodegradable polymers such as polyethylene oxide (PEO), polyvinyl Alcohol (PVA) [17-18], polyvinylpyrrolidone (PVP) [19], and Polyethylene Terephthalate (PET) [20]. Electrospinning nanofiber mats from these blends were more advantageous over the electrospinning of pure chitosan in terms of enhancing the mechanical properties of the chitosan nanofibers by the addition of PVA, PEO, PVP and PET [1]. However, antibacterial properties of chitosan could be compromised if chitosan is electrospun by blending it with other polymers because of reduced percentage of chitosan in nanofiber web. Thus, electrospinning of pure chitosan is important if it is being used in wound dressing material.

Subsequently, successful electrospinning of pure chitosan in TFA and acetic acid was reported by Ohkawa et al.[21] and Bhattarai et al.[22], respectively. Because of its poor mechanical properties, crosslinking of chitosan nanofibers using glutaraldehyde vapor was studied by Schiffman and Schauer [23]. Thermally cross-linked electrospun fibers were prepared from chitosan/PVA in aqueous acrylic acid solutions and Triethylene glycol

dimethacrylate (TEGDMA) was added with chitosan/PVA solution to improve the mechanical property of the resulting fibers [24].

It is necessary to find an alternative way which would use no chemicals to modify the surface of 100% chitosan nanofibers and improve the mechanical properties of nanofibers without affecting its antibacterial and wound healing properties. In our previous work in our laboratory, atmospheric pressure plasma technology has been used to modify the structures and properties of various materials (especially textile materials). We have shown that plasma treatment can: i) improve surface bonding or adhesive ability [25,26], ii) increase mechanical strength by crosslinking [26-28], iii) change fiber surface hydrophobicity [29], iv) roughen fiber surfaces [28,30], v) increase crystallinity [25-27,29-31].

Researchers are currently exploring ways to improve mechanical stability and handling properties of nanofibers webs [32, 33]. Recently, Vitchuli et al. [33] successfully improved the adhesion between nylon nanofibers and nylon/cotton fabric substrates. If chitosan is used in nanofibrous form in wound dressing, it is important to get rid of the shortcomings of nanofibers. In this study, atmospheric pressure plasma has been utilized to improve the adhesion and durability of chitosan nanofiber coating on a cotton gauze substrate

Our aim is to design and develop advanced electrospun nanofiber/textile composite wound dressings and utilize atmospheric pressure plasma technology to improve the interfacial adhesion between nanofiber mats and substrate and thus improve the durability of the nanofiber coating. The composite bandages were characterized to determine effect of plasma on

- Bonding between nanofiber mat and 100% cotton substrate using peel test and gelbo flex test
- Crystallinity and glass transition temperature of chitosan nanofiber web using XRD and DSC, respectively
- Storage modulus of chitosan nanofiber web using DMA
- Surface properties of chitosan nanofibers and cotton substrate after plasma treatment using XPS

## **6.3 MATERIALS AND METHODS**

### **6.3.1 Materials**

Chitosan (Sigma Aldrich, Molecular Weight: 190kDa-375kDa, Degree of Deacetylation: 85%) was used for electrospinning onto a 100% cotton gauze substrate (Carolina Narrow Fabric Co. Inc.). Trifluoroacetic acid (Sigma Aldrich) was selected as the solvent.

### **6.3.2 Electrospinning of nanofiber webs onto substrates**

Electrospinning of chitosan nanofibers was carried out on to cotton substrates using the electrospinning setup with collecting rotating drum. The setup consisted of a syringe pump (New Era Pump System, Inc.), collecting rotating drum, and a high voltage power supply (Gamma High voltage Res. Inc.). Syringe was filled with the solution of chitosan in TFA and was fixed to the extrusion system. Extrusion system was used to control the feed rate of the spinning solution and was maintained at 1.5 ml/hr. A positive charge was applied to the tip of the needle by fixing a high voltage power supply of 25 kV. The collection system for the nanofibers included a cylindrical polyvinyl chloride (PVC) drum (5.2 cm in diameter and

16.3 cm in circumference) with a grounded metal ring at one end. A constant distance of 15 cm was maintained between rotating drum and syringe during electrospinning. The speed of the drum was maintained at 20 rpm, i.e., surface speed of 3.3 m/min using a motor. Because PVC is a non-conducting material, a metal rod was attached to the ring and ran along the length of the cylinder. In order to make the rotating drum surface conductive, aluminium foil was wound over the drum in contact with the metal rod. The textile substrates of dimension 1 cm × 5 cm were wrapped around the aluminium foil to enable deposition of electrospun nanofibers onto it.

### **6.3.3 Plasma pre-treatment of Substrate**

The atmospheric pressure audio frequency glow discharge system was designed and developed at North Carolina State University. The capacitively-coupled dielectric-barrier-discharge (DBD) consists of two parallel copper electrodes, each embedded within a Lexan polycarbonate insulator as shown in Figure 6.1. The device has an active exposure area of approximately 60 × 60 cm<sup>2</sup> between two copper electrodes with an adjustable 5 cm gap separation. The dielectric-barrier non-equilibrium discharge generates a low-temperature (1-2eV), low electron number density (10<sup>14</sup>-10<sup>16</sup> /m<sup>3</sup>) pseudo-glow discharge plasma, which is typical for dielectric-barrier discharges at atmospheric pressure. Stable and uniform plasma was achieved at low (audible) frequency, 1.373 kHz during the operation. The voltage across the plates was ~6.3 kVrms and 7.6 kVmax for 100% He plasma and ~6.6 kVrms and 7.85 kVmax for 99% He plus 1% O<sub>2</sub>. A gas flow of 20 lit/min for Helium gas and 0.3 lit/min for oxygen gas was used.

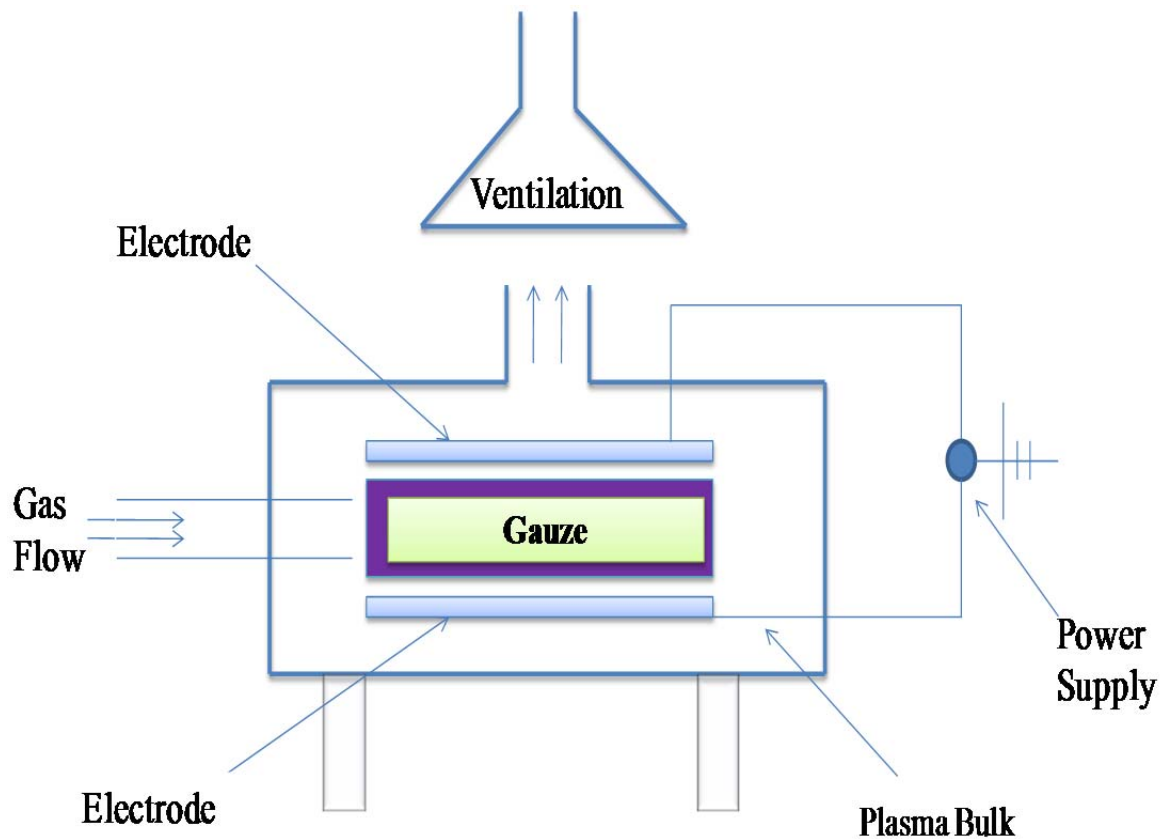


Figure 6.1. Schematic diagram of atmospheric pressure plasma system

Two types of protocol were followed. In the first case, the fabrics were pre-treated with 100% He- plasma or 99%He/1%O<sub>2</sub> plasma prior to electrospinning. The gauze substrates were placed on a nylon grid suspended in the middle of the test cell to enable complete and uniform plasma exposure from all sides. In second case, plasma pre-treated/untreated gauze fabric coated with chitosan nanofiber web was treated in plasma chamber. These samples were considered as plasma post-treated samples. The ability of atmospheric plasma treatment to enhance adhesion and durability of the composite bandage was investigated by characterization of four sample sets:

- 1) No plasma pre-treatment of the substrate and no plasma post-treatment of the composite bandages,
- 2) Plasma pre-treatment of the substrate and no plasma post-treatment of the composite bandages,
- 3) No plasma pre-treatment of the substrate and plasma post-treatment of the composite bandages, and
- 4) Plasma pre-treatment of the substrate and plasma post-treatment of the composite bandages.

These composite bandages were tested for adhesion force between nanofibers and substrates, whereas chitosan nanofibers were tested for storage modulus, crystallinity, glass transition temperature and surface chemical composition.

#### **6.3.4 Adhesion between nanofiber mats and supporting fabrics**

##### **Peel Test**

A peel test method was devised for evaluating the adhesion between the nanofiber mat and the fabric substrate based on ASTM D2261-*Tearing strength of woven fabrics by tongue (Single Rip) method* [34] using an Instron Tensile Tester. The 90° peel test was used. This method allows the user to control the rate of delamination and the locus of failure. Substrate samples with chitosan nanofibers deposited on them, of dimensions 5 cm × 1 cm were used. The two layers, *i.e.*, substrate (fabric) and nanofiber mat were fixed to the lower and upper jaws, respectively. The speed of the upper jaw was kept constant at 50 mm/min. A 50 gm load cell with a gauge length of 1.27 cm was used to measure the force of adhesion. For each

sample, 6-8 specimens were tested on Instron Tensile Tester and average force to peel off the nanofiber layer off the substrate was recorded.

### **Gelbo Flex Test**

In order to assess the ability of nanofiber mats electrospun on the substrate to withstand repetitive strain, Gelbo Flex testing was employed (modification of ASTM F 392-93, *Standard Test Method for Flex Durability of Flexible Barrier Materials*) [35]. Nanofiber-deposited fabric samples were attached to two circular clamping disks, via hose clamps, and the samples of dimensions 5 cm × 1 cm were twisted and flexed for 1000 cycles. Results of Gelbo Flex testing provided a visual adhesion assessment which was observed under (JEOL 6400 Field Emission SEM).

### **6.3.5 Dynamic mechanical analysis (DMA)**

A Rheometrics Solid Analyzer RSA III in the tensile mode (film tension clamp) was used to study the dynamic mechanical behavior of the specimens. Rectangular specimens of approximately  $38 \pm 1$  mm,  $6 \pm 0.5$  mm, with the same thickness were mounted on a film tension clamp. Specimens were cut from the nanofiber web in machine direction. Special care was taken to avoid variation in thickness of the sample by cutting the samples from the same electrospun mat. The test was run with oscillation frequency of 1 Hz at a heating rate of 3 °C/min to 250 °C. The initial static force and force track was kept at 0.01 N and 125% respectively.

### **6.3.6 Differential Scanning Calorimetry (DSC)**

DSC measurements were carried out on Perkin Elmer Diamond DSC-7 instrument to study the effect of plasma surface treatment on chitosan nanofibers. About 3-5 mg of sample

was hermetically sealed in an aluminum pan for these measurements. The samples were heated from 150 to 225 °C at a rate of 5 °C/min. Nitrogen was used as the purge gas. DSC data were analyzed by using Pyris software.

### **6.3.7 Wide angle X-ray Diffraction (WAXD)**

The crystallinity of the samples was measured with Rigaku SmartLab X-ray diffractometer. The diffractometer was equipped with Be-filtered Cu K $\alpha$  radiation with a wavelength of 1.54 Å and generated at 40 kV and 44 mA. The fiber samples were mounted onto the sample holder and placed inside the chamber. The samples were scanned in the 2 $\theta$  range from 10° to 30° with an increment of 0.05° at the speed of 1°/min. Crystallinity of the sample was determined using PDXL software for WAXD.

### **6.3.8 X-Ray Photoelectron Spectroscopy (XPS)**

X-Ray Photoelectron Spectroscopy data were taken using a Riber LAS-3000 with MgK $\alpha$  excitation (1254 eV). Energy calibration was established by referencing to adventitious Carbon (C1s line at 284.5 eV binding energy). A takeoff angle of ~75° from surface was used with an X-Ray incidence angle of ~20° and an x-ray source to analyzer angle of ~55°. Base pressure in the analysis chamber was in 10<sup>-10</sup> Torr range. CASA XPS software was used for data reduction. X-ray photoelectron spectroscopy (XPS) was carried out to investigate the changes in the surface chemical composition of 100% cotton gauze substrate and chitosan nanofiber as a result of changes in plasma parameters (percentage of Helium and oxygen).

## **6.4 RESULTS AND DISCUSSION**

### **6.4.1 Electrospinning of nanofiber webs onto substrates**

Chitosan nanofibers were electrospun in the range of 2 – 7% concentration in trifluoroacetic acid (TFA) (Figure 6.2). Electrospinning of 2% concentration of chitosan in TFA showed beads formation with no fiber formation. However, as the concentration increased from 3 to 7%, an obvious reduction in number of beads, with an increase in fiber forming tendency was observed. A 1% increment in concentration from 3 to 7% yielded an increase in diameter from 97, 105, 116, 165, and 252 nm, respectively. In order to create a robust nanofiber layer and higher production, 7% concentration of chitosan in TFA solvent was used for the further experiments. Concentration above 7% needs more amount of polymer, thus increasing the cost. A chitosan concentration of 7% in TFA was therefore selected for subsequent experiments.

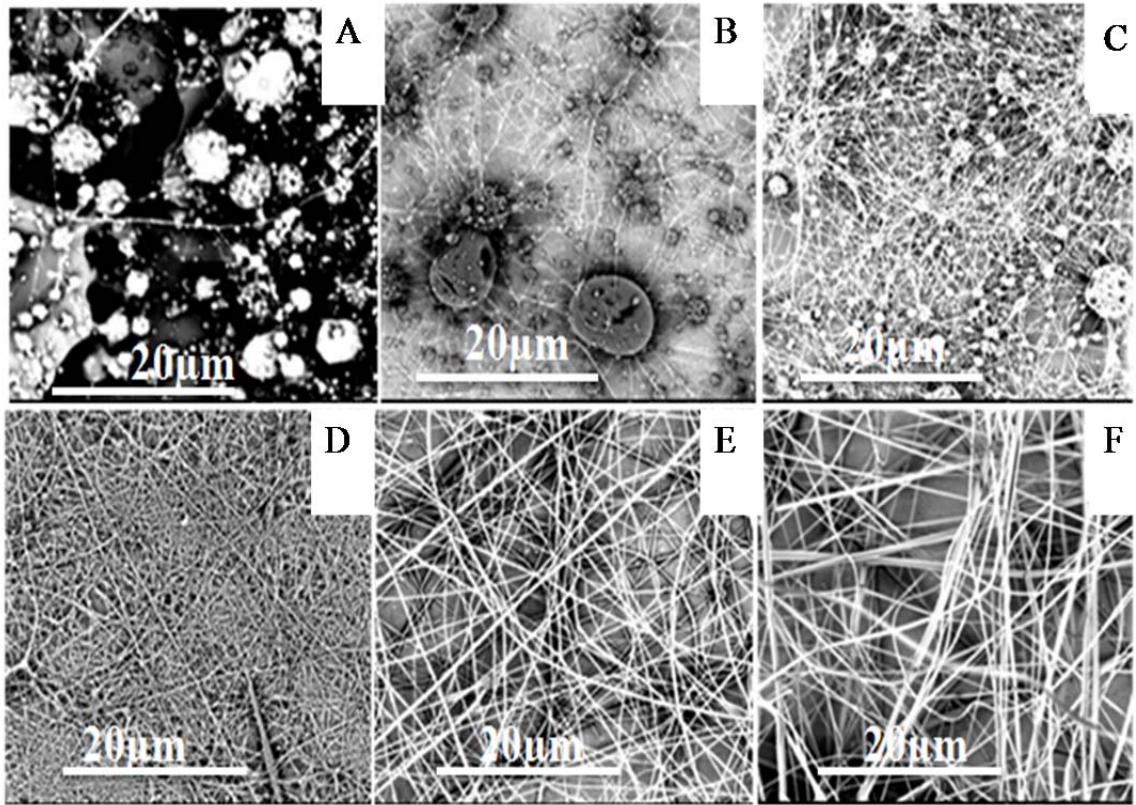


Figure 6.2. SEM images of Chitosan nanofibers Concentration: a) 2%, b) 3%, c) 4%, d) 5%, e) 6%, and f) 7% in TFA. (Scale: 20  $\mu\text{m}$ )

## 6.4.2 Adhesion between nanofiber mats and supporting fabrics

### Peel Test

To analyze the adhesion between nanofiber web and substrate quantitatively, peel test was carried out. Table 6.1 shows the average adhesion strengths between chitosan nanofiber mats and cotton gauze fabric substrates. It was observed that after treating the substrate with 100% helium plasma and 99% helium/1% oxygen plasma, the force required to peel off the nanofiber layer from substrate increased by up to 4 times as compared to untreated controls. In this case, no post-treatment was given. Increase in interfacial adhesion can be attributed to the formation of free radicals and other forms of active species at the surface of cotton substrate. These active sites on the surface of cotton substrate were available for the crosslinking between the cottons substrate and cationic groups of chitosan nanofibers to be electrospun on them.

Table 6.1. Measurement of adhesion between nanofiber mats and supporting fabrics.

Load (gf) required to peel the chitosan nanofibers layer off the substrate			
Treatment to chitosan nanofibers	No post-treat	He post-treat	He/O <sub>2</sub> post-treat
<b>No pre-treat, gf</b>	11.05 ± 1.9	25.30 ± 5.8	27.38 ± 1.7
<b>He pre-treat, gf</b>	42.28 ± 6.1	36.63 ± 5.1	45.10 ± 5.6
<b>He/O<sub>2</sub> pre-treat, gf</b>	31.23 ± 1.2	34.05 ± 3.0	47.43 ± 3.7

Post-treatment and no pre-treatment showed an increase in adhesion up to 2.5 times as that of untreated/control composite bandages. As the substrate was not given the plasma pre-treatment, no active species were formed on the surface of substrate prior to deposition of nanofibers causing no crosslinking with the nanofibers to be electrospun on cotton gauze fabric. However, because of post-treatment of composite bandages after electrospinning, there was formation of active sites on both the surfaces of nanofibers and substrate causing crosslinking between them but at lower level. The effect of plasma treatment would have been better if the substrate was pre-treated. Thus, the adhesion force was lower in case of only post-treated samples as compared to the samples in which substrates were given plasma pre-treatment and both plasma pre/post-treatment.

If average forces required to peel off the nanofiber layer from the substrates were compared, it was observed that irrespective of post-treatment; he-plasma pre-treatment (42.2, 36.6 and 45.1 gf) showed higher interfacial adhesion than that of He/O<sub>2</sub> plasma pre-treated composite bandages (31.2, 34.0 and 47.4 gf). Exception was He/O<sub>2</sub> plasma pre- and post-treated samples which showed highest adhesion force (47.4 gf) required to peel the nanofiber webs off the substrate. This is due to higher amount oxygen radicals present in the plasma reacting with chitosan as well as with the cotton substrate. During such circumstances, more amount of cross-linking can occur between nanofibers and substrate because of oxidation of the surfaces.

While conducting the peel test it was observed that, nanofiber webs were removed intact in case of control sample; whereas tearing of the nanofiber web was observed on plasma pre-

treated substrates and post-treated composite bandages. This indicated improved adhesion between nanofiber layer and the substrate.

### **Gelbo Flex Test**

To analyze the interfacial adhesion between composite wound dressing qualitatively, gelbo flex testing was performed on the samples and their morphology was observed in SEM at 15 × magnification as shown in Figure 6.3.

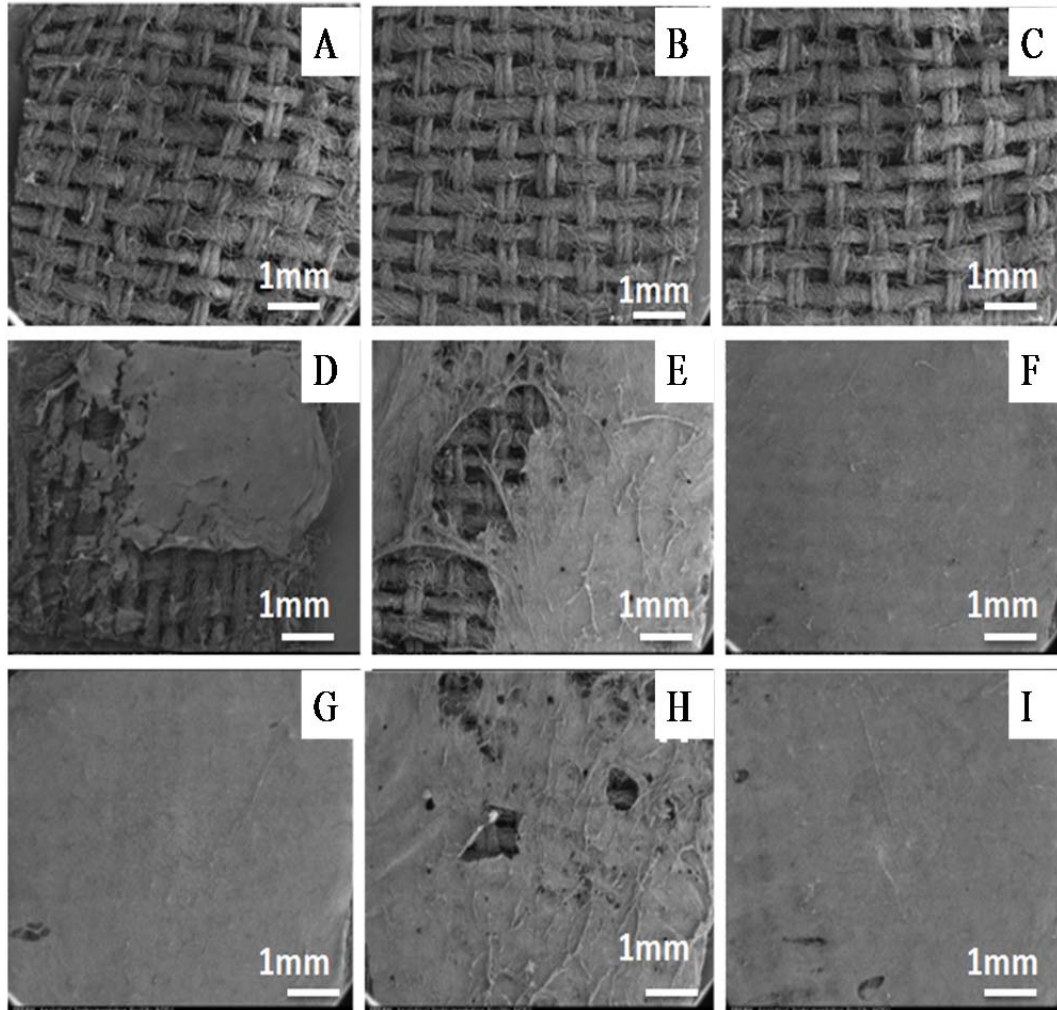


Figure 6.3 Distortion of chitosan nanofibers after 1000 cycles of Gelbo flex test, electrospun on 100% cotton gauze First row: no plasma pre-treatment, second row: He plasma pre-treatment, third row: He/O<sub>2</sub> plasma pre-treatment, First column: no plasma post-treatment, second column: He plasma post-treatment, third column: He/O<sub>2</sub> plasma post-treatment

It was observed that the nanofiber layer was badly damaged after 1000 cycles in the case of untreated substrate (Figure 6.3 A), whereas it showed much better adhesion when the substrate was pre-treated by plasma (Figures 6.3 D and G). Without pre-treating the substrate with plasma, only post-treatment of composite bandages did not show any resistance to 1000

cycles of flexing and twisting (Figures 6.3 B and C). This showed that pre-treatment of cotton substrate is necessary in order to have better adhesion. The qualitative results also support that along with the pre-treatment of the substrate, post-treatment of the composite bandages showed increase in adhesion with the substrate. The nanofiber layer was intact and firmly adhered to the substrate as a whole layer as shown in (Figures 6.3 E, F, H and I). When the composite bandages were given a pre-treatment to the substrate and post-treatment to the composite bandages, it was observed that the nanofiber layer was least damaged. The rolling off of the nanofibers from the top layer indicated that in spite of having vigorous flexing of 1000 cycles, the bottom of the layer was still intact and firmly adhered to the substrate.

Concluding the results from Gelbo flex testing and peel testing, higher adhesion can be explained by the fact that plasma treatment induces active sites which are likely to increase nanofiber adhesion to the substrate. Along with the active species formed at the surface of substrate during pre-treatment and nanofibers during post-treatment, an increase in adhesion can also be attributed to the roughness caused by etching of the substrate surface during pre-treatment in plasma [36], which increases the frictional force between the two layers.

### **6.4.3 Dynamic Mechanical Analysis**

Dynamic mechanical properties are the mechanical properties of materials as they are deformed under periodic forces. Viscoelastic properties of plasma treated chitosan nanofiber webs were mainly evaluated by the storage modulus  $E'$ . The storage modulus is approximately similar to the Young's or elastic modulus, or stiffness and these dynamic mechanical properties are usually studied over a wide temperature range. Figure 6.4 shows

the storage modulus of the untreated/control, He-plasma treated and He/O<sub>2</sub>-plasma treated electrospun chitosan nanofibers respectively. Curves obtained in DMA analysis for plasma treated and untreated nanofiber webs showed similar behavior with increase in temperature. When the polymer is heated up through the glass transition (T<sub>g</sub>) region, the storage modulus of a polymer decreased rapidly. Reduction in storage modulus after T<sub>g</sub> with temperature is caused due to mobility of amorphous regions.

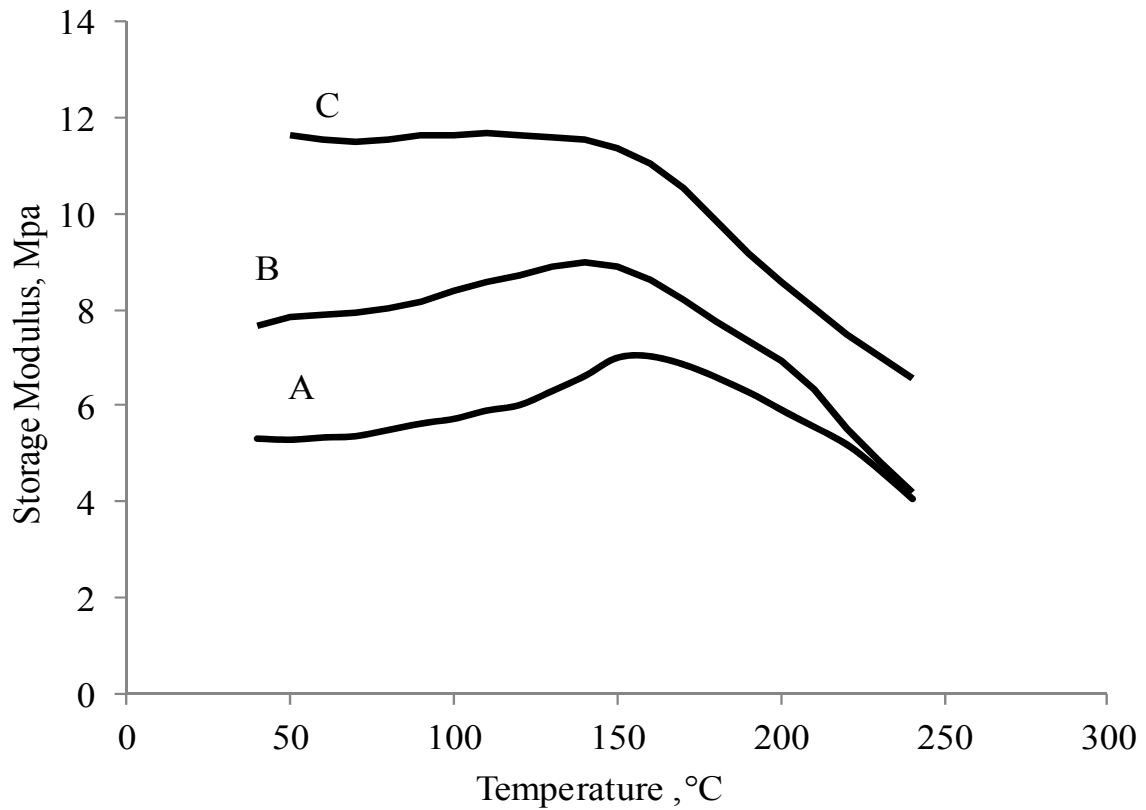


Figure 6.4 Storage modulus for the A) plasma untreated, B) He/O<sub>2</sub> plasma treated, and C) He-plasma treated chitosan nanofiber web.

As expected the plasma treatment of chitosan nanofiber web increased the storage modulus because of increased cross-linking between the active sites available on adjacent nanofibers [37] and roughness caused by etching of the nanofibers [36]. It was observed that storage modulus was higher when the nanofibers were subjected to He-plasma treatment as compared to when subjected to He/O<sub>2</sub>-plasma treatment. Untreated chitosan nanofiber web showed the lowest storage modulus as compared to both plasma treated nanofiber webs. At 50°C (Figure 6.4), the He-plasma treated nanofiber web showed highest storage modulus of 12 MPa, whereas He/O<sub>2</sub> treated showed storage modulus of 8 MPa. Control i.e. untreated nanofiber web showed lowest storage modulus of 5 MPa. Previously Sakurai et al. [19] carried out DMA analysis of chitosan films to determine its glass transition temperature. In another work, DMA (dynamic mechanical analysis) measurements were conducted to observe T<sub>g</sub> of the Polylactide/Chitosan blend membrane [38]. However, mechanical properties of 100% pure chitosan nanofibers and effect of plasma on the storage modulus of chitosan nanofibers are not analyzed yet.

XPS analysis (discussed in XPS section) of chitosan nanofibers also confirmed that He-plasma is responsible for more amount of C-O scission which causes removal of hydroxyl groups, opening of cellulosic ring in the chitosan and etching of the nanofibers. Etching is accountable for increased frictional forces between the nanofibers and reduced diameter of nanofibers which in turn increases the storage modulus of nanofiber web after plasma treatment. Reduced diameter of nanofibers after treating the electrospinning solution with plasma has been observed by Shi et al.[39]. They found that the atmospheric plasma treatment of pre-electrospinning solutions helped to form finer and smoother nanofibers with

fewer micro-beads and increased crystallinity. XPS also showed formation of active sites on the surface causing cross-linking within nanofibers. A similar type of behavior was observed when nanofibers and the cotton/nylon substrate were treated with atmospheric pressure plasma [33]. From DSC it was observed that the glass transition temperature of plasma treated chitosan nanofiber was increased as compared to the untreated nanofiber web which is an indication of increased crystallinity of the chitosan nanofibers after the plasma treatment

#### **6.4.4 Differential Scanning Calorimetry**

DSC, a widely used thermo-analytical technique, was employed to assess changes in the glass transition temperature of the plasma treated and untreated chitosan nanofiber webs. The results of the DSC study further strengthened our notion that the treatment of chitosan nanofibers with atmospheric pressure plasma leads to an alteration of the surface properties of chitosan nanofibers. The differential heat flow curves for untreated, He-plasma and He/O<sub>2</sub>- plasma treated chitosan nanofibers are shown in Figure 6.5. According to literature, glass transition temperature of chitosan is approximately 203 °C [19].

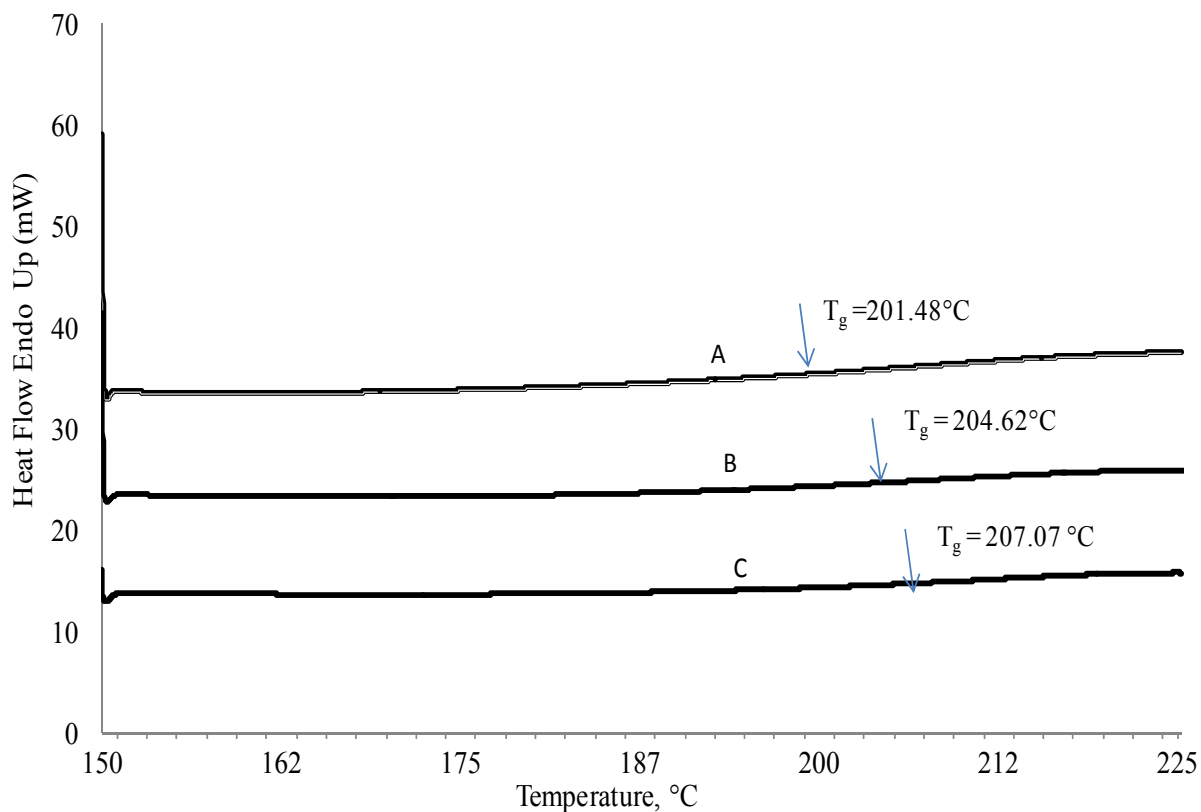


Figure 6.5. DSC heating curves of A) plasma untreated, B) He/O<sub>2</sub> plasma treated, and C) He-plasma treated chitosan nanofibers

In this study, The glass transition temperature ( $T_g$ ) of the untreated chitosan nanofibers was found to be 201.48°C which was increased to 207.07 °C and 204.62°C after He-plasma and He/O<sub>2</sub> plasma treatment of nanofiber web, respectively. Since effect of plasma treatment is only a surface phenomenon, the increase in glass transition temperature after plasma treatment was expected to be low. The increase in  $T_g$  showed that plasma treatment increased the crystallinity of the chitosan nanofibers by etching the amorphous region from the chitosan nanofibers [36] and also caused cross-linking between active sites created on the surface of adjacent nanofibers [33].

### 6.4.5 Wide angle X-ray Diffraction (WAXD)

Figure 6.6 shows the crystalline structure changes of chitosan nanofibers with the plasma treatment. With the He- and He/O<sub>2</sub>- plasma treatment, the WAXD intensities of peaks at 2 theta value of 14° and 17° increased. Percentage crystallinity of the untreated, He and He/O<sub>2</sub> treated chitosan nanofibers as calculated from PDXL software is as shown in Table 6.2.

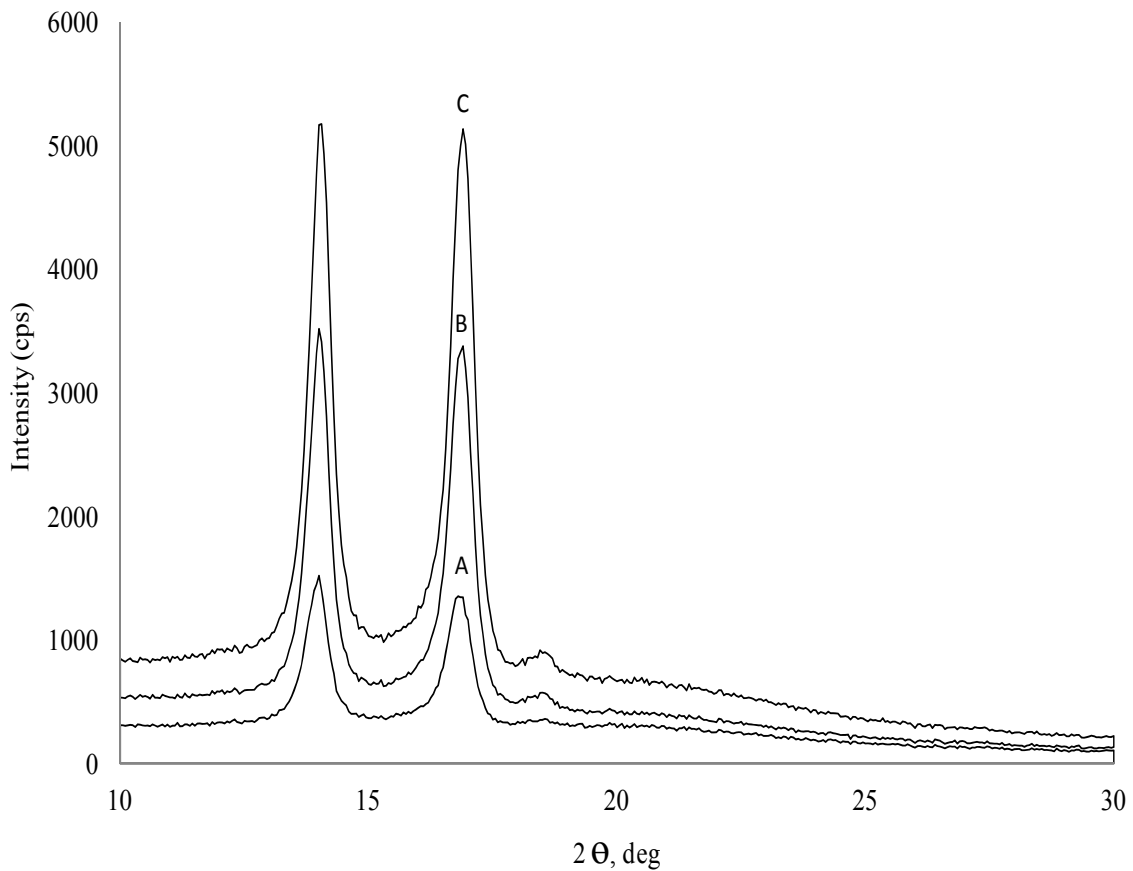


Figure 6.6 XRD patterns of A) plasma untreated, B) He/O<sub>2</sub> plasma treated, and C) He-plasma treated chitosan nanofibers. Plasma treatment showed increased crystallinity with the plasma treatment.

Table 6.2 Crystallinity of untreated, He-plasma treated and He/O<sub>2</sub> plasma treated chitosan nanofiber webs using WAXD

<b>Treatment to Chitosan nanofibers</b>	<b>Crystallinity, %</b>
Untreated	35.5
He/O <sub>2</sub> plasma	44.9
He plasma	56.1

In this work, crystallinity of untreated chitosan nanofibers was found to be 35.5%, which approximately matches with the literature value of the crystallinity of chitosan (DD = 87%) [40]. After treating the nanofibers layer with He- and He/O<sub>2</sub>-plasma, the crystallinity was increased to 56.1% and 44.9% respectively. This increase in crystallinity can be attributed to the removal of amorphous region from the surface of chitosan nanofibers. These results support the increase in glass transition temperature and increase in storage modulus of the chitosan nanofibers. In DSC, He-plasma treated chitosan showed highest glass transition temperature. In WAXD, He-plasma treated chitosan showed highest crystallinity i.e. 56.1 % and in DMA, He-plasma treated chitosan showed highest storage modulus as compared to that of untreated chitosan nanofibers.

#### **6.4.6 XPS Analysis of Substrate after Plasma Treatment**

To analyze the mechanism of improved adhesion in qualitative and quantitative assessment of the composite wound dressings, surface elemental analysis of cotton substrate

was carried out and is as shown in Table 6.3. The carbon content in the control sample was found to be 84.88 %. Typical cellulose would have a carbon content of 66.9 % [29]. This atypical cellulose composition may be due to the presence of residual long chains of hydrocarbons [41] on the cotton fiber surface which remain even after aqueous processing, or may be due to the composition of the cotton fiber outer wall which consists of mixture of fats, waxes and resin [42].

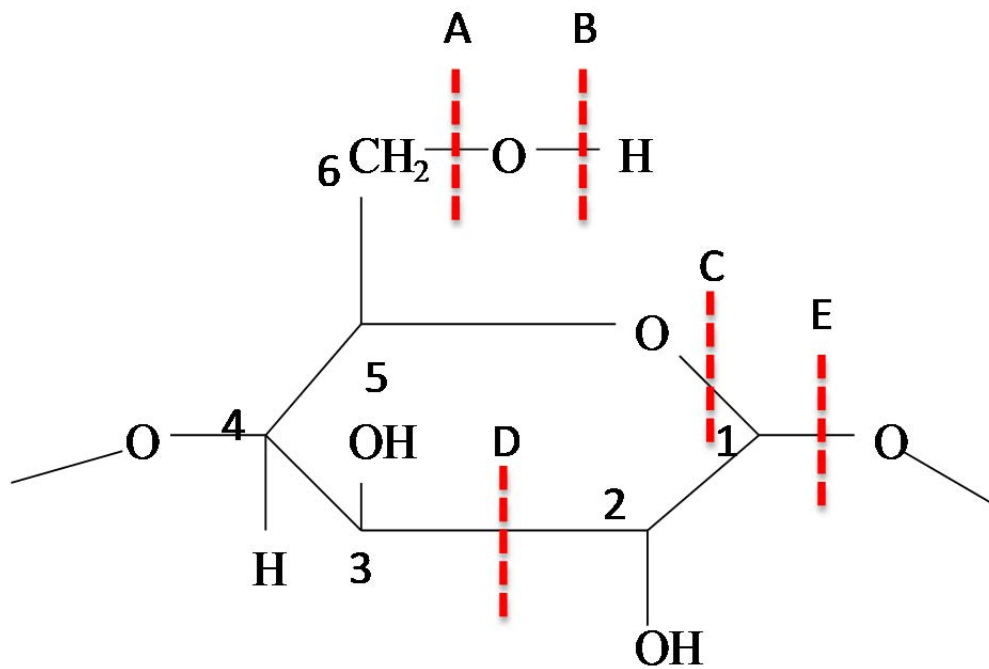


Figure 6.7. Possible sites for scission of cotton substrate after plasma treatment (A) Dehydroxylation, B) Dehydrogenation, C) scission between C1 and ring oxygen, D) dehydrogenation/dehydroxylation, E) scission between C1 and glycosidic oxygen

Previous studies in our lab showed possible radical formation on surface of cotton fabric due to fluorinated radio frequency plasma [29]. Table 6.3 shows a reduction in the carbon content of the cotton substrate from 84.88% to 77.62% and 81.18% after He- and He/O<sub>2</sub> - plasma treatment. This effect was more pronounced for the He treated substrate than for the He/O<sub>2</sub> plasma treated substrate. Reduction in surface carbon content is due to the etching of some of the long chain hydrocarbons from the surface as a result of plasma treatment which results in roughness of the surface. Oxygen content of the cotton substrate was increased from 15.12 % to 22.38 % and 18.82 % after He- and He/O<sub>2</sub> plasma treatment respectively. This indicates that He-plasma treatment created more sites for oxidation on the surface of cotton substrate as compared to He/O<sub>2</sub> plasma treated substrate. This led to more crosslinking between cotton substrate and nanofibers via ionic bond or covalent bond formation.

Table 6.3 Results of surface elemental analysis for atmospheric pressure plasma treated and untreated Cotton substrate

<b>100% cotton Substrate</b>	<b>C-spectra</b>			<b>Overall</b>	
	C-C (%)	C-O (%)	COO-(%)	O (%)	C (%)
<b>No treatment</b>	85	14	1	15.12	84.88
<b>He Plasma treated</b>	82	9	9	22.38	77.62
<b>He-O<sub>2</sub> plasma treated</b>	82	8	10	18.82	81.18

The scission at sites 'C' and 'E' produced radicals that could react with active groups of the chitosan nanofibers. In addition, dehydrogenation or dehydroxylation at site 'B' and 'A' in -C-O-H groups (figure 6.7) on cellulose can make cotton substrate susceptible to react with chitosan nanofibers at C6. Due to abundance of hydroxyl groups on chitosan as well as on cotton substrate formed by plasma treatment, there are high chances of hydrogen bonding at the nanofiber-substrate interface as well as within the chitosan nanofibers.

C1s spectral analysis showed that there was formation of new functional groups on the cotton substrates after treating them with He- or He/O<sub>2</sub>-plasma. Increases in COO- (289.1eV) indicate formation of polar groups available for cross-linking with hydroxyl or cationic amide groups of chitosan nanofibers. After treating the cotton substrate with plasma, breaking of cellulose ring occurred due to scission at site 'C' and 'E'. This scission can be explained by the reduced intensities of C-C and C-O bonds in C1 spectra and can be responsible for crosslinking between the substrate and nanofibers to be deposited on it. Considering all these factors, it is likely that increased functionality and surface roughness as a result of plasma treatment are responsible for the increased adhesion. Qualitative assessment of the surface roughness of nanofibers is technically challenging because of presence of convolutions on to the cotton fabric and was not characterized in this study.

#### 6.4.7 XPS analysis of Plasma treated chitosan nanofiber webs

In order to study the active groups created and breaking of chains/etching on the surface of chitosan nanofibers after the He-Plasma or He/O<sub>2</sub>- plasma treatment, XPS analysis of the samples was carried out.

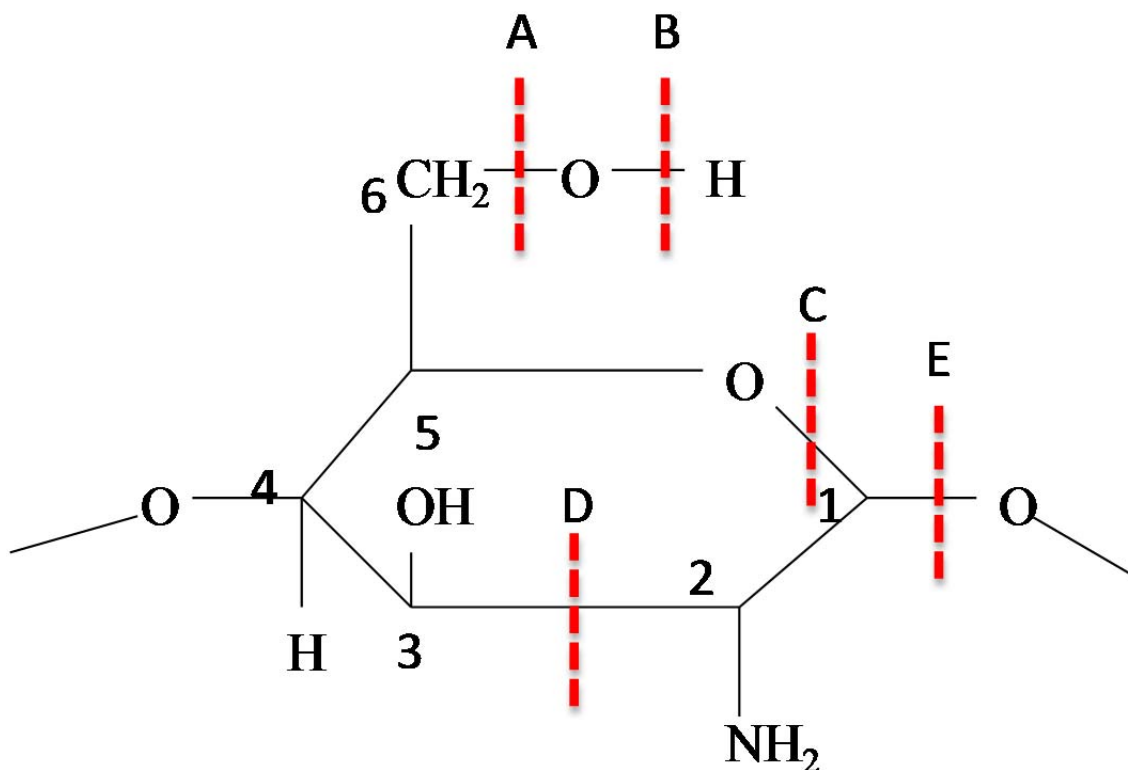


Figure 6.8. Possible sites for scission of chitosan after plasma treatment  
A) Dehydroxylation, B) Dehydrogenation, C) scission between C1 and ring oxygen, D) dehydrogenation/dehydroxylation, E) scission between C1 and glycosidic oxygen

As it can be seen in elemental analysis (Table 6.4), carbon content of chitosan nanofibers decreased after He- and He/O<sub>2</sub>- plasma treatment. This indicates scission at site 'D' (Figure. 6.8) and removal of some the carbon containing groups from the ring, particularly CH<sub>2</sub>-OH groups at C5. This removal can be responsible for formation of active

site at C5 and possible cross-linking, formation of covalent bond and ionic bond between the surfaces of nanofibers as well as with the cotton substrate. On the other hand, oxygen content was increased after the plasma treatment. This might be due to radical creation and subsequent oxygen group formation on the surface of the chitosan nanofibers during atmospheric pressure plasma treatment.

Table 6.4 Results of surface elemental analysis for atmospheric pressure plasma treated and untreated chitosan nanofibers

Plasma Treatment	C-spectra				N spectra		Overall		
	C-O	C-C	C=O	C-N	N-H	N-C	O	C	N
Control	30.52	21.69	26.58	21.21	55.44	44.56	32.53	61.27	6.20
He	24.40	23.93	26.77	24.91	54.72	45.28	35.23	58.99	5.78
He/ O <sub>2</sub>	25.51	18.07	26.12	30.30	54.04	45.96	35.11	58.84	6.05

Decreased C-O percentage showed scission at sites A, C, E (Figure 6.8) creating active sites on the surface of chitosan nanofibers. Whereas, increased C-N percentage showed cross-linking between cationic amide group and active sites available on the adjacent nanofiber and on the cotton substrate. This explains the results from peel test showing higher adhesion force between nanofibers and cotton substrate. Cross-linking between adjacent nanofibers increased the storage modulus of nanofiber web when treated with atmospheric pressure plasma.

## **6.5 Conclusion**

Chitosan nanofibers were electrospun onto 100% cotton gauze substrate to form composite bandages. Atmospheric pressure plasma technology was utilized to improve the adhesion and durability of the nanofiber coating. Peel test showed that treatment of the substrate with 100% He plasma and 99% He/1% O<sub>2</sub> plasma increased the adhesion between nanofiber layers and substrates by up to 4 times. This force was further increased approximately by up to 4.5-5 times after treating the composite bandages with plasma i.e. post-treatment. Also, plasma pretreatment of the gauze fabric prior to electrospinning significantly reduced degradation of the nanofiber layer due to repetitive flexing. From both gelbo and peel tests, it was found that only post-treatment of composite bandages was not as effective as both pre-treatment of substrate and pre & post-treatment of the composite bandages in improving the adhesion between two layers.

DMA results also showed that there was increase in storage modulus of the chitosan nanofibers after He- or He/O<sub>2</sub>-plasma treatment. DSC curves showed that the glass transition temperature of the chitosan nanofibers was increased after treating them with atmospheric

pressure plasma. This increase in  $T_g$  indicated etching of the amorphous region from the surface of chitosan nanofibers and increase in crystallinity of the nanofibers. Wide angle X-ray diffraction showed increase in percentage crystallinity of chitosan nanofibers after plasma treatment which supported the increase in  $T_g$  and increase storage modulus of chitosan nanofibers after plasma treatment. From DSC, DMA and WAXD, it was concluded that He plasma was most effective in improving the surface properties of chitosan nanofibers. XPS analysis showed that after treating the substrate and chitosan nanofibers with plasma, the surface carbon content (C1s) was decreased and oxygen content was increased. Plasma treatment created surface oxidation, which was responsible for the increased adhesion between the substrate and chitosan nanofibers through cross-linking between the active sites.

## References:

1. Jayakumar R, Prabakaran M, Nair SV, Tamura H. Novel chitin and chitosan nanofibers in biomedical applications. *Biotechnol Adv* 2010;28:142-150.
2. Sokolsky-Papkov M, Agashi K, Olaye A, Shakesheff K, Domb AJ. Polymer carriers for drug delivery in tissue engineering. *Adv Drug Deliv Rev* 2007;59:187-206.
3. Agarwal S, Wendorff JH, Greiner A. Use of electrospinning technique for biomedical applications. *Polymer* 2008;49:5603-5621.
4. Ito Y, Hasuda H, Kamitakahara M, Ohtsuki C, Tanihara M, Kang I, Kwon OH. A composite of hydroxyapatite with electrospun biodegradable nanofibers as a tissue engineering material. *Journal of Bioscience and Bioengineering* 2005;100:43-49.
5. Chen Z, Mo X, He C, Wang H. Intermolecular interactions in electrospun collagen-chitosan complex nanofibers. *Carbohydr Polym* 2008;72:410-418.
6. Duan YY, Jia J, Wang SH, Yan W, Jin L, Wang ZY. Preparation of Antimicrobial Poly( $\epsilon$ -caprolactone) Electrospun Nanofibers Containing Silver-Loaded Zirconium Phosphate Nanoparticles. 2007;106:1208-1214.
7. Loh XJ, Peh P, Liao S, Sng C, Li J. Controlled drug release from biodegradable thermoresponsive physical hydrogel nanofibers. *J Controlled Release* 2010;143:175-182.
8. Luo Z, Wang S, Zhang S. Fabrication of self-assembling d-form peptide nanofiber scaffold d-EAK16 for rapid hemostasis. *Biomaterials* 2011;32:2013-2020.
9. Zhang Y, Lim C, Ramakrishna S, Huang Z. Recent development of polymer nanofibers for biomedical and biotechnological applications RID A-9865-2008 RID C-9542-2009. *Journal of Materials Science-Materials in Medicine* 2005;16:933-946.
10. Francesko et al A. Developments in the processing of chitin, chitosan and bacterial cellulose for textile and other applications. 2010:288.
11. Abdel-Halim ES, Abdel-Mohdy FA, Al-Deyab SS, El-Newehy MH. Chitosan and monochlorotriazinyl- $\beta$ -cyclodextrin finishes improve antistatic properties of cotton/polyester blend and polyester fabrics. *Carbohydr Polym* 2010;82:202-208.
12. Chitins and chitosans for the repair of wounded skin, nerve, cartilage and bone. *Carbohydr Polym* 2009;76:167.

13. Development of a chitosan-based wound dressing with improved hemostatic and antimicrobial properties. *Biomaterials* 2008;29:4323.
14. Aoyagi S, Onishi H, Machida Y. Novel chitosan wound dressing loaded with minocycline for the treatment of severe burn wounds. 2007;330:138-145.
15. Mi F, Shyu S, Wu Y, Lee S, Shyong J, Huang R. Fabrication and characterization of a sponge-like asymmetric chitosan membrane as a wound dressing. *Biomaterials* 2001;22:165-173.
16. Min B, Lee SW, Lim JN, You Y, Lee TS, Kang PH, Park WH. Chitin and chitosan nanofibers: electrospinning of chitin and deacetylation of chitin nanofibers. *Polymer* 2004;45:7137-7142.
17. Deepthy M. Control of nanostructures in PVA, PVA/chitosan blends and PCL through electrospinning. *Bull Mater Sci* 2008;31:343.
18. Duan B, Yuan X, Zhu Y, Zhang Y, Li X, Zhang Y, Yao K. A nanofibrous composite membrane of PLGA–chitosan/PVA prepared by electrospinning. *European Polymer Journal* 2006;42:2013-2022.
19. Sakurai K, Maegawa T, Takahashi T. Glass transition temperature of chitosan and miscibility of chitosan/poly(N-vinyl pyrrolidone) blends. *Polymer* 2000;41:7051-7056.
20. Jung K, Huh M, Meng W, Yuan J, Hyun SH, Bae J, Hudson SM, Kang I. Preparation and antibacterial activity of PET/chitosan nanofibrous mats using an electrospinning technique. *J Appl Polym Sci* 2007;105:2816-2823.
21. Ohkawa K, Cha D, Kim H, Nishida A, Yamamoto H. Electrospinning of Chitosan. *Macromolecular Rapid Communications* 2004;25:1600-1605.
22. Bhattarai N, Edmondson D, Veiseh O, Matsen FA, Zhang M. Electrospun chitosan-based nanofibers and their cellular compatibility. *Biomaterials* 2005;26:6176-6184.
23. Schiffman J, Shauer C. Cross-linking of chitosan Nanofibers. 2007;8:594-601.
24. Zhou Y, Yang D, Nie J. Electrospinning of chitosan/poly(vinyl alcohol)/acrylic acid aqueous solutions. *J Appl Polym Sci* 2006;102:5692-5697.
25. Hwang YJ, McCord MG, Kang BC. Helium/oxygen atmospheric pressure plasma treatment on poly(ethylene terephthalate) and poly(trimethylene terephthalate) knitted fabrics: Comparison of low-stress mechanical/surface chemical properties. 2005;6:113-120.

26. Shin Y, Son K, Yoo DI, Hudson S, McCord M, Matthews S, Whang Y. Functional finishing of nonwoven fabrics. I. Accessibility of surface modified PET spunbond by atmospheric pressure He/O<sub>2</sub> plasma treatment. *J Appl Polym Sci* 2006;100:4306-4310.
27. Hwang YJ, McCord MG. Surface modification of organic polymer films treated in atmospheric Plasmas. 2004;151:495-501.
28. McCord MG, Hwang YJ, Hauser PJ, Qiu Y, Cuomo JJ, Hankins OE, Bourham MA, Canup LK. Modifying Nylon and Polypropylene Fabrics with Atmospheric Pressure Plasmas. *Textile Research Journal* 2002;72:491-498.
29. McCord MG, Hwang YJ, Qui Y, Hughes LK, Bourham MA. Surface Analysis of Cotton Fabrics Fluorinated in RadioFrequency Plasma. 2003;88:2038-2047.
30. Cai Z, Qui Y, Hwang YJ, Zhang C, McCord MG. The Use of Atmospheric Pressure Plasma Treatment in Desizing PVA on Viscose Fabrics. 2003;32:223-232.
31. Hwang YJ, Mccord MG, An JS, Kang BC, Park SW. Effects of Helium Atmospheric Pressure Plasma Treatment on Low-Stress Mechanical Properties of Polypropylene Nonwoven Fabrics. *Textile Research Journal* 2005;75:771-778.
32. Graham K, Gibson H, Gogins M. Incorporation of Electrospun Nanofibers into Functional Structures. 2003.
33. Vitchuli N, Shi Q, Nowak J, Nawalakhe R, Sieber M, Bourham M, McCord M, Zhang X. Plasma-Electrospinning Hybrid Process and Plasma Pretreatment to Improve Adhesive Properties of Nanofibers on Fabric Surface. *Plasma Chem Plasma Process* 2012;32:275-291.
34. ASTM D2261. Tearing strength of woven fabrics by tongue (Single Rip) Procedure (Constant-Rate-of-Extension Tensile Testing Machine). .
35. ASTM F 392-93. Standard Test Method for Flex Durability of Flexible Barrier Materials. 2004.
36. Matthews SR, Hwang YJ, Mccord M, Bourham M. Investigation into etching mechanism of polyethylene terephthalate (PET) films treated in helium and oxygenated-helium atmospheric plasmas. *Journal of Applied Polymer Science* 2004;94:2383-2389.
37. Qiu Y, Zhang C, Hwang YJ, Bures BL, McCord M. The effect of atmospheric pressure helium plasma treatment on the surface and mechanical properties of ultrahigh-modulus polyethylene fibers. 2002;16:99-107.

38. Ying W, Hua W, Axi Y, Dijiang W. Biodegradable Polylactide/Chitosan Blend Membranes. *Biomacromolecules* 2007;7:1362-1372.
39. Shi Q, Vitchuli N, Nowak J, Lin Z, Guo B, Mccord M, Bourham M, Zhang X. Atmospheric plasma treatment of pre-electrospinning polymer solution: A feasible method to improve electrospinnability. *Journal of Polymer Science Part B: Polymer Physics* 2010;49:115-122.
40. Trung TS, Thein-Han WW, Qui NT, Ng C, Stevens WF. Functional characteristics of shrimp chitosan and its membranes as affected by the degree of deacetylation. *Bioresour Technol* 2006;97:659-663.
41. Mitchell R, Carr CM. Surface chemical analysis of raw cotton fibers and associated materials. 2005;12:629-639.
42. Narjès R, Michel N, Jean-Yves D, Richard F. Comparison of surfaces properties of different types of cotton fibers by inverse gas chromatography. 2010;17:25-32.

## Chapter 7

### Electrospinning of Silk Fibroin Nanofibers: Improving its Mechanical Properties and Adhesion with the Cotton Gauze with the help of Atmospheric Pressure Plasma

**Electrospinning of Silk Fibroin Nanofibers: Improving its  
Mechanical Properties and Adhesion with the Cotton Gauze with  
the help of Atmospheric Pressure Plasma**

Rupesh Nawalakhe,<sup>1</sup> Narendiran Vitchuli,<sup>1</sup> Quan Shi,<sup>1</sup> Mohamed A. Bourham,<sup>2,\*</sup> Xiangwu  
Zhang,<sup>1,\*</sup> and Marian G. McCord<sup>1,3,\*</sup>

<sup>1</sup> *Fiber and Polymer Science Program, Department of Textile Engineering, Chemistry and  
Science, North Carolina State University, Raleigh, NC 27695-8301, USA*

<sup>2</sup> *Department of Nuclear Engineering, North Carolina State University, Raleigh, NC  
27695-7909, USA*

<sup>3</sup> *Joint Department of Biomedical Engineering, North Carolina State University, Raleigh,  
NC 27695-7115, USA, and University of North Carolina, Chapel Hill, NC, 27599, USA*

\* Corresponding author:

E-mail address: bourham@ncsu.edu (Mohamed A. Bourham);

E-mail address: xiangwu\_zhang@ncsu.edu (Xiangwu Zhang);

E-mail address: mmccord@ncsu.edu (Marian G. McCord).

## 7.1 Abstract

Objective of this research is to develop advanced electrospun silk fibroin (SF) nanofiber/textile wound dressings and utilize atmospheric pressure plasma technology to improve the adhesion and durability of the nanofiber coating. This paper will mainly focus on improving the mechanical properties of SF nanofibers. SF nanofibers were treated with atmospheric pressure He or He/O<sub>2</sub> plasma on capacitively coupled device at low (audible) frequency of 1.373 kHz with a gas flow of 20 lit/min for Helium gas and 0.3 lit/min for oxygen gas. The nanofiber layer was treated for 5 min. Dynamic mechanical analysis (DMA) of untreated, He and He/O<sub>2</sub> plasma treated SF nanofiber web was studied to observe the effect of plasma treatment on the storage modulus of nanofibrous structure. Plasma treated SF nanofiber web showed higher storage modulus as compared to untreated SF nanofiber web. The SF nanofiber webs were subjected to differential scanning calorimetry (DSC) to study the changes in glass transition temperature of nanofiber web after He- or He/O<sub>2</sub> plasma treatment. It was observed that glass transition temperature of SF nanofibers was increased after plasma treatment. Wide angle X-ray diffraction (WAXD) showed increased in the crystallinity of SF nanofibers after plasma treatment which supported the data from DSC and DMA. To understand the mechanism of improved mechanical properties, XPS surface elemental analysis of plasma treated silk fibroin nanofibers were carried out. XPS analysis showed formation of active sites on the surface of plasma treated silk fibroin nanofibers responsible for cross linking between adjacent nanofibers. MTT assay of untreated, He-plasma treated, and He/O<sub>2</sub> -plasma treated silk fibroin was carried out to study cell viability of human epidermal keratinocytes (HEK).

## 7.2 Introduction

Electrospinning has been recognized as an efficient technique for the fabrication of polymer nanofibers. Electrospun nanofibers have broad application in tissue engineering, controlled drug release, wound dressings, medical implants, nanocomposites for dental restoration, molecular separation, biosensors, and preservation of bioactive agents where their unique properties contribute to product functionality[1-5]. However, electrospun nanofiber mats are inherently weak, and hence they are often deposited on mechanically-strong substrates such as porous woven fabrics [6]. In such cases, nanofiber layer can act as primary functional layer and substrate can act as strong backing material. In last paper we have shown that plasma treatment of substrate prior to electrospinning can improve the adhesion between nanofiber layer and substrate. In this paper our main focus will be improving durability of nanofibers by treating the nanofiber layer with atmospheric pressure He or He/O<sub>2</sub>- plasma.

[7]Plasma treatment of polymer surfaces is an environmentally friendly process as compared to conventional chemical treatments [7,8]. The plasma consists of highly active charged species, electrons, ions and radicals, and can create highly unusual environments to interact with material surfaces. Plasma treatment of polymer materials results in surface modification through functionalization, etching, chain scission, and cross linking [7,9-12]. . In our previous work in our laboratory, atmospheric pressure plasma technology has been used to modify the structures and properties of various materials (especially textile materials). We have shown that plasma treatment can: i) improve surface bonding or adhesive ability [10,12], ii) increase mechanical strength by crosslinking [8,8,8,10,13], iii)

change fiber surface hydrophobicity [14], iv) roughen fiber surfaces [13,15], v) increase crystallinity [7,8,10,12,14,15]. Therefore, plasma can be used to enhance the durability of nanofiber mats.

Polymers based on protein are of specific interest in healthcare applications because of their biocompatibility, combined strength and toughness. Silk fibroin (SF) is a natural protein, mainly consisting of amino acids with small side groups, such as glycine, alanine and serine. Previous studies on silk fibroin have shown excellent biocompatibility, biodegradability [16-22], high oxygen and water permeability [18], desirable drug permeability [23] and effective resistance against enzymatic degradation [24]. These properties make SF useful for a broad range of biomedical applications, including surgical sutures [25], skin treatments [26], wound dressing materials [27], cell culture substrates [28], controlled drug-delivery, cosmetics, and food additives [27][29].

Silk fibroin was selected as a primary wound dressing material to be electrospun on to the cotton substrate and effect of plasma on storage modulus, glass transition temperature, and crystallinity of nanofibers was studied. Plasma treatment makes polymer surface hydrophilic [30-32]

## **7.3 Materials and Methods**

### **7.3.1 Materials**

Raw silk (Grade 5A produced in Brazil) was degummed before electrospinning. Sericin was removed from raw silk in boiling water with 0.25 % (w/v) sodium lauryl sulfate and 0.25% (w/v) sodium carbonate, bath ratio of 1:100 (w/v), for 1 hour. Fibroin obtained after this treatment was washed in boiling water for 1 hour to remove leftover sericin and surfactants, and then rinsed with distilled water. Degummed silk was used for electrospinning onto a 100% cotton gauze substrate (Carolina Narrow Fabric Co. Inc.). Trifluoroacetic acid (Sigma Aldrich) was selected as the solvent.

### **7.3.2 Electrospinning of nanofiber webs onto substrates**

Electrospinning of SF nanofibers was carried out using the electrospinning setup with collecting rotating drum as shown in the picture of Figure 7.1. The setup consisted of a syringe pump (New Era Pump System, Inc.), collecting rotating drum, and a high voltage power supply (Gamma High voltage Res. Inc.). Syringe was filled with the solution of SF in TFA and was fixed to the extrusion system. Extrusion system was used to control the feed rate of the spinning solution and was maintained at 1 ml/hr. A positive charge was applied to the tip of the needle by fixing a high voltage power supply of 25 kV. The collection system for the nanofibers included a cylindrical polyvinyl chloride (PVC) drum (5.2 cm in diameter and 16.3 cm in circumference) with a grounded metal ring at one end. The speed of the drum was maintained at 20 rpm, i.e., surface speed of 3.3 m/min using a motor. Because PVC is a non-conducting material, a metal rod was attached to the ring and ran along the length of the cylinder. In order to make the rotating drum surface conductive, aluminium foil was wound

over the drum in contact with the metal rod. The textile substrate was then wrapped around the aluminium foil to enable deposition of electrospun nanofibers onto it.

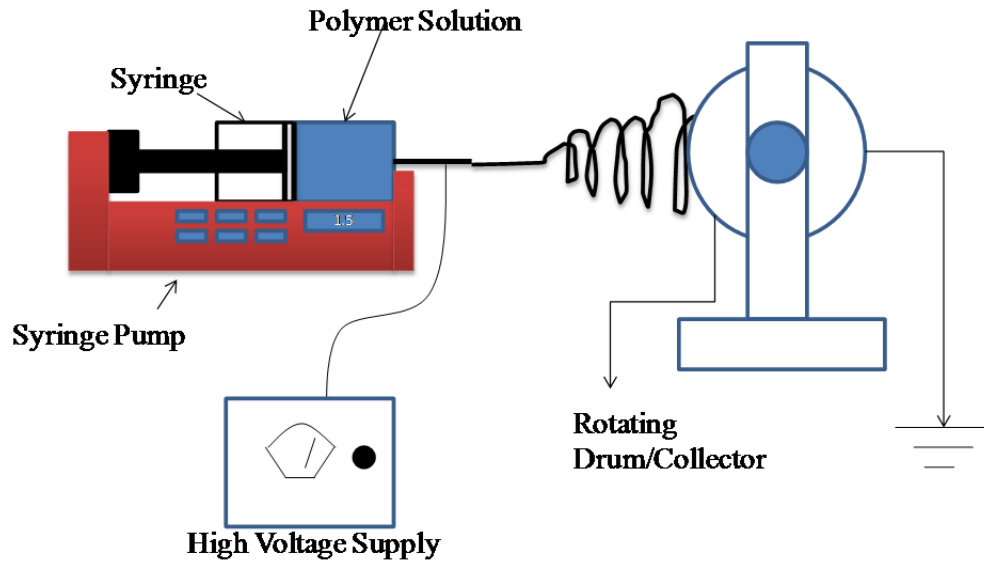


Figure 7.1. Depositing nanofibers onto the fabric by rotating collector.

### 7.3.3 Plasma pre-treatment of Substrate

The atmospheric pressure audio frequency glow discharge system was designed and developed at North Carolina State University. The capacitively-coupled dielectric-barrier-discharge (DBD) consists of two parallel copper electrodes, each embedded within a Lexan polycarbonate insulator. The device has an active exposure area of approximately  $60 \times 60 \text{ cm}^2$  between two copper electrodes with an adjustable 5 cm gap separation. The dielectric-barrier non-equilibrium discharge generates a low-temperature (1-2eV), low electron number density ( $10^{14}$ - $10^{16} / \text{m}^3$ ) pseudo-glow discharge plasma, which is typical for dielectric-barrier discharges at atmospheric pressure. Stable and uniform plasma was achieved at low (audible)

frequency, 1.373 kHz during the operation. The voltage across the plates was  $\sim 6.3$  kVrms and 7.6 kVmax for 100% He plasma and  $\sim 6.6$  kVrms and 7.85 kVmax for 99% He plus 1% O<sub>2</sub>. A gas flow of 20 lit/min for Helium gas and 0.3 lit/min for oxygen gas was used.

Composite bandages were treated with 100% He- plasma or 99%He/1%O<sub>2</sub> plasma. The composite bandages were placed on a nylon grid suspended in the middle of the test cell to enable complete and uniform plasma exposure from all sides. Nanofiber layer was removed from the substrate in order to carry out the characterization which included dynamic mechanical analysis, differential scanning calorimetry measurements, surface elemental analysis, and wide angle X-ray diffraction. Composite bandages were also tested for MTT assay to observe the effect of plasma treatment on cell viability.

#### **7.3.4 Dynamic mechanical analysis (DMA)**

A Rheometrics Solid Analyzer RSA III in the tensile mode (film tension clamp) was used to study the dynamic mechanical behavior of the specimens. Rectangular specimens of approximately  $38 \pm 1$  mm,  $6 \pm 0.5$  mm, with the same thickness were mounted on a film tension clamp. Specimens were cut from the nanofiber web in machine direction. Special care was taken to avoid variation in thickness of the sample by cutting the samples from the same electrospun mat. The test was run with oscillation frequency of 1 Hz at a heating rate of 3 °C/min to 250 °C. The initial static force and force track was kept at 0.01 N and 125% respectively.

#### **7.3.5 Differential Scanning Calorimetry (DSC)**

DSC measurements were carried out on Perkin Elmer Diamond DSC-7 instrument to study the effect of plasma surface treatment on SF nanofibers. About 3-5 mg of sample was

hermetically sealed in an aluminum pan for these measurements. The samples were heated from 150 to 225 °C at a rate of 5 °C/min. Nitrogen was used as the purge gas. DSC data were analyzed by using Pyris software.

### **7.3.6 Wide angle X-ray Diffraction (WAXD)**

The crystallinity of the samples was measured with Rigaku SmartLab X-ray diffractometer. The diffractometer was equipped with Be-filtered Cu Ka radiation with a wavelength of 1.54 Å and generated at 40 kV and 44 mA. The fiber samples were mounted onto the sample holder and placed inside the chamber. The samples were scanned in the  $2\theta$  range from 10° to 30° with an increment of 0.05° at the speed of 1°/min. Crystallinity of the sample was determined using PDXL software for WAXD.

### **7.3.7 MTT assay: Viability Assessment of SF Substrates**

Composite bandages with SF nanofibers as a primary layer and cotton substrate as secondary layer were cut to fit the wells of a 6-well plate (3.5cm diameter; 9.6cm<sup>2</sup>). The bandages were sterilized with UVB light in the cell culture hood. Both surfaces were exposed to the light, with substrate rotated 90 degrees after a minimum 4h light exposure per side. The materials were transferred to sterile 6-well culture plates and anchored with sterile stainless steel washers with an effective growth area of 1.5cm<sup>2</sup>. The composite bandages were then equilibrated in cell culture medium in the incubator until seeded with human epidermal keratinocytes (HEK).

Cryopreserved first pass neonatal HEK (Lonza; Walkersville, MD) were seeded in 75cm<sup>2</sup> flasks and grown to 75% confluency, harvested, and seeded on each membrane (n=4) in 6-well plates at 293,000 cells per well. Cells were also seeded in the wells alone (well

control; n=2/plate) to monitor cell growth. Once the HEK in the well controls reached approximately 70% confluency, the media was changed and the cells were grown for an additional 24h. To assess cell viability, the cell culture medium was replaced with MTT medium and the HEK incubated for 3h. The media was aspirated, the cells carefully rinsed in Hank's Balanced Salt Solution (HBSS), and 3ml of isopropyl alcohol added to HEK in each well and agitated to solubilize the formazan crystals within the cells. The isopropyl alcohol (100 $\mu$ l) was transferred to a new 96-well plate and the absorbance quantitated at 550nm in a Multiskan RC plate reader (Labsystems). MTT assay was quantified on 1<sup>st</sup> day, 7<sup>th</sup> day and 14<sup>th</sup> day to see the effect of plasma treatment of composite bandages on cell viability.

#### **7.7.8 XPS Analysis of Substrate and SF Nanofibers after Plasma Treatment**

X-ray photoelectron spectroscopy (XPS) was carried out to investigate the changes in the surface chemical composition SF nanofibers as a result of plasma treatment and changes in plasma parameters (percentage of helium and oxygen). XPS data were taken using a Riber LAS-3000 with MgK $\alpha$  excitation (1254 eV). Energy calibration was established by referencing to adventitious Carbon (C1s line at 284.5 eV binding energy). A take-off angle of  $\sim 75^\circ$  from the surface was used with an X-Ray incidence angle of  $\sim 20^\circ$  and an x-ray source to analyzer angle of  $\sim 55^\circ$ . Base pressure in the analysis chamber was in  $10^{-10}$  Torr range. CASA XPS software was used for data reduction.

### **7.4 Results and discussion**

#### **7.4.1 Electrospinning of SF nanofibers**

Silk nanofibers were electrospun in trifluoroacetic acid (TFA) for 2 hrs with an extrusion rate of 1 ml/hr, applied voltage of 25 kV, and distance of 15 cm between the

rotating drum and the needle tip. The concentration varied from 5 to 10 wt%. The average diameters of nanofibers obtained in the range of 5 - 10% concentrations were 95, 220, 560, 620, 1270, and 1760 nm, respectively, as shown in Figure 7.2. In order to create a robust nanofiber layer, 9% concentration was selected for the further experiments to get sturdy structure and higher production of nanofibers. All further experiments were performed at that concentration. Concentrations above 9% were not considered because the increase of average diameter will significantly decrease the specific surface area and porosity of the nanofiber web.

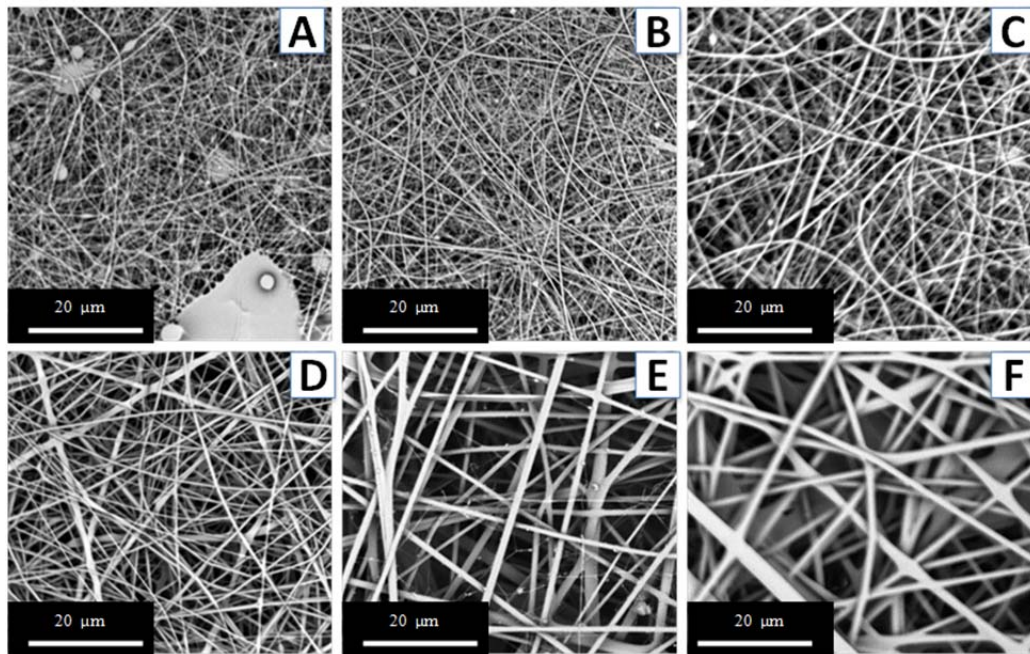


Figure 7.2. SEM images of SF nanofibers electrospun at concentrations of A) 5%, B) 6%, C) 7%, D) 8%, E) 9%, F) 10% in TFA. Magnification: 2500 ×.

### 7.4.2 Dynamic mechanical analysis (DMA)

Viscoelastic properties of plasma treated SF nanofiber webs were mainly evaluated by the storage modulus  $E'$ . When the SF nanofibers were treated with He- and He/O<sub>2</sub>- plasma, it creates radicals and active sites on the surface of nanofibers. Plasma treatment also increased the roughness on the nanofibers causing higher frictional forces between adjacent nanofibers. As expected the plasma treatment of SF nanofiber web increased the storage modulus because of increased cross-linking between the active sites available on adjacent nanofibers [33] and roughness caused by etching of the nanofibers [34].

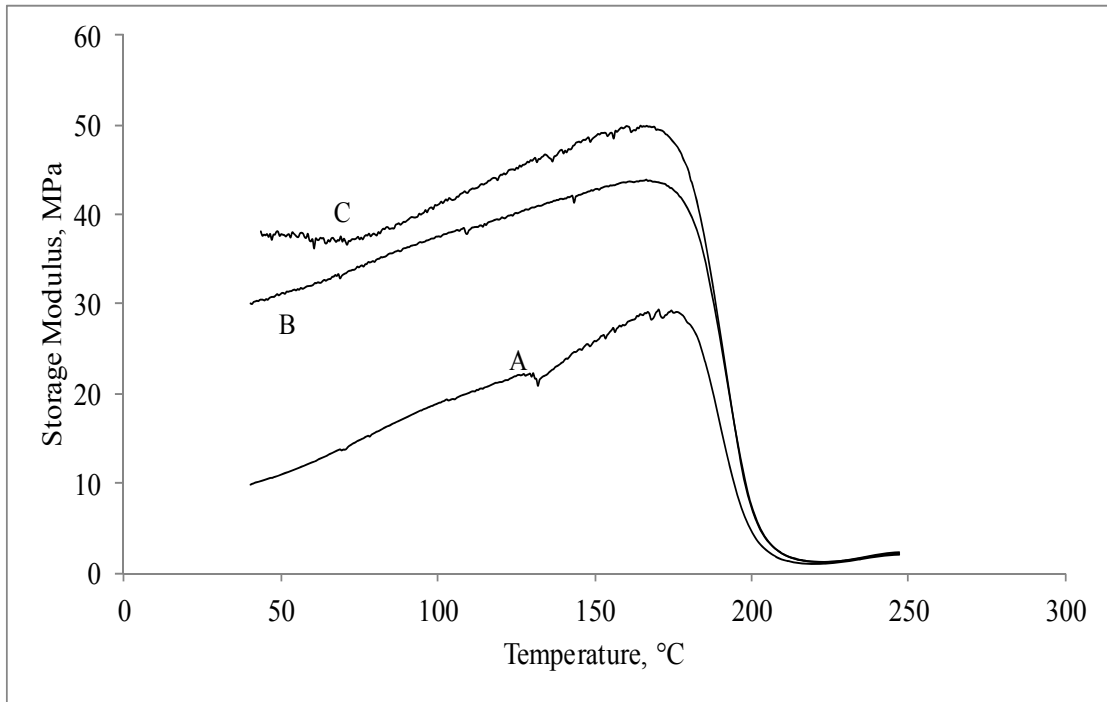


Figure 7.3. Storage modulus for the A) plasma untreated, B) He/O<sub>2</sub> plasma treated, and C) He-plasma treated SF nanofiber web.

It was observed that storage modulus was higher when the nanofibers were subjected to He-plasma treatment as compared to when subjected to He/O<sub>2</sub>-plasma treatment. Untreated SF nanofiber web showed the lowest storage modulus as compared to both plasma treated nanofiber webs. At 50°C, the He-plasma treated nanofiber web showed highest storage modulus of 39 MPa, whereas He/O<sub>2</sub> treated showed storage modulus of 31 MPa. Control i.e. untreated nanofiber web showed lowest storage modulus of 11 MPa (Figure 7.3). Previously Minoura et al. [18] carried out DMA analysis of silk fibroin membranes to determine the effect methanol treatment for different time. It was observed that the modulus increased with increasing treatment time, that is, the silk fibroin membrane became elastic. In another work, films of silk fibroin cast from fibroin–water solutions at different casting temperatures and untreated or treated after casting with methanol, were characterized by dynamic mechanical analysis [35]. However, mechanical properties of 100% SF nanofibers and effect of plasma on the storage modulus of SF nanofibers are not analyzed yet.

#### **7.4.3 Differential Scanning Calorimetry (DSC)**

DSC, a widely used thermo-analytical technique, was employed to assess changes in the glass transition temperature of the plasma treated and untreated SF nanofiber webs. The results of the DSC study further strengthened our notion that the treatment of SF nanofibers with atmospheric pressure plasma leads to an alteration of the surface properties of SF nanofibers. The differential heat flow curves for untreated, He-plasma and He/O<sub>2</sub>-plasma treated SF nanofibers are shown in Figure 7.4. According to literature, glass transition temperature of SF is approximately 175 °C [36][37].

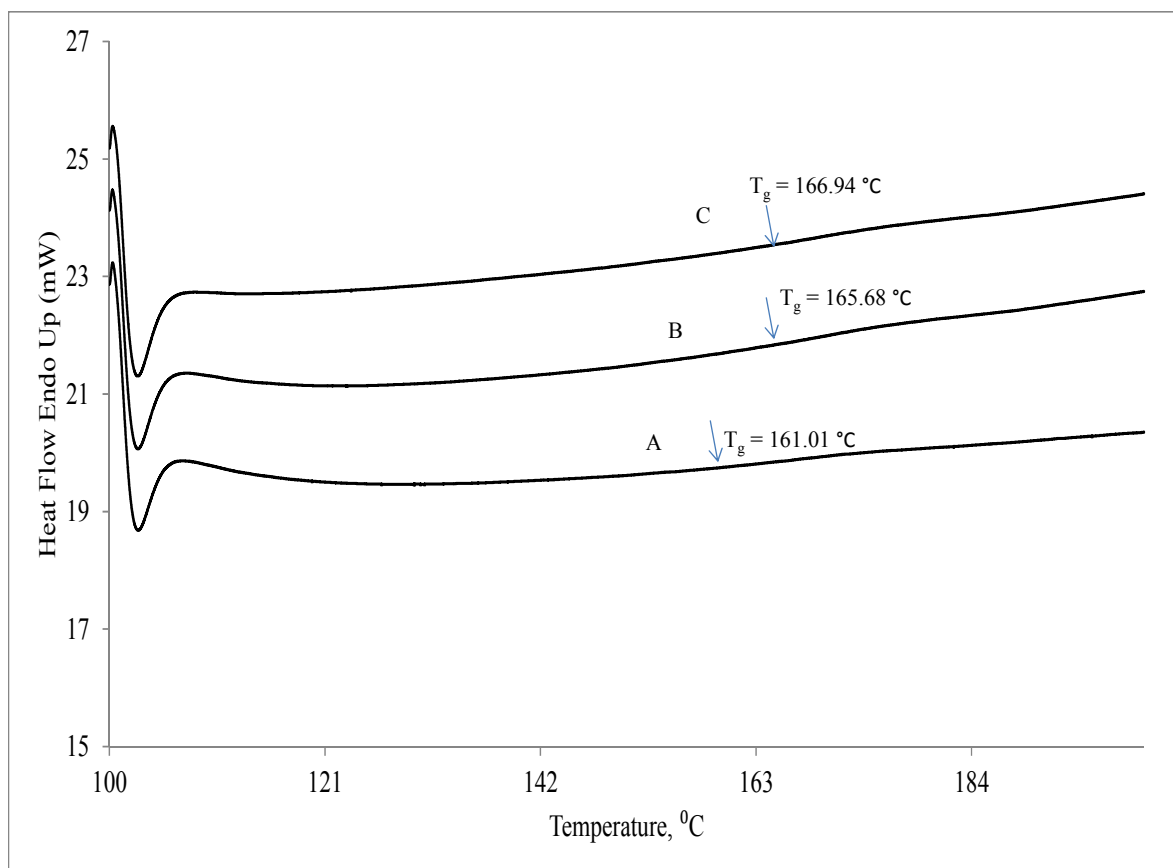


Figure 7.4. DSC heating curves of A) plasma untreated, B) He/O<sub>2</sub> plasma treated, and C) He-plasma treated SF nanofibers.

In this study, the glass transition temperature ( $T_g$ ) of the untreated SF nanofibers was found to be 161.01°C which was increased to 166.94 °C and 165.68°C after He-plasma and He/O<sub>2</sub> plasma treatment of nanofiber web, respectively. Since effect of plasma treatment is only a surface phenomenon, the increase in glass transition temperature after plasma treatment was expected to be low. The increase in  $T_g$  showed that plasma treatment increased the crystallinity of the SF nanofibers by etching the amorphous region from the SF nanofibers [34] and also caused cross-linking between active sites created on the surface of adjacent nanofibers [6].

#### 7.4.4 Wide angle X-ray Diffraction (WAXD)

Figure 7.5 shows the crystalline structure changes of SF nanofibers with the plasma treatment. With the He- and He/O<sub>2</sub>- plasma treatment, the WAXD intensities of peaks at 2 theta value of 14° and 17° increased. Percentage crystallinity of the untreated, He and He/O<sub>2</sub> treated SF nanofibers as calculated from PDXL software is as shown in Table 7.1. In this work, crystallinity of untreated SF nanofibers was found to be 32.59%. After treating the nanofibers layer with He- and He/O<sub>2</sub>-plasma, the crystallinity was increased to 62.12% and 43.48% respectively.

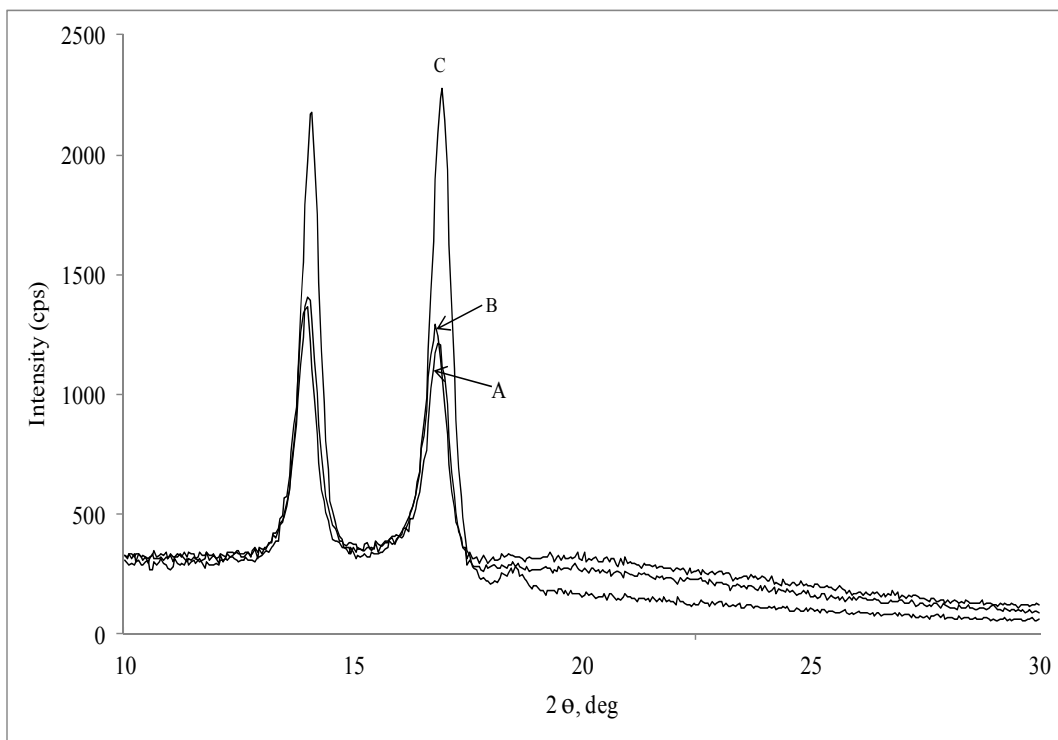


Figure 7.5 XRD patterns of A) plasma untreated, B) He/O<sub>2</sub> plasma treated, and C) He-plasma treated SF nanofibers. Plasma treatment showed increased crystallinity with the plasma treatment.

Table 7.1 Crystallinity of untreated, He-plasma treated and He/O<sub>2</sub> plasma treated SF nanofiber webs using WAXD

<b>Plasma treatment</b>	<b>Crystallinity, %</b>
SF Untreated	32.59
SF He	62.12
SF He/O <sub>2</sub>	43.48

This increase in crystallinity can be attributed to the removal of amorphous region from the surface of SF nanofibers. These results support the increase in glass transition temperature and increase in storage modulus of the SF nanofibers. In DSC, He-plasma treated SF showed highest glass transition temperature. In WAXD, He-plasma treated SF showed highest crystallinity i.e. 56.1 % and in DMA, He-plasma treated SF showed highest storage modulus as compared to that of untreated SF nanofibers.

#### **7.4.5 MTT assay: Viability Assessment of SF Substrates**

HEK were grown on the three composite bandages, viz. untreated, He-plasma treated and He/O<sub>2</sub> plasma treated SF composite bandages. HEK remained stable in the wells resulting in fairly consistent data. A comparison of viability on the different composite bandages found that cell growth on the He treated SF composite bandages was significantly greater ( $p < 0.05$ ) than the He/O<sub>2</sub> treated bandages which was significantly greater ( $p < 0.05$ ) than that of untreated SF composite bandages (Figure 7.6). This higher cell viability can be explained by the effect of atmospheric pressure plasma which increases the hydrophilicity of the SF nanofibers greatly. [19]. The He- and He/O<sub>2</sub>-plasma treated SF nanofibers showed higher cellular activities for both human epidermal keratinocytes (HEK) than the untreated ones.

He- plasma was more effective than that He/ O<sub>2</sub> plasma. As XPS surface analysis of silk nanofibers showed, the oxygen content was increased to 26.71% when treated with He plasma making the nanofiber layer more hydrophilic and suitable for the cell growth. The differences in chemical composition, conformation and hydrophilicity of nanofibrous matrices affect the cellular activities [38]. It was observed that the as compared to 1<sup>st</sup> day, 14<sup>th</sup> day showed significant increase in cell viability. Thus it is expected that He plasma treatment of SF composite bandages can improve the hydrophilicity of silk fibroin nanofiber and increase the cell viability. SF nanofibers can also act as a scaffold material for regeneration of skin cells and improve the healing rate of wound.

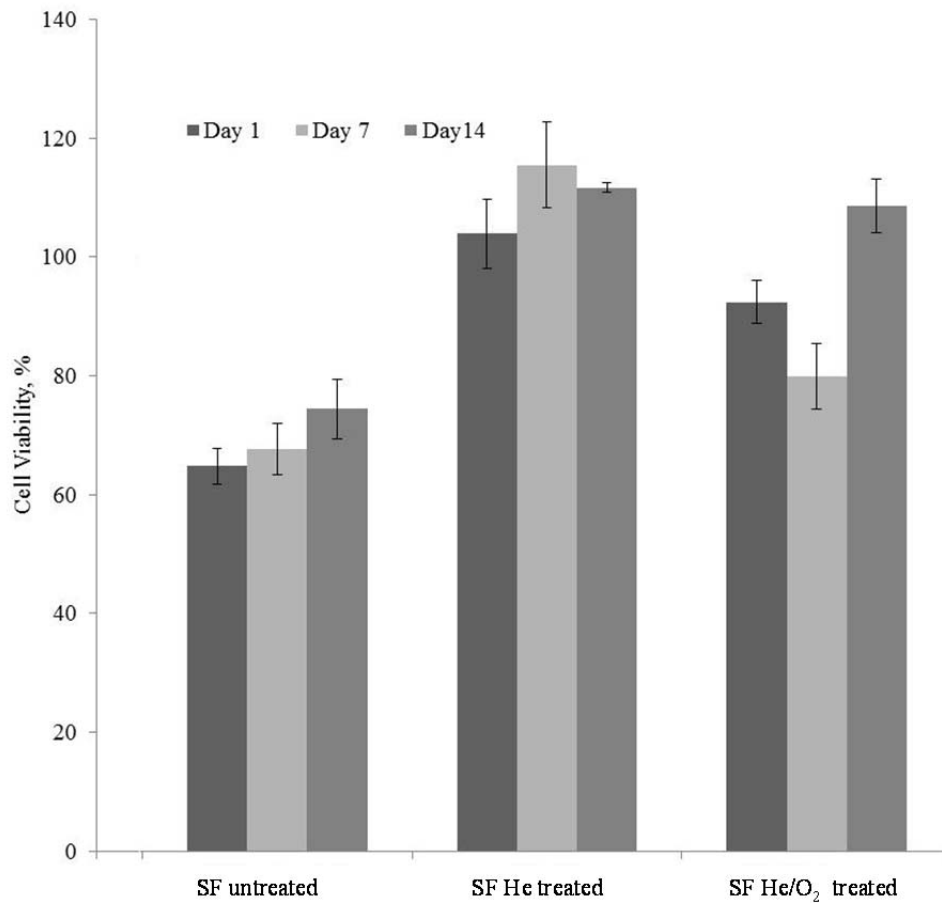


Figure 7.6 MTT viability of HEK grown on untreated, He plasma treated and He/O<sub>2</sub> plasma treated SF composite bandages.

#### 7.4.6 XPS analyses of silk fibroin nanofibers

To study the effect of plasma post-treatment, SF nanofibers were also analyzed using XPS spectroscopy to study the surface chemical structure before and after plasma treatment. Table 2 shows the surface chemical composition of untreated, He and He/O<sub>2</sub> plasma treated SF nanofibers. The XPS spectra of the SF nanofibers after the plasma treatment showed three strong peaks in the region of 200–600 eV. The first (290 eV), second (400 eV) and third

peaks (530 eV) were assigned to C1 s, N1 s and O1 s, respectively. Table 2 shows C1 spectra, N1 spectra and overall elemental composition of SF nanofibers with and without plasma treatment. C1s spectral analysis showed formation of new groups. The intensities of C-C (285.0 eV) and C-N bonds decreased with both the plasma treatments (Figure 7.7 and table 2). This is probably due to the creation of free radicals on the surface of SF nanofibers (Figure 8). The percentage of N-C=O (288 eV) bonds increased due to plasma treatment, as shown in Table 7.2. The increases in N-C=O and N-H bonds after plasma treatment are likely due to scission of the C-C linkage (Figure 7.8) from -HN-C-CO-NH- group. Etching of the surface of silk nanofiber may also play a role in increasing the frictional force between SF nanofibers; however, this was not assessed in this study.

Table 7.2. Results of chemical composition of C1s, N1 peaks and overall elemental analysis for treated and untreated SF nanofibers with atmospheric pressure plasmas.

Silk Nanofibers	C1 - spectra (%)				N1 - spectra (%)		Overall Elemental analysis (%)		
	C-O/C-N	C-C/C-H	N-C=O	C=O	N-H	N-C	O	C	N
<b>Un-treated</b>	20.57	32.66	10.73	36.04	82.87	17.13	21.26	61.28	17.45
<b>He Plasma</b>	21.63	27.05	11.70	39.62	85.38	14.62	26.71	57.45	15.83
<b>He-O<sub>2</sub> plasma</b>	15.40	24.40	28.41	31.80	93.06	6.94	22.67	61.23	16.06

N1 spectra of untreated and plasma treated SF nanofibers showed increased percentages of N-H groups (85.38% and 93.06 %) and decreased percentages of N-C (14.62% and 6.94% ) groups when treated with He and He/O<sub>2</sub> plasma. This clearly indicates scission of C-N bond

from -HN-C-CO- linkage and formation of free radicals on the surface of SF nanofibers. Both of these effects will result in possible crosslinking/covalent bonding between active groups of SF (-NH and -OH groups).

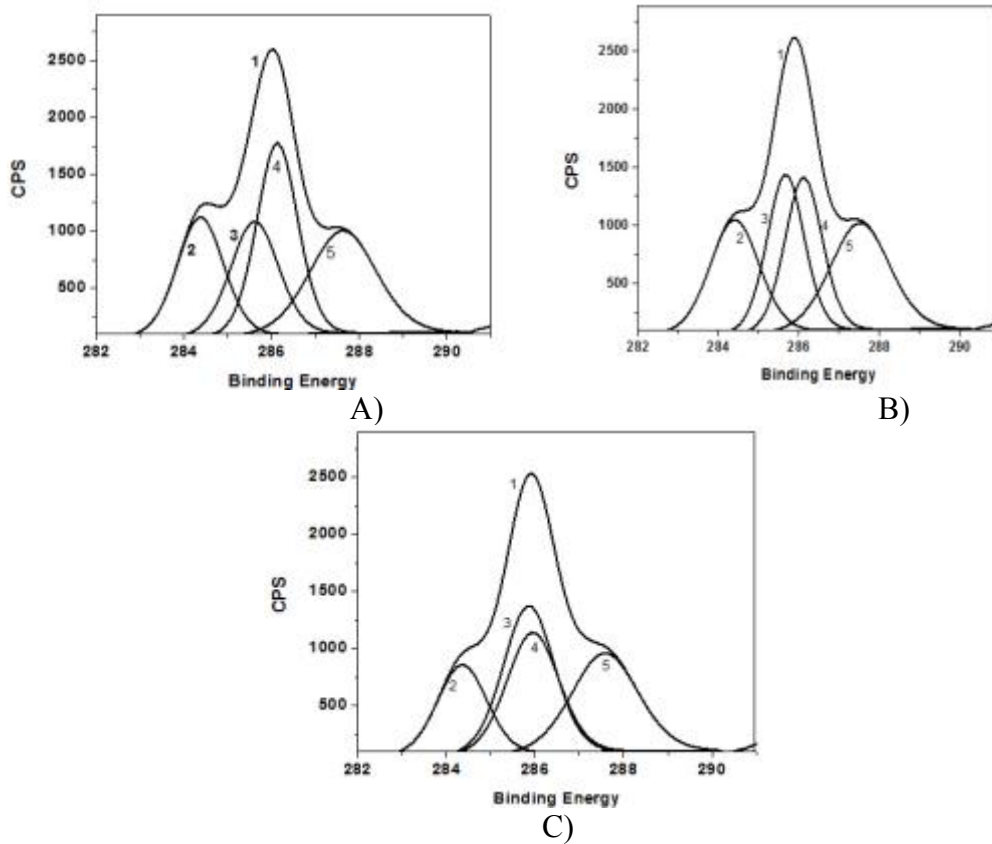


Figure 7.7. Chemical composition of plasma-treated and untreated silk fibroin nanofibers with Atmospheric A) Untreated, B) He-plasma treated and C) He/O<sub>2</sub> plasma treated SF nanofibers .1: Envelope, 2: C=O, 3: C=O/N-C=O, 4: C-O/C-N, 5: C-C/C-H.

In addition, SF nanofibers treated by He- and He/O<sub>2</sub>- plasmas exhibited relatively higher amounts of oxygen-containing chemical groups than those untreated with plasma. Oxygen content is higher for He- plasma treated nanofibers than for He/O<sub>2</sub> plasma treated nanofibers, which indicates higher number of active site on the surface of nanofibers available for cross-

linking with nanofibers. This is reflected in the higher storage modulus, higher crystallinity and higher cell viability of SF nanofibers in case of the He-plasma treatment.

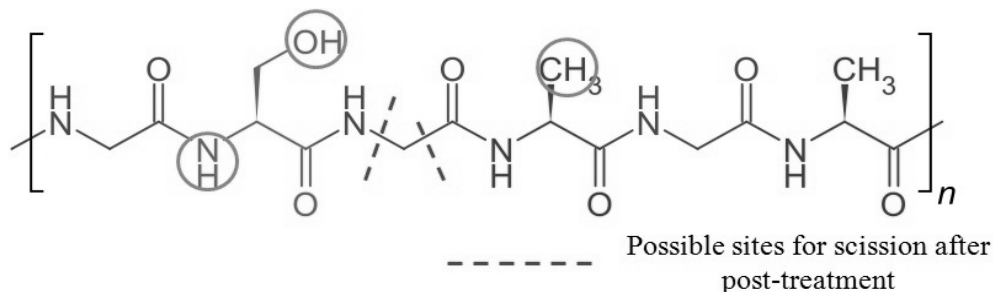


Figure 7.8. Possible sites for scission after plasma treatment of SF nanofibers.

Encircled regions in Figure 7.8 show the available sites for cross-linking and hydrogen bonding between and within SF nanofibers. The surface activation of SF nanofibers by plasma treatment can lead to the hydrogen bonding between  $-OH$  and  $-NH$  groups of adjacent SF nanofibers. As it can be seen in Table 7.2, the percentage of C-H groups was reduced from 32.66% to 27.05% and 24.40% after treating the composite bandages with He-plasma and He/O<sub>2</sub> plasma, respectively. Reduction in C-H groups is expected to lead to the formation of free radicals which are available for cross-linking with active groups of SF nanofibers such as  $-OH$  and  $-NH$  groups.

Thus, formation of active sites on the surfaces of the SF nanofibers, chain scission, hydrogen and covalent bonding, creating roughness on the surface and interfacial cross-linking within SF nanofibers are responsible for increased mechanical properties of SF nanofibers.

## 7.5 Conclusion

SF nanofibers were electrospun onto 100% cotton gauze substrate to form composite bandages. Atmospheric pressure plasma technology was utilized to improve durability of the nanofiber coating. DMA results showed that there was increase in storage modulus of the SF nanofibers after He- or He/O<sub>2</sub>-plasma treatment. DSC curves showed that the glass transition temperature of the SF nanofibers was increased after treating them with atmospheric pressure plasma. The increase in T<sub>g</sub> indicated etching of the amorphous region from the surface of SF nanofibers and increase in crystallinity of the nanofibers. Wide angle X-ray diffraction showed increase in percentage crystallinity of chitosan nanofibers after plasma treatment which supported the increase in T<sub>g</sub> and increase storage modulus of chitosan nanofibers after plasma treatment. From DSC, DMA and WAXD, it was concluded that He plasma was most effective in improving the surface properties of chitosan nanofibers. XPS analysis showed that after treating the SF nanofibers with plasma, the surface carbon content (C1s) was decreased and oxygen content was increased. Plasma treatment created surface oxidation, which was responsible for the increased mechanical properties of SF nanofibers through cross-linking between the active sites. MTT assay showed that He plasma treatment made the SF nanofibers more hydrophilic, thereby increasing cell viability of bandages as compared to untreated SF composite bandages. Thus composite bandage made up of SF nanofibers as a primary layer and cotton gauze as a backing material can act as promising wound dressing material.

## 7.6 References

1. Jayakumar R, Prabakaran M, Nair SV, Tamura H. Novel chitin and chitosan nanofibers in biomedical applications. *Biotechnol Adv* 2010;28:142-150.
2. Sokolsky-Papkov M, Agashi K, Olaye A, Shakesheff K, Domb AJ. Polymer carriers for drug delivery in tissue engineering. *Adv Drug Deliv Rev* 2007;59:187-206.
3. Agarwal S, Wendorff JH, Greiner A. Use of electrospinning technique for biomedical applications. *Polymer* 2008;49:5603-5621.
4. Ito Y, Hasuda H, Kamitakahara M, Ohtsuki C, Tanihara M, Kang I, Kwon OH. A composite of hydroxyapatite with electrospun biodegradable nanofibers as a tissue engineering material. *Journal of Bioscience and Bioengineering* 2005;100:43-49.
5. Chen Z, Mo X, He C, Wang H. Intermolecular interactions in electrospun collagen-chitosan complex nanofibers. *Carbohydr Polym* 2008;72:410-418.
6. Vitchuli N, Shi Q, Nowak J, Nawalakhe R, Sieber M, Bourham M, McCord M, Zhang X. Plasma-Electrospinning Hybrid Process and Plasma Pretreatment to Improve Adhesive Properties of Nanofibers on Fabric Surface. *Plasma Chem Plasma Process* 2012;32:275-291.
7. Hwang YJ, McCord MG, An JS, Kang BC, Park SW. Effects of Helium Atmospheric Pressure Plasma Treatment on Low-Stress Mechanical Properties of Polypropylene Nonwoven Fabrics. *Textile Research Journal* 2005;75:771-778.
8. Hwang YJ, McCord MG. Surface modification of organic polymer films treated in atmospheric Plasmas. 2004;151:495-501.
9. Tendero C, Tixier C, Tristant P, Desmaison J, Leprince P. Atmospheric pressure plasmas: A review. *Spectrochimica Acta Part B: Atomic Spectroscopy* 2006;61:2-30.
10. Shin Y, Son K, Yoo DI, Hudson S, McCord M, Matthews S, Whang Y. Functional finishing of nonwoven fabrics. I. Accessibility of surface modified PET spunbond by atmospheric pressure He/O<sub>2</sub> plasma treatment. *J Appl Polym Sci* 2006;100:4306-4310.
11. Cornelius C. Atmospheric Plasma Characterization and Mechanism of Substrate Surface Modification. 2006.
12. Hwang YJ, McCord MG, Kang BC. Helium/oxygen atmospheric pressure plasma treatment on poly(ethylene terephthalate) and poly(trimethylene terephthalate) knitted fabrics: Comparison of low-stress mechanical/surface chemical properties. 2005;6:113-120.

13. McCord MG, Hwang YJ, Hauser PJ, Qiu Y, Cuomo JJ, Hankins OE, Bourham MA, Canup LK. Modifying Nylon and Polypropylene Fabrics with Atmospheric Pressure Plasmas. *Textile Research Journal* 2002;72:491-498.
14. McCord MG, Hwang YJ, Qui Y, Hughes LK, Bourham MA. Surface Analysis of Cotton Fabrics Fluorinated in RadioFrequency Plasma. 2003;88:2038-2047.
15. Cai Z, Qui Y, Hwang YJ, Zhang C, McCord MG. The Use of Atmospheric Pressure Plasma Treatment in Desizing PVA on Viscose Fabrics. 2003;32:223-232.
16. Gandhi M, Heejae Y, Frank K. regeneration of bombyx mori silk by Electrospinnin: A comparative study of biocompatibility of natural and synthetic polymers for tissue engineering applications. 2007;1:274-281.
17. Ohgo K, Zhao C, Kobayashi M, Asakura T. Preparation of non-woven nanofibers of Bombyx mori silk, Samia cynthia ricini silk and recombinant hybrid silk with electrospinning method. *Polymer* 2003;44:841-846.
18. Minoura N, Aiba S, Gotoh Y, Tsukada M, Imai Y. Attachment and growth of cultured fibroblast cells on silk protein matrices. *J Biomed Mater Res* 1995;29:1215-1221.
19. Jeong L, Yeo I, Kim HN, Yoon YI, Jang DH, Jung SY, Min B, Park WH. Plasma-treated silk fibroin nanofibers for skin regeneration. *Int J Biol Macromol* 2009;44:222-228.
20. Kim K, Jeong L, Park H, Shin S, Park W, Lee S, Kim T, Park Y, Seol Y, Lee Y, Ku Y, Rhyu I, Han S, Chung C. Biological efficacy of silk fibroin nanofiber membranes for guided bone regeneration. *J Biotechnol* 2005;120:327-339.
21. Park KE, Jung SY, Lee SJ, Min B, Park WH. Biomimetic nanofibrous scaffolds: Preparation and characterization of chitin/silk fibroin blend nanofibers. *Int J Biol Macromol* 2006;38:165-173.
22. Zarkoob S, Eby RK, Reneker DH, Hudson SD, Ertley D, Adams WW. Structure and morphology of electrospun silk nanofibers. *Polymer* 2004;45:3973-3977.
23. Gibson P, Schreuder-Gibson H, Rivin D. Transport properties of porous membranes based on electrospun nanofibers. *Colloids Surf Physicochem Eng Aspects* 2001;187-188:469-481.
24. Gu J, Yang X, Zhu H. Surface sulfonation of silk fibroin film by plasma treatment and in vitro antithrombogenicity study. *Materials Science and Engineering: C* 2002;20:199-202.

25. von Fraunhofer JA, Sichina WJ. Characterization of surgical suture materials using dynamic mechanical analysis. *Biomaterials* 1992;13:715-720.
26. Zhang Y. Natural silk fibroin as a support for enzyme immobilization. *Biotechnol Adv* 1998;16:961-971.
27. Santin M, Motta A, Freddi G, Cannas M. In vitro evaluation of the inflammatory potential of the silk fibroin. *J Biomed Mater Res* 1999;46:382-389.
28. Gotoh Y, Tsukada M, Minoura N, Imai Y. Synthesis of poly(ethylene glycol)-silk fibroin conjugates and surface interaction between L-929 cells and the conjugates. *Biomaterials* 1997;18:267-271.
29. Amiraliyan N, Nouri M, Kish MH. Effects of Some Electrospinning Parameters on Morphology of Natural Silk-Based Nanofibers. *J Appl Polym Sci* 2009;113:226-234.
30. Sun S, Qiu Y. Influence of moisture on wettability and sizing properties of raw cotton yarns treated with He/O<sub>2</sub> atmospheric pressure plasma jet. *Surf Coat Technol* 2012;206:2281-2286.
31. Chen K, Liao S, Lin S, Hung T, Tsao S, Wu H, Inagaki N, Chen W. Improvement of Thermoplastic Polyurethane Nonwoven Hydrophilicity by Atmospheric Pressure Plasma Treatment with He and N<sub>2</sub> Mixed Gases. *Jpn J Appl Phys* 2012;51:01AJ06.
32. Tian L, Nie H, Chatterton NP, Branford-White CJ, Qiu Y, Zhu L. Helium/oxygen atmospheric pressure plasma jet treatment for hydrophilicity improvement of grey cotton knitted fabric. *Appl Surf Sci* 2011;257:7113-7118.
33. Qiu Y, Zhang C, Hwang YJ, Bures BL, McCord M. The effect of atmospheric pressure helium plasma treatment on the surface and mechanical properties of ultrahigh-modulus polyethylene fibers. 2002;16:99-107.
34. Matthews SR, Hwang YJ, Mccord M, Bourham M. Investigation into etching mechanism of polyethylene terephthalate (PET) films treated in helium and oxygenated-helium atmospheric plasmas. *Journal of Applied Polymer Science* 2004;94:2383-2389.
35. Ying W, Hua W, Aixi Y, Dijiang W. Biodegradable Polylactide/Chitosan Blend Membranes. *Biomacromolecules* 2007;7:1362-1372.
36. MAGOSHI J, NAKAMURA S. Studies on Physical-Properties and Structure of Silk - Glass-Transition and Crystallization of Silk Fibroin. *J Appl Polym Sci* 1975;19:1013-1015.

37. Schoeser M. *Silk*. USA: Yale University Press, 2007.
38. Jeong L, Yeo I, Kim HN, Yoon YI, Jang DH, Jung SY, Min B, Park WH. Plasma-treated silk fibroin nanofibers for skin regeneration. *Int J Biol Macromol* 2009;44:222-228.

Chapter 8  
Conclusion and Future Recommendation

## 8.1 Conclusions

In this research, we were able to prepare nanofibers based novel composite wound dressings. Fabrication of composite bandages was found to be useful in terms of functionality and durability. Two types of biopolymers were studied viz. chitosan and silk fibroin. Chitosan nanofiber layer was useful in providing antibacterial and hemostatic properties whereas SF nanofibers layer was useful in improving the cell viability. Nanofibers layer was deposited on to cotton gauze which acted as secondary absorbent wound dressing material.

The study also focused on removing the drawbacks of application of nanofibers in wound dressing. Nanofibers are inherently weak and difficult to handle. Atmospheric pressure plasma was used to improve the adhesion between cotton substrate and nanofibers. Substrate when treated with atmospheric pressure plasma creates active site on its surface available for cross-linking with the nanofibers to be deposited on it.

The conclusion can be divided into two sections one for chitosan nanofibers based composite wound dressing and other for SF nanofibers based composite wound dressing.

### *Chitosan nanofibers based composite wound dressing*

Electrospinning of chitosan was possible in the range of 3%-7% concentration of chitosan in trifluoroacetic acid. Chitosan nanofibers were electrospun onto 100% cotton gauze substrate to form composite bandages. Atmospheric pressure plasma technology was utilized to improve the adhesion and durability of the nanofiber coating. Peel test showed that treatment of the substrate with 100% He plasma and 99% He/1% O<sub>2</sub> plasma increased the adhesion between nanofiber layers and substrates by up to 4 times. This force was further increased approximately by up to 4.5-5 times after treating the composite bandages with

plasma i.e. post-treatment. Also, plasma pretreatment of the gauze fabric prior to electrospinning significantly reduced degradation of the nanofiber layer due to repetitive flexing. From both gelbo and peel tests, it was found that only post-treatment of composite bandages was not as effective as both pre-treatment of substrate and pre & post-treatment of the composite bandages in improving the adhesion between two layers.

Antibacterial results showed that with plasma pre-treatment of the substrate, the antibacterial properties of chitosan were retained against Gram positive (*Bacillus cereus*) and Gram negative bacteria (*Escherichia coli*). Air permeability and moisture vapor transport were reduced due to the presence of a nanofiber layer upon the substrate, which is expected to aid in keeping the wound moist, resulting in better wound healing. XPS analysis showed that after the substrate was treated by plasma, the surface carbon content (C1s) was decreased and oxygen content was increased. Also, plasma treatment created active sites on surface of substrate, which was responsible for the increased adhesion between the substrate and chitosan nanofibers through crosslinking between the active sites. As compared to uncoated gauze alone, gauze coated with chitosan nanofibers had on average a 68-82% higher absorbency, which is likely to enhance absorption of wound exudates and blood.

DMA results demonstrated increase in storage modulus of the chitosan nanofibers after He- or He/O<sub>2</sub>-plasma treatment. DSC curves showed that the glass transition temperature of the chitosan nanofibers was increased after treating them with atmospheric pressure plasma. This increase in T<sub>g</sub> indicated etching of the amorphous region from the surface of chitosan nanofibers and increase in crystallinity of the nanofibers. Wide angle X-ray diffraction showed increase in percentage crystallinity of chitosan nanofibers after plasma treatment

which supported the increase in  $T_g$  and increase storage modulus of chitosan nanofibers after plasma treatment. From DSC, DMA and WAXD, it was concluded that He plasma was most effective in improving the surface properties of chitosan nanofibers. XPS analysis showed that after treating the chitosan nanofibers with plasma, the surface carbon content (C1s) was decreased and oxygen content was increased. Plasma treatment created surface oxidation, which was responsible for the increased adhesion between the substrate and chitosan nanofibers through cross-linking between the active sites.

*SF nanofibers based composite wound dressing:*

SF nanofibers were electrospun onto 100% cotton gauze substrates to form composite bandages. Atmospheric pressure plasma treatment was utilized to improve the adhesion and durability of the nanofiber coating. Substrates were pre-treated with atmospheric plasma prior to electrospinning of SF nanofibers to study the effect of pre-treatment and plasma post-treatment was performed on composite bandages to study effect of plasma post-treatment. The durability and adhesion of the nanofibers to the substrates was investigated using peel tests and Gelbo Flex tests. Other properties evaluated included MVTR, surface chemical composition via X-ray photoelectron spectroscopy, absorbency and air permeability. The peel test showed that plasma pre-treatment of the substrates and plasma post-treatment of composites with 100% He-plasma and 99% He/1% O<sub>2</sub>-plasma increased the forces required to peel off the nanofiber layer. This confirmed that the pre-treatment of the substrate with atmospheric plasma followed by electrospinning of SF nanofiber produced durable composite bandages. The peel force required to peel the nanofibers off the pre-treated substrate was further increased after post treatment of the composite bandages. These results

were supported by the Gelbo flex testing carried out on the composite bandages. Air permeability and moisture vapor transport were reduced due to the presence of a nanofiber layer upon the substrate which is expected to aid in keeping the wound moist, resulting in better wound healing.

DMA results showed that there was increase in storage modulus of the SF nanofibers after He- or He/O<sub>2</sub>-plasma treatment. DSC curves showed that the glass transition temperature of the SF nanofibers was increased after treating them with atmospheric pressure plasma. The increase in T<sub>g</sub> indicated etching of the amorphous region from the surface of SF nanofibers and increase in crystallinity of the nanofibers. Wide angle X-ray diffraction showed increase in percentage crystallinity of chitosan nanofibers after plasma treatment which supported the increase in T<sub>g</sub> and increase storage modulus of chitosan nanofibers after plasma treatment. From DSC, DMA and WAXD, it was concluded that He plasma was most effective in improving the surface properties of chitosan nanofibers. MTT assay showed that He plasma treatment made the SF nanofibers more hydrophilic, thereby increasing cell viability of bandages as compared to untreated SF composite bandages. Thus composite bandage made up of SF nanofibers as a primary layer and cotton gauze as a backing material can act as promising wound dressing material.

The results of surface elemental analysis of the cotton substrate showed formation of oxygen rich active sites on the surface after plasma treatment. Plasma treatment creates surface oxidation, which may be responsible for the crosslinking and formation of covalent bonds between the substrate and SF nanofibers. It was concluded from XPS analysis that plasma treatment creates active sites on the surface making them available for crosslinking

with the active sites created on nanofibers. Study of C1 spectra and N1-spectra of SF nanofibers showed scission of C-C and C-N linkages which indicates the formation of radicals on the surface and etching of the surfaces of SF nanofibers. This increase in roughness can cause higher frictional forces between adjacent layer of nanofibers and between nanofibers and substrate; thereby, increasing the storage modulus of nanofibers and interfacial adhesion between nanofibers layer and substrate.

## **8.2 Recommendations**

In this dissertation research, the fabrication of composite wound dressing, deposition of biopolymer based electrospun fibers on cotton fabric to improve the wound healing properties and interfacial adhesion between nanofibers layer and substrate by treating the composite bandage with atmospheric pressure plasma were examined. Some of our recommendations for future research are discussed below.

### a) Use of different gases

In this research, gases used in generating plasma were 100% He and mixture of 99% He/1% oxygen gases. The XPS analyses showed that the He plasma treatment created more number of active sites on the surface of polymers than that of Helium and oxygen gas plasma. This can be explained by the fact that oxygen molecule is difficult to break into radicals. The active chemical groups on polymer surfaces facilitate the formation of cross-linking between nanofibers and substrates, and improve adhesion strength. We would recommend using other plasma carrier gases such as N<sub>2</sub>, CO<sub>2</sub> and NH<sub>3</sub> to explore its effect on creation of active sites on the surface of polymers.

#### b) Cell viability assessment

In this work it was observed that plasma increased the hydrophilicity of silk and chitosan nanofibers and made suitable environment for cell growth. It was observed that cell viability was higher when treated He and He/O<sub>2</sub> plasma as compare to when no plasma treatment was given to composite bandages. During cell viability study, even after multiple trials cell proliferation on the nanofiber layer could not be observed under scanning electron microscope. This might be because less number of cell were mounted on to the samples because of which there was no cell proliferation was observed. It is recommended that more number of cells should be mounted on the samples so as to get cell proliferation.

#### c) Polymers other than Chitosan and silk fibroin should be studied.

We carried out studies on chitosan and silk. Other polymers such as fibrinogen, collagen, cellulose acetate, etc. should be explored in the form of nanofibers for their application in wound dressing.

#### d) Utilize Hybrid Plasma

Increased adhesion between nanofiber layer and substrate was achieved by treating the substrate in atmospheric plasma chamber and post treating composite wound dressing in the same atmospheric plasma chamber. Hybrid plasma system in which nanofibers can be electrospun through the plasma curtain can further enhance the properties of nanofibers to be deposited on to the substrate. This hybrid plasma system should be utilized to create more active sites on the nanofiber, thereby improving the mechanical properties of nanofibers.

## APPENDICES

Appendix A

**Moisture Vapor Transmission rate**

Moisture Vapor Transmission rate of Chitosan and Silk Nanofiber Based composite wound dressings

Moisture vapor transmission rate of Chitosan Nanofibers based composite wound dressings							
		1	2	3	4	5	<b>Avg. g/m<sup>2</sup>/day</b>
Gauze	(Final wt. -initial wt.), gms	3.65	3.82	3.64	3.76	3.72	<b>3.7 ± 0.07</b>
	MVTR, g/m <sup>2</sup> /day	868.7	909.1	866.3	894.8	885.3	<b>885.3 ± 18.0</b>
Gauze + Chitosan	(Final wt. -initial wt.), gms	3.2	3.13	3.07	3.15	3.1	<b>3.13 ± 0.04</b>
	MVTR, g/m <sup>2</sup> /day	761.6	744.9	730.6	749.7	737.8	<b>744.9 ± 11.7</b>
He treated gauze + chitosan	(Final wt. -initial wt.), gms	3.22	3.08	3.17	3.13	3.26	<b>3.17 ± 0.071</b>
	MVTR, g/m <sup>2</sup> /day	766.3	733.0	754.4	744.9	775.8	<b>754.4 ± 16.9</b>
He/O <sub>2</sub> treated gauze + chitosan	(Final wt. -initial wt.), gms	3.32	3.16	3.18	3.15	3.29	<b>3.2 ± 0.07</b>
	MVTR, g/m <sup>2</sup> /day	790.1	752.0	756.8	749.7	783.0	<b>766.3 ± 18.8</b>

Moisture vapor transmission rate of Silk fibroin Nanofibers based composite wound dressings							
		1	2	3	4	5	<b>Avg., g/m<sup>2</sup>/day</b>
Gauze	(Final wt. -initial wt.), gms	3.7	3.54	3.64	3.76	3.55	<b>3.64 ± 0.09</b>
	MVTR, g/m <sup>2</sup> /day	880.6	842.5	866.3	894.8	844.9	<b>866.3 ± 22.6</b>
Gauze + SF	(Final wt. -initial wt.), gms	2.98	3.16	3.07	3.15	3.1	<b>3.09 ± 0.07</b>
	MVTR, g/m <sup>2</sup> /day	709.2	752.0	730.6	749.7	737.8	<b>735.4 ± 17.2</b>
He treated gauze + SF	(Final wt. -initial wt.), gms	3.2	3.06	3.17	3.13	3.24	<b>3.16 ± 0.06</b>
	MVTR, g/m <sup>2</sup> /day	761.6	728.2	754.4	744.9	771.1	<b>752.0 ± 16.4</b>
He/O <sub>2</sub> treated gauze + SF	(Final wt. -initial wt.), gms	2.88	3.06	3	2.91	3.1	<b>2.99 ± 0.09</b>
	MVTR, g/m <sup>2</sup> /day	685.4	728.2	714	692.5	737.8	<b>711.6 ± 22.4</b>

## Appendix B

### Absorbency

Absorbency of Gauze Fabric and Chitosan Nanofiber coated composite wound dressings

	Initial wt. gms	final wt, gms	difference, gms	Average	Absorbency, %	<b>Avg. absorbency, %</b>
Gauze	0.127	0.248	0.121	0.12	95.9	<b>91.2±5.5</b>
	0.131	0.246	0.115		87.7	
	0.130	0.255	0.125		96.3	
	0.133	0.243	0.111		83.5	
	0.135	0.260	0.125		92.6	
Gauze + Chitosan	0.143	0.346	0.203	0.22	142.5	<b>152.8±10.2</b>
	0.140	0.372	0.232		166.5	
	0.147	0.359	0.212		144.1	
	0.144	0.373	0.230		159.7	
	0.149	0.375	0.226		151.4	
He treated gauze + Chitosan	0.130	0.336	0.226	0.23	174.3	<b>164.4±7.2</b>
	0.138	0.369	0.231		167.5	
	0.142	0.366	0.224		157.6	
	0.143	0.378	0.235		165.1	
	0.138	0.355	0.217		157.2	
He/O <sub>2</sub> treated gauze + Chitosan	0.147	0.379	0.232	0.24	157.9	<b>166.3±9.3</b>
	0.149	0.383	0.234		157.6	
	0.136	0.378	0.243		179.3	
	0.142	0.377	0.235		165.4	
	0.144	0.391	0.247		171.5	

Absorbency of Gauze fabric and Silk Fibroin (SF) Nanofiber coated composite wound dressings

	Initial wt. gms	final wt, gms	difference, gms	Average	Absorbency, %	<b>Avg. absorbency, %</b>
Gauze	0.126	0.247	0.1213	0.119	95.8	<b>91.18±5.5</b>
	0.131	0.246	0.115		87.6	
	0.129	0.254	0.125		96.3	
	0.132	0.243	0.1106		83.47	
	0.135	0.26	0.125		92.59	
Gauze + SF	0.142	0.346	0.2434	0.236	170.5	<b>163.79±6.5</b>
	0.139	0.361	0.2222		159.2	
	0.147	0.399	0.252		171.3	
	0.143	0.373	0.2296		159.6	
	0.149	0.384	0.2358		158.1	
He treated gauze + SF	0.129	0.336	0.2663	0.242	205.1	<b>176.31±18.1</b>
	0.138	0.379	0.2412		174.7	
	0.142	0.365	0.2238		157.6	
	0.142	0.377	0.2352		165.0	
	0.137	0.384	0.2468		178.9	
He/O <sub>2</sub> treated gauze + SF	0.146	0.388	0.242	0.249	164.7	<b>174.23±11.2</b>
	0.148	0.392	0.244		164.3	
	0.135	0.394	0.259		191.1	
	0.142	0.397	0.255		179.4	
	0.144	0.391	0.247		171.5	

## Appendix C

### Air Permeability

Air Permeability Gauze fabric and Chitosan nanofiber coated composite wound dressings

	Cotton Gauze	Untreated gauze+ Chitosan	He treated gauze+ Chitosan	He/O <sub>2</sub> treated gauze+ Chitosan
1	523.8	6.67	9.82	16.74
2	546	6.57	9.48	17.25
3	531.2	6.77	9.56	17.25
4	509	6.57	9.75	17.08
5	538.6	6.97	9.82	17.59
6	523.8	6.57	9.48	17.59
7	538.6	6.67	9.48	17.76
8	531.2	6.26	9.69	17.42
9	494.2	6.26	9.62	16.57
10	516.4	6.46	9.48	17.76
Std Dev	15.52	0.21	0.14	0.40
Average, ft <sup>3</sup> /ft <sup>2</sup> /min	523.8	6.67	9.62	17.25
<b>Air permeability, in cm<sup>3</sup>/cm<sup>2</sup>/sec</b>	<b>265.68±7.87</b>	<b>3.38±0.11</b>	<b>4.88±0.07</b>	<b>8.75±0.20</b>

Air Permeability Gauze fabric and Silk Fibroin (SF) nanofiber coated composite wound dressings

	Cotton Gauze	Untreated gauze+ SF	He treated gauze+ SF	He/O <sub>2</sub> treated gauze+ SF
1	523.8	17.76	33.9	33.9
2	546	17.93	33.5	34.7
3	531.2	16.91	32.7	35.1
4	509	16.91	31.06	33.9
5	538.6	17.59	31.5	33.5
6	523.8	18.1	31.5	33.1
7	538.6	16.91	32.3	32.3
8	531.2	17.25	30.62	31.9
9	494.2	17.08	30.62	35.1
10	516.4	17.76	30.62	34.7
Std Dev	15.52	0.46	1.21	1.12
Average, ft <sup>3</sup> /ft <sup>2</sup> /min	523.8	17.42	31.9	33.9
<b>Air permeability, in cm<sup>3</sup>/cm<sup>2</sup>/sec</b>	<b>265.68±7.87</b>	<b>8.84±0.23</b>	<b>16.19±0.61</b>	<b>17.20±0.57</b>

## Appendix D

### 90-degree peel test.

<b>Peel Force required to peel chitosan nanofibers off the substrate, gf</b>									
Pretreatment/Post-treatment									
	no/no	He/no	HeO <sub>2</sub> /no	no/He	He/He	HeO <sub>2</sub> /He	no/ HeO <sub>2</sub>	He/ HeO <sub>2</sub>	HeO <sub>2</sub> / HeO <sub>2</sub>
	13.5	36.2	31.9	31.5	42.6	37.7	30.1	52.2	52.7
	9.3	39.6	29.7	19.2	34.9	30.3	26.5	38.5	42.1
	10.1	48.9	32.3	23.1	35.9	32.8	28.9	49.6	49.2
	13.2	51.1	29.9	25.3	30.8	31.3	25.6	41.3	44.6
	9.0	38.2	31.3	33.2	42.9	37.2	27.2	40.9	47.7
	11.3	39.8	32.3	19.9	32.7	35.1	25.8	48.3	48.2
<b>Avg., gf</b>	<b>11.1± 1.9</b>	<b>42.3± 6.1</b>	<b>31.2± 1.2</b>	<b>25.4± 5.9</b>	<b>36.6± 5.1</b>	<b>34.1± 3.1</b>	<b>27.4± 1.8</b>	<b>45.1± 5.6</b>	<b>47.4± 3.7</b>

<b>Peel Force required to peel silk fibroin nanofibers off the substrate, gf</b>									
Pretreatment/Post-treatment									
	no/no	He/no	HeO <sub>2</sub> /no	no/He	He/He	HeO <sub>2</sub> /He	no/HeO <sub>2</sub>	He/HeO <sub>2</sub>	HeO <sub>2</sub> /HeO <sub>2</sub>
	35.5	41.3	44.3	59.6	44.4	56.7	41.3	46.7	54.4
	25.7	39.8	37.7	57.8	37.1	43.3	34.1	51.8	34.3
	28.7	38.5	42.7	47.5	35.1	56.0	33.4	37.0	32.7
	23.6	42.6	43.7	46.0	47.5	47.3	43.8	39.8	48.3
	29.6	37.5	38.7	50.4	46.8	46.5	40.3	36.3	45.7
	32.0	37.2	44.6	53.0	37.0	42.1	32.2	43.1	50.2
<b>Avg., gf</b>	<b>29.2± 4.3</b>	<b>39.5± 2.2</b>	<b>41.9± 3.0</b>	<b>52.4± 5.5</b>	<b>41.3± 5.5</b>	<b>48.7± 6.3</b>	<b>37.5± 4.9</b>	<b>42.4± 6.0</b>	<b>44.3± 8.8</b>